# A Dynamic Model for Algal Growth in the Vaal River

**SW Schoombie • A Cloot • G le Roux**

Report to the Water Research Commission
by the
Department of Mathematics and Applied Mathematics
University of the Orange Free State

**WRC Report No 536/1/97**

# A DYNAMIC MODEL FOR ALGAL GROWTH IN THE VAAL RIVER

WRC Report

submitted to the Water Research Commission

by

SW Schoombie, A Cloot and G le Roux

Department of Mathematics and Applied Mathematics
University of the Orange Free State
BLOEMFONTEIN 9300
South Africa

WRC Report No. 536/1/97
ISBN 1 86845 325 1

# Acknowledgements

This is a report on a research project funded by the Water Research Commission and entitled:

" The development of a dynamic model for algal growth in the Vaal River".

The steering Committee responsible for this project, consisted of the following persons:

| | |
|---|---|
| Mr G Offringa | Water Research Commission (Chairman) |
| Mr H M du Plessis | Water Research Commission |
| Mrs A M du Toit | Water Research Commission (Secretary) |
| Prof J Haarhoff | Rand Afrikaans University |
| Dr C W S Dickens | Umgeni Water |
| Prof J H Swart | University of Natal |
| Prof A J H Pieterse | University of Potchefstroom |
| Mr G Quibell | Department of Water Affairs and Forestry |
| Prof J F Botha | University of the Orange Free State |
| Dr J C Roos | University of the Orange Free State |

The financing of the project by the Water Research Commission is acknowledged gratefully.
This project was only possible with the co-operation of many individuals and institutions. The authors therefore wish to record their sincere thanks to the following:

The Western Transvaal Regional Water Company, in particular Mrs. M Kruger, Mr. J Pietersen and Mr. K Morgan, for the Stilfontein data.

The Institute of Ground Water Studies at the U.O.F.S., in particular
Prof J F Botha, for the use of their graphics software.

The Department of Botany and Genetics at the U.O.F.S., for expert advice about the behaviour of algae.

Mrs. M van der Westhuizen and everyone at the Department of Applied Mathematics who worked on the project at various stages with patience and diligence.

# Executive summary

## Motivation for the research project

The Vaal River is one of the principal sources of potable water for the most populous part of South Africa. This resource is used for industrial and domestic purposes in many different ways that can often be quite conflicting. On the one hand, the river is used as a conduit for industrial and domestic wastes, and on the other hand water from the same river is purified and used for domestic purposes. The waste products in the river, as well as dissolved fertilizer washed into the river from neighbouring agricultural areas, often cause high concentrations of dissolved phosphate and nitrogen, leading to eutrophication. This, in its turn, helps to create favourable conditions for algal blooms, i.e. an increase of algae in the water to such an extent that the water is visibly discoloured. Such high algal concentrations in the water affects the water quality adversely, and creates difficulties in the water purification plants along the river. Thus, the prediction of possible algal blooms is of primordial importance in water resource management.

## Objectives

The main objective of the research project was to develop a mathematical model with the following properties:

a) It should be able to predict the occurrence of algal blooms at least at specified points along the river, and at least a few weeks in advance.

b) It should also be able to distinguish between different algal species, or at least genera, and give a good indications of which algae would be dominant in the predicted bloom.

c) It should take into account all those environmental factors which are known to have a major effect on the growth of algae in the Vaal River.

d) It should be based on sound biological, physical and chemical principles, and be compatible with reported observations of the effect of environmental factors on algal growth.

e) It should be properly calibrated, using existing data sets.

f) It should be thoroughly tested with respect to its sensitivity to changes in input parameters and its predictive abilities.

g) The model should be implemented as computer software for a desk top computer.

## Results and conclusions

A site specific, multi-algal species mathematical model was developed which took into account six environmental factors which have a major effect on algal growth, namely water temperature, under water light, turbidity, dissolved silicon, dissolved nitrogen and dissolved phosphorus. The model was developed progressively, starting with a basic kernel which involved only the effects of under water light and temperature on algal growth. To this was added mathematical expressions which simulate the effect of first silicon and then that of the other nutrients.

A unique feature of the model is its ability to distinguish between different algal species, or at least different groups of algae, each consisting of species with similar properties. This makes it possible to predict not only an algal bloom, but also to give an indication of the type of algae which would be dominant.

Two versions of the model were developed. The first does not take river flow explicitly into account, and is referred to as the stationary model. This version of the model was implemented as a FORTRAN computer program called ALGSTMOD, which should be able to run well on any personal computer with at least an Intel Pentium or equivalent processor.

The stationary model is recommended for predictions of algal blooms at specific sites (e.g. water purification plants), and was calibrated and validated at such a site at Stilfontein. In the report a full sensitivity analysis and the results of verification tests are given for this model. The sensitivity analysis showed that temperature, under water light, and the ratio between dissolved nitrogen and dissolved phosphorus are the parameters in the model which affect algal growth most. The calibration at Stilfontein consists of sets of parameter values for fourteen different algal groups. Some of these groups could be correlated with specific algal genera. With this calibration it was possible to make fairly satisfactory predictions.

The other version of the model does take river flow explicitly into account, and was implemented as another FORTRAN program called ALGDYMOD. It is a more complicated model, and would take up more computer time and resources than the stationary model. It is therefore recommended that users who wish to use such a model at a specific site only, should first try ALGSTMOD. Only if it turns out that the assumption of fairly slow, steady flow on which the stationary model is based, is not true at that site, or if the user wishes to consider an entire stretch of the river, should ALGDYMOD be used.

## Recommendations for further research

Although both a stationary model and a flow dependent model was developed, a full calibration and verification was only performed for the former. Much of this calibration can be (and has been) used for the flow dependent model as well, but more remains to be done, possibly in collaboration with a user or users of the model. It would probably be best to incorporate the model into an existing water quality model. The stationary model is mainly suitable for use at specific sites along the river, but could also be used be used to manage the river system or at least parts of it. One possibility would be to calibrate this model ast a restricted number of sites, and simulate algal growth only at these sites. This should give the managers of the river system a quick idea of the general effects of a planned action on the river.

Another extension to this research project would be to build a comprehensive data bank of algal groups. In this report a calibration involving 14 algal groups are described, with at least some of them associated with known algal genera. By continuing the calibration-verification process described in the report, using more data sets, it would be possible to parameterise more algal groups, and eventually compile a library of parameter sets for algal genera which occur in the river.

# Contents

# List of Tables

# List of Figures

# List of symbols

1. Latin symbols

| | | |
|---|---|---|
| $Chl-\alpha$ | : | Chlorophyll-$\alpha$ concentration |
| $CO_2$ | : | Dissolved concentration of carbon dioxide |
| $CO_{2_s}$ | : | Saturation concentration of dissolved carbon dioxide |
| $c_s$ | : | Light extinction coefficient of suspended inorganic solids in the water |
| $H$ | : | Solar zenith angle |
| $H_f$ | : | Enthalpy of formation of a chemical substance |
| $I$ | : | Underwater light energy |
| $I_{Inhib}$ | : | Inhibiting light intensity for algal photosynthesis |
| $I_{opt}$ | : | Optimal light intensity for algal growth |
| $K$ | : | Chemical equilibrium constant |
| $K_{CO_2}$ | : | Inverse of characteristic time of restitution for $CO_2$ saturation concentration |
| $k_D$ | : | Dying rate of algae |
| $k_{G_{opt}}$ | : | Optimal growth rate of algae |
| $K_{O_2}$ | : | Inverse of characteristic time of restitution for $O_2$ saturation concentration |
| $K_{PO_4}$ | : | Inverse of characteristic time of restitution for $PO_4$ saturation concentration |
| $k_S$ | : | Settling rate of algae |
| $k_{Si}$ | : | Inverse of characteristic time of restitution for $Si$ saturation concentration |
| $k_T$ | : | Vertical light extinction coefficient of water |
| $k_w$ | : | Vertical light extinction coefficient of pure water |
| $k_x$ | : | Self-shading coefficient of algae |
| $[N]$ | : | Dissolved nitrogen concentration |
| $N_{sat}$ | : | Dissolved nitrogen saturation concentration for algal absorption |
| $[NH_4]$ | : | Dissolved concentration of ammonium |
| $N/P$ | : | Ratio of dissolved nitrogen and phosphorus concentration |
| $(N/P)^{opt}$ | : | Optimal $N/P$ ratio for algal growth |
| $O_2$ | : | Concentration of dissolved oxygen |
| $O_{2_s}$ | : | Saturation concentration of dissolved oxygen |
| $[P]$ | : | Dissolved phosphorus concentration |
| $P_{CO_{2_g}}$ | : | Partial pressure of $CO_2$ in the atmosphere |
| $P_{sat}$ | : | Dissolved phosphorus saturation concentration for algal absorption |
| $PS$ | : | Photosynthetic rate of algae |
| $PS_{max}$ | : | Maximum photosynthetic rate of algae |
| $Q$ | : | Water discharge |
| $R$ | : | Universal gas constant |
| $R_\beta$ | : | Fraction of light reflected by the water surface |

| | | |
|---|---|---|
| $S$ | : | Concentration of suspended inorganic solids in the water |
| $Si$ | : | Concentration of dissolved Silicon in the water |
| $Si_S$ | : | Saturation concentration of dissolved silicon in the absence of algae |
| $\bar{Si}^{cr}$ | : | Saturation concentration of dissolved Silicon for algal growth |
| $\bar{Si}^{min}$ | : | Minimum concentration of dissolved Silicon for algal growth |
| $Si^{cr}$ | : | Saturation concentration of dissolved Silicon for absorption by algae |
| $Si^{min}$ | : | Minimum concentration of dissolved Silicon for absorption by algae |
| $S_{shape}$ | : | Model sensitivity coefficient |
| $S_{val}$ | : | Model sensitivity coefficient |
| $t$ | : | time variable |
| $T$ | : | Temperature of the water |
| $T_{min}$ | : | Minimum temperature for algal growth |
| $T_{opt}$ | : | Optimal temperature for algal growth |
| $T_{PS}^{opt}$ | : | Optimal temperature for algal photosynthetic activity |
| $V$ | : | Silicon absorption rate by algae |
| $V_{max}$ | : | Maximum silicon absorption rate by algae |
| $x_{i_1}$ | : | Concentration of live algae of $i$-th group in the water |
| $x_{i_2}$ | : | Concentration of dead algae of $i$-th group in the water |
| $z_0$ | : | Depth of the mixed layer |

2 Greek symbols

| | | |
|---|---|---|
| $\chi$ | : | Dispersion coefficient for algal silicon absorption transfer function |
| $\chi_N$ | : | Dispersion coefficient for algal nitrogen absorption |
| $\chi_P$ | : | Dispersion coefficient for algal phosphorus absorption |
| $\chi_{N/P}$ | : | Dispersion coefficient for $N/P$ ratio |
| $\chi_{PS}$ | : | Slope of the photosynthetic curve as $I \rightarrow 0$ |
| $\gamma_i$ | : | Chemical activity of substance "i" |
| $\mu$ | : | Cosine of the zenith angle |
| $\tau_{D_i}$ | : | Characteristic time of decomposition of dead algae of the $i$-th group |

# Chapter 1

# Introduction

The Vaal River is one of the principal sources of potable water for the most populous part of South Africa. This resource is used for industrial and domestic purposes in many different ways that can often be quite conflicting. On the one hand, the river is used as a conduit for industrial and domestic wastes, and on the other hand water from the same river is purified and used for domestic purposes. The waste products in the river, as well as dissolved fertilizer washed into the river from neighbouring agricultural areas, often cause high concentrations of dissolved phosphate and nitrogen, leading to eutrophication. This, in its turn, helps to create favourable conditions for algal blooms, i.e. an increase of algae in the water to such an extent that the water is visibly discoloured. Such high algal concentrations in the water affects the water quality adversely, and creates difficulties in the water purification plants along the river. Some of these, and other adverse effects are ( Walmsley, 1980):
a) Increased purification costs of water for potable purposes.
b) Tastes and odours produced by algae in water intended for potable purposes.
c) Toxins produced by certain types of algae can result in losses of livestock such as fish and may have subsequent effects on humans.
d) Interferences with irrigation due to clogging of canals by algal growth.

Thus it would be very useful if the occurrence of such algal blooms could be predicted well in advance. Water purification plants could then make suitable preparations in a cost effective way.

The main objective of the research reported in this document was therefore to develop a mathematical model with the following properties:
a) It should be able to predict the occurrence of algal blooms at least at specified points along the river, and at least a few weeks in advance.
b) It should also be able to distinguish between different algal species, or at least genera, and give a good indications of which algae would be dominant in the predicted bloom.
c) It should take into account all those environmental factors which are known to have a major effect on the growth of algae in the Vaal River.
d) It should be based on sound biological, physical and chemical principles, and be compatible with reported observations of the effect of environmental factors on algal growth.
e) It should be properly calibrated, using existing data sets.

f) It should be thoroughly tested with respect to its sensitivity to changes in input parameters and its predictive abilities.
g) The model should be implemented as computer software for a desk top computer.

During the course of this three year project, these objectives were met reasonably well. In some cases expectations were exceeded. For instance, instead of predictions a few weeks in advance some algal blooms were predicted months in advance during the testing phase (Details can be found in chapter 8).

The end results were two FORTRAN programs, ALGSTMOD and ALGDYMOD. Detailed instructions on the use of these two programs can be found in Appendix B. The program ALGSTMOD would be most useful for users who are interested in predicting algal blooms at one particular site only (e.g. water purifying plants). It is the implementation of a version of the model in which the flow of the river is not taken into account explicitly. (Henceforth we shall refer to this version as the stationary model.) This made it possible to use a system of ordinary differential equations instead of more complicated partial differential equations, resulting in a smaller and faster model. This implementation is discussed in detail in Chapters 3 to 5, as well as Chapters 7 and 8. Those readers who only wish to get a quick idea of the basic model structure and inherent assumptions, need only read Chapters 2 and 3 in detail, and scan the rest. Chapter 2 describes the structure of the model and the modelling assumptions, and Chapter 3 describes the basic building block of the model, namely that part which simulates the effect of underwater light climate and water temperature on algal growth. (Readers who are more mathematically inclined, may also find the analysis of this basic model in Appendix A interesting.) Chapters 4 and 5 contains detailed descriptions of the rather complicated parts of the model which simulate the effect of available nutrients on algal growth. In Chapter 7 the results are given of sensitivity tests performed on the stationary model. The reader who wants to see tests of the predictive abilities of the stationary model, will find that in Chapter 8.

The program ALGDYMOD is an implementation of a more complicated version of the model, in which the flow of the river is taken into account explicitly. Because this version of the model makes use of partial differential equations which are solved in space as well as in time, it is much more complicated. Chapter 6 describes the modifications which were made to the stationary model. For the sake of a more simple representation, only the incorporation of flow effects into the basic light-temperature part of the model is considered in this chapter. In the program ALGDYMOD, however, flow effects were included in the whole model. Because ALGDYMOD did not, as far as it was tested up to this point, give results which differed significantly from those of ALGSTMOD when used to simulate algal growth at one particular site only, under steady flow conditions, it is not recommended to those users who may wish to use it for that purpose. ALGSTMOD would give virtually the same results much faster and use much less computer resources. ALGDYMOD is meant for users who wish to simulate algal growth along a significant stretch of the river. Even so, it would probably be necessary to use this program together with a standard water quality model, or even to incorporate it as a sub model into a more comprehensive model. In the concluding remarks in Chapter 9, more will be said about this.

# Chapter 2

# Model structure and modelling assumptions

The interactions between algae and their environment are most complicated, and it would be futile to account for each and every one in a model. Such a model would not only be very difficult to build, but it would be so complicated that it would be almost useless in practice. Thus the model described in this document involves only those environmental factors which are fairly dominant. In this way an acceptable description of the real situation is still obtained without an unnecessarily complicated model.

In Figure 2.1 the conceptual model is shown on which the mathematical model is based. The central circle represents the entire phytoplankton population of the Vaal River. Each factor which is assumed to play a significant role in the growth of algae is represented by a rectangular box, and arrows are used to indicate the ways in which these factors influence each other and the algal population. Since some factors would influence only certain specific categories of algae, the algal population is subdivided into three different groups, represented by triangular boxes. These are diatoms, and other algae which are either nitrogen fixing or not. Whenever some factor affects only one of these algal types, an arrow points towards one of the triangles rather than to the central circle.

To gain a proper insight in the model, it should be realised that environmental factors represented in Figure 2.1 were grouped into five different categories, namely:

1. Under water light climate and turbidity.
2. Silicon uptake by diatoms.
3. Photosynthesis and respiration.
4. Nutrient uptake and recycling.
5. The effect of flow.

Since there are only fairly weak interactions between these five categories (with the exception of the first and the fifth), it was possible to start with category 1 as the basic

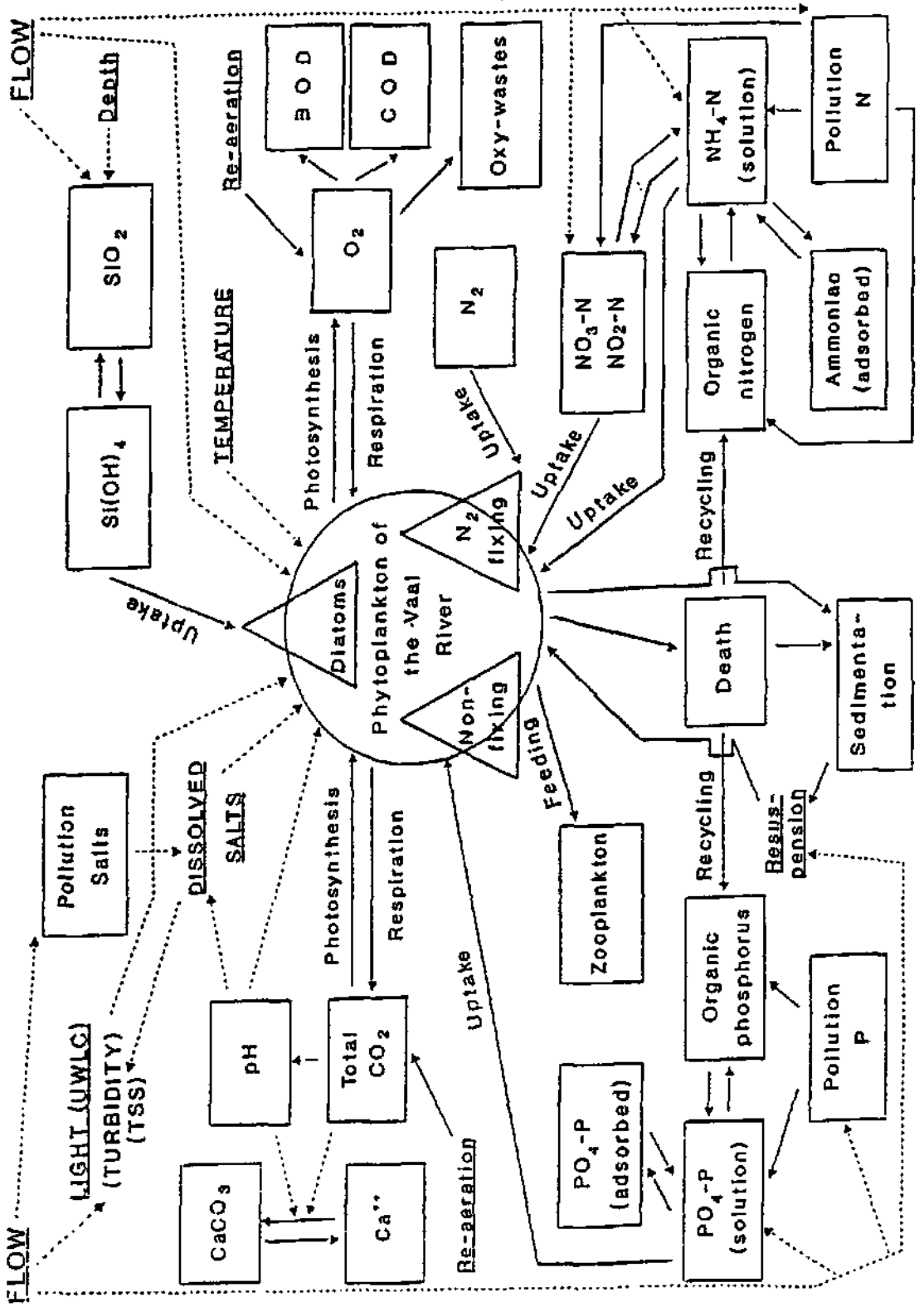


Figure 2.1: Environmental variables associated with algae in the Vaal River, as implemented in the mathematical model.

building block of the model, and then add on each of the other sets of environmental factors in turn, from 2 through five.

In the rest of this report we shall start with a description of the basic building block (category 1), and then indicate how each of the other modules are incorporated into the model.

During the modelling process the following main assumptions were made:

1. The most important factors affecting algal growth are water temperature, under water light climate, the concentration of dissolved silicon (for diatoms only), the concentration of dissolved nitrogen and the concentration of dissolved phosphorus.
2. Other environmental factors either have a small effect on algal growth, or else remain fairly constant.

It was also necessary to make some assumptions about the effect of the flow of the river on algal growth. Two versions of the model were actually developed, with different assumptions about river flow. The first version was based on the assumptions that the river flow is steady (i.e. does not change with time at a fixed point in the river), that the gradient of the flow velocity along the river is very slight, and that the flow velocity itself is relatively small. This version will be referred to henceforth as the stationary model, and it turned out to be very effective for the prediction of algal growth at a specific site along the river. To understand why, the reader is referred to Figure 2.2. This figure

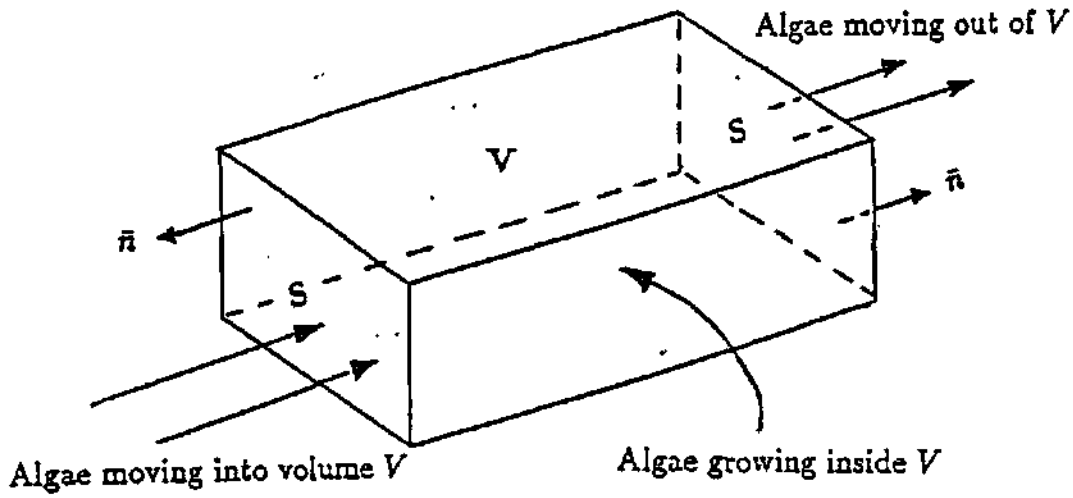


Figure 2.2: Graphic representation of the change in algal concentration due to the flow.

shows a small control volume $V$ at a specific point in the river. The rate of change in

algal biomass in this volume is equal to the rate of change in biomass of algae within the volume (governed by their growth rate and dying rate), plus the biomass flowing per unit time into the volume through the surface $S$, minus that flowing out of the volume per unit time. Under the assumptions stated, the inflow of algal biomass is very nearly equal to the outflow, and the stationary model ignores these contributions altogether. Any remaining effects of river flow is effectively incorporated into the other model parameters during model calibration, which is partly done by fitting model output onto measurements of algal biomass.

*Of course, these rather restricting assumptions are idealisations,* and at times, and at some sites along the river they would not hold. For this reason a second version of the model was developed, as described in Chapter 6, which is not based on such assumptions, and take the effect of river flow explicitly into account.

# Chapter 3

# A basic light-temperature model for algal blooms

The basic building block of the model, which involves the effect of under water light and temperature on algal growth, can be viewed as a model in its own right, albeit a very rough one. The other environmental factors are then either neglected as second order effects, or considered to remain unchanged.

An important feature of not only this sub model, but also the complete model, is that the algal biomass is divided into a number of algal groups. The algae in each group is assumed to have fairly similar properties, at least in terms of those properties taken into account by the model. Such a group could consist of a single genus or even (but less likely) a single algal species. If we now assume that there are $N$ of these algal groups, then the basic light-temperature model can be represented by the scheme shown in Figure 3.1

A straightforward transcription of the scheme in Figure 3.1 in terms of mathematical relations leads to a system of $N$ pairs of coupled non-linear differential equations

$$\begin{aligned} \dot{x}_{i_1} &= [-(k_{D_i} + k_{S_i}) + k_{G_i}(T, I, \underline{K}_j; j = 1, N)]x_{i_1} \\ \dot{x}_{i_2} &= k_{D_i}x_{i_1} - k_{S_i}x_{i_2} \end{aligned} \tag{3.1}$$

where $x_{i_1}$ is the chlorophyll-$a$ concentration of living algae belonging to the i-th category and $x_{i_2}$ represents the dead algae belonging to the same group, also expressed in term of chlorophyll-$a$ concentration. Furthermore, $k_{D_i}$, $k_{S_i}$, $k_{G_i}$ are the dying rate, the settling rate and the growth rate respectively, corresponding to the i-th algal category. The dying and settling rates are throughout this report assumed to be constants, and the growth rates are functions of available light, $I$, water temperature, $T$, and a set of further variables represented by the vector $\underline{K}_i$. These variables consist of both environmental variables, and variables which are characteristic of a specific algal group. The functional dependence of the growth rates on these variables will be described in the next two sections.

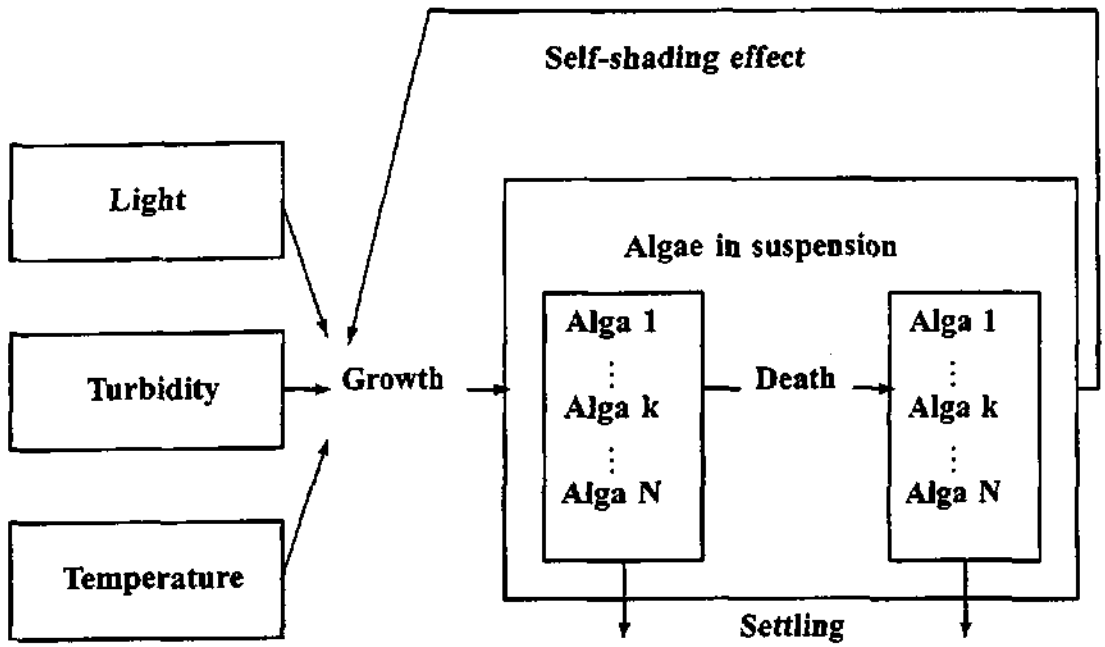


Figure 3.1: A schematic representation of the basic light-temperature growth model.

## 3.1 Modelling the light dependence of algal growth

To determine the function $k_{G_i}$, an approach similar to that in (Wofsy, 1983) and (Whitehead and Hornberger, 1984) was followed: A function was constructed which corresponds fairly well to experimental data on the dependence of growth rate on available light.

Such experimental data is available in the literature for various types of algae (see Jorgensen (1979) and references therein). As a rule algal growth rate is an increasing function of light intensity up to a certain optimal value (which will be denoted by $I_{opt}$ henceforth) where the growth rate takes on its maximum value $k_{G_{opt}}$. At higher light intensities the algal growth rate decreases again. The specific values of the optimal light intensity and the optimal growth rate vary a great deal for different algal species. Thus each algal category would have its own set of values for $I_{opt}$ and $k_{G_{opt}}$.

A function which is at once simple enough to facilitate easy incorporation into the model on the one hand, and versatile enough to fit this type of experimental data set, is

$$k_{G_i} = k_{G_{opt_i}}(\bar{I}/I_{opt_i}) \exp[1 - \bar{I}/I_{opt_i}], \tag{3.2}$$

where $I_{opt_i}$ is the optimal average irradiance for which the i-th algal group has the maximum growth coefficient $k_{G_{opt_i}}$ and $\bar{I}$ is the average light available under the water surface. In Figure 3.2 measured values of growth rate for various values of $\bar{I}$ is shown for the diatom *Ditylum brightwellii* at 20°. These were taken from Eppley (1977), and the figure also shows how well the function (3.2) can be made to fit this data.

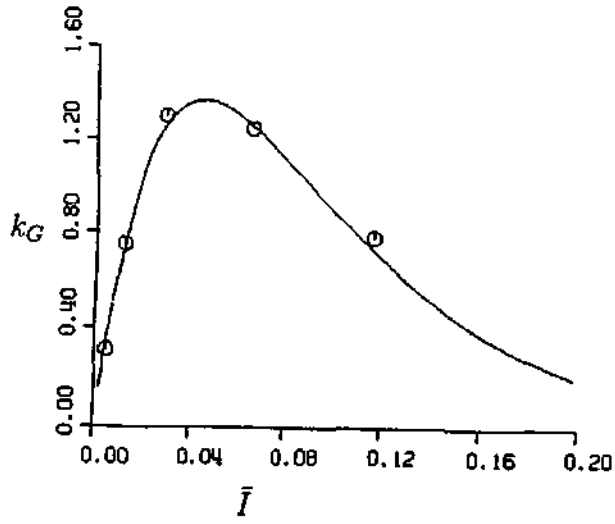


Figure 3.2: $k_G$ as a function of $\bar{I}$, for $I_{opt} = 0.045 cal/cm^2$ and $k_{G_{opt}} = 1.37$ divisions /day. The circles represent measured values.

To find an expression for the average light energy $\bar{I}$, it was first assumed that available underwater light for photosynthesis is attenuated according to the formula

$$I(z,t) = I_0(t)\exp(-k_T z/\mu(t)), \tag{3.3}$$

where $z$ is the depth, $I_0(t)$ is the solar irradiance just below the surface of the water, $k_T$ is the vertical light extinction coefficient, and $\mu(t)$ is the cosine of the solar zenith angle at time $t$ during daylight hours (i.e. the cosine of the angle between a vertical line through an observer's position on earth and a line from that position to the sun). Then the average available light in the so called mixed layer of depth $z_0$ at a certain point in the river at time $t$ can be calculated as follows:

$$\begin{aligned} \bar{I} &= \frac{1}{z_0}\int_0^{z_0} I_0 \exp[-k_T z/\mu]dz \\ &= \frac{\mu I_0}{k_T z_0}[1-\exp[-k_T z_0/\mu]] \end{aligned} \tag{3.4}$$

Furthermore, the vertical extinction coefficient is assumed to be of the form

$$k_T = k_w + c_s S + \sum_{i=1}^{N} k_{x_i}(x_{i_1} + x_{i_2}), \tag{3.5}$$

where $k_w$ is the extinction coefficient for pure water, S is the concentration of suspended inorganic solids, with $c_s$ its specific extinction coefficient, and $k_{x_i}$ is the specific extinction coefficient for the total mass per unit volume of living and dead algae belonging to the i-th group. Note that in an attempt to keep the number of variables as small as possible, the assumption is made that the self-shading coefficient $k_{x_i}$ is the same for living and dead algae. This is of course an approximation, and in cases where it should turn out to be very far removed from reality, it would be a simple matter to change the model appropriately.

For typical values of the parameters, $k_T z_0$ is usually large enough for the exponent in (3.4) to be negligible and in the model this equation is replaced by the approximate version

$$\bar{I} = \frac{\mu I_0}{z_0[k_w + c_s S + \sum_{i=1}^{N} k_{x_i}(x_{i_1} + x_{i_2})]}. \tag{3.6}$$

Finally, the irradiance $I_0(t)$ can be represented by the formula

$$I_0(t) = I_{max}(1 - R_\beta(t)), \tag{3.7}$$

where $I_{max}$ is the irradiance on the water surface for a zero solar zenith angle and $R_\beta$ is the fraction of light reflected by the water surface. Assuming this surface to be reasonably smooth and flat, the following expression for $R_\beta$ can be used (Golterman, 1975) :

$$R_\beta = \frac{1}{2}\left(\left[\frac{\sin(H(t) - r)}{\sin(H(t) + r)}\right]^2 + \left[\frac{\tan(H(t) - r)}{\tan(H(t) + r)}\right]^2\right), \tag{3.8}$$

where $H(t) = \arccos \mu$ is the solar zenith angle , and

$$\sin r = \sin H / 1.33 \ . \tag{3.9}$$

Note that most of the parameters in the model can be determined by direct measurement, and the rest by calibrating the model on actual data. The system (3.1) of ordinary differential equations can then be solved numerically by a fourth order Runge-Kutta method.

This model is still simple enough to be amenable to analysis, and some dynamical aspects are discussed in Appendix A. A more comprehensive analysis can also be found in Cloot and Schoombie (1994).

## 3.2 Temperature dependence of the growth rate

To incorporate the effect of temperature into the model, the constant parameter $k_{G_{opt_i}}$ in (3.2) is replaced by a function $G_i(T)$ of the temperature $T$, so that (3.2) now reads:

$$k_{G_i} = G_i(T)(\bar{I}/I_{opt_i} \exp[1 - \bar{I}/I_{opt_i}]. \tag{3.10}$$

Experimental data show that the growth rate is, as in the case of light dependence, an increasing function of temperature up to a certain optimal temperature, after which it decreases again. There is, however, a certain threshold value $T_{min_i}$ below which no algal growth will take place, and which is characteristic of a specific algal group (see Canale and Vogel (1974) and the references therein).

The following form for $G_i(T)$ turned out to be most representative of experimental data, and simple enough for the purposes of the model:

$$G_i(T) = \begin{cases} k_{G_{opt_i}} s_i^4 \exp[1 - s_i^4] & \text{if } T \geq T_{min_i} \\ 0 & \text{if } T < T_{min_i} \end{cases} \tag{3.11}$$

with $s_i$ given by

$$s_i = \frac{T - T_{min_i}}{T_{opt_i} - T_{min_i}}$$

and where $T_{opt_i}$ is the optimal temperature for the i-th algal group. Note that $k_{G_{opt_i}}$ is now the overall maximum growth rate at both optimal light and temperature conditions.

Figures 3.3 through 3.5 show the transfer function (3.11) fitted onto measurements of growth rates at various temperatures in the case of three different algal species:

The diatom *Asterionella formosa* (Fig. 3.3); The green alga *Dunaliella tertiolecta* with an optimal temperature of about 28° (Fig. 3.4) , and *Chlorella pyrenoidosa*, a green alga with an unusually high optimal temperature of around 40°$C$ (Fig. 3.5).

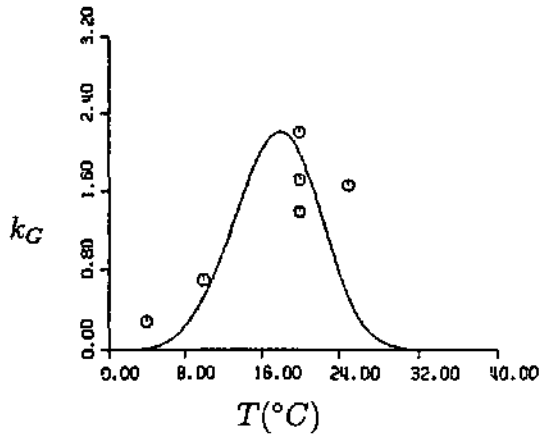


Figure 3.3: Comparison between eq. 3.11 and experimental data for the *Asterionella formosa*: $k_{G_{opt}} = 2.2$; $T_{min} = 0°C$; $T_{opt} = 18°C$.

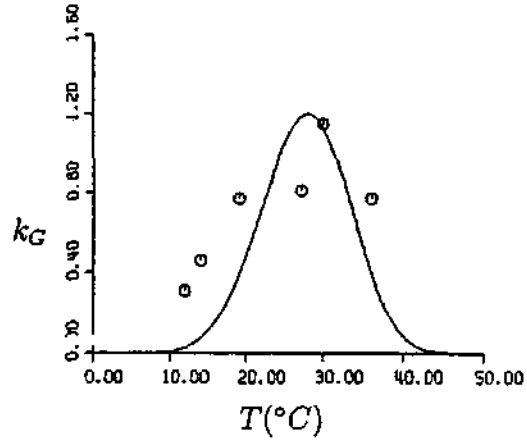


Figure 3.4: Comparison between eq. 3.11 and experimental data for *Dunaliella tertiolecta*: $k_{G_{opt}} = 1.2$; $T_{min} = 5°C$; $T_{opt} = 28°C$.

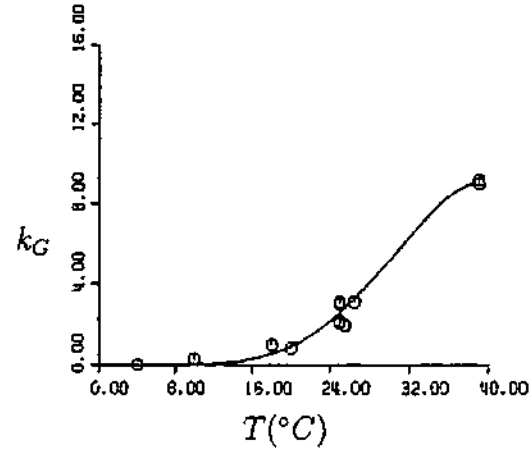


Figure 3.5: Comparison between eq. 3.11 and experimental data for the *Chlorella pyrenoidosa*: $k_{G_{opt}} = 9.2$; $T_{min} = 4°C$; $T_{opt} = 40°C$.

## 3.3 Simulation of winter algal blooms with the basic model

The parameters which were represented by the vector $\underline{K_i}$ in (3.1), have now all been defined, and are, for convenience, listed below in tables 3.1 and 3.2. Henceforth the subscript $i$ will be dropped unless specifically required.

| | | |
|---|---|---|
| $I_0$ | : | maximal irradiance available under the water surface $(cal/cm^2.min)$ |
| $\mu(t)$ | : | cosine of solar zenith angle |
| $T$ | : | the water temperature $(°C)$ |
| $c(t)$ | : | concentration of inorganic material suspended in the water $(mg/l)$ |
| $z_0$ | : | depth of the mixed layer $(m)$ |
| $k_C$ | : | light extinction coefficient for suspended inorganic material $(m^{-1})$ |

Table 3.1: Basic set of environmental parameters

| | | |
|---|---|---|
| $I_{opt}$ | : | optimal light intensity for growth $(cal/cm^2.min)$ |
| $T_{opt}$ | : | optimal temperature for growth $(°C)$ |
| $T_{min}$ | : | minimum temperature for growth $(°C)$ |
| $k_{G_{opt}}$ | : | maximum growth rate $(d^{-1})$ |
| $k_x$ | : | self-shading algal coefficient $((\mu g$ Chl-$a$ /l.m$)^{-1})$ |
| $k_D$ | : | dying rate $(d^{-1})$ |
| $k_S$ | : | algal settling rate $(d^{-1})$ |

Table 3.2: Parameter set governing algal growth (basic model)

As stated before, the model up to now, can serve as a model in its own right under appropriate conditions. Since it is the basic building block of the comprehensive model discussed in this report, it is worthwhile to show how it performs as a model.

Now since this basic model only takes variations in under water light climate and water temperature into account, it can only simulate algal growth in the river realistically when other environmental factors have either a negligible effect, or remain fairly constant. This is probably not true most of the time. However, over relatively short periods of time and at a single site in the river, the model could simulate actual algal growth fairly well.

Simulations were performed of the winter algal blooms at Stilfontein during each of the years 1985 through 1987. Figures 3.6 through 3.8 show the total chlorophyll-$a$ values which were measured in the river at this site during these years.

In all three years two strong chlorophyll-$a$ peaks occurred during the winter months, which suggested that two algal groups might be sufficient to simulate algal growth during these months reasonably well. The algal growth parameters were calibrated partly by using published algal data, and by fitting model output onto measured chlorophyll-$a$. These

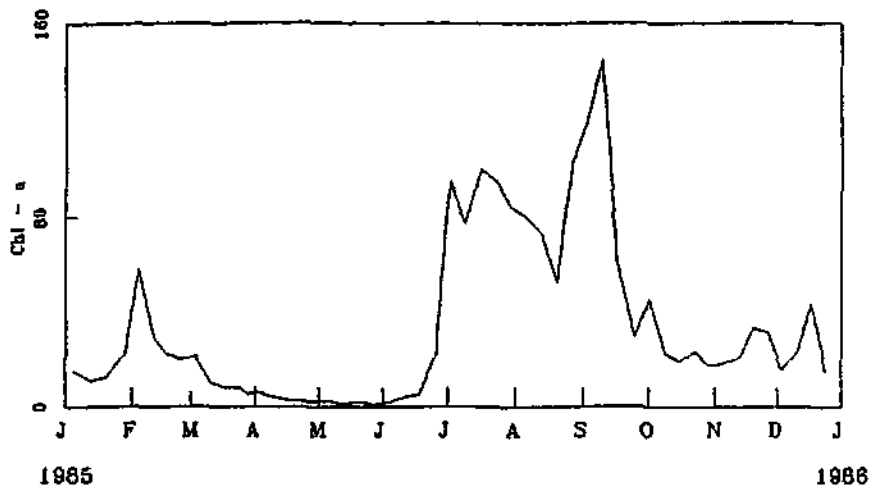


Figure 3.6: Chlorophyll-*a* profile for the year 1985 at the Stilfontein site.

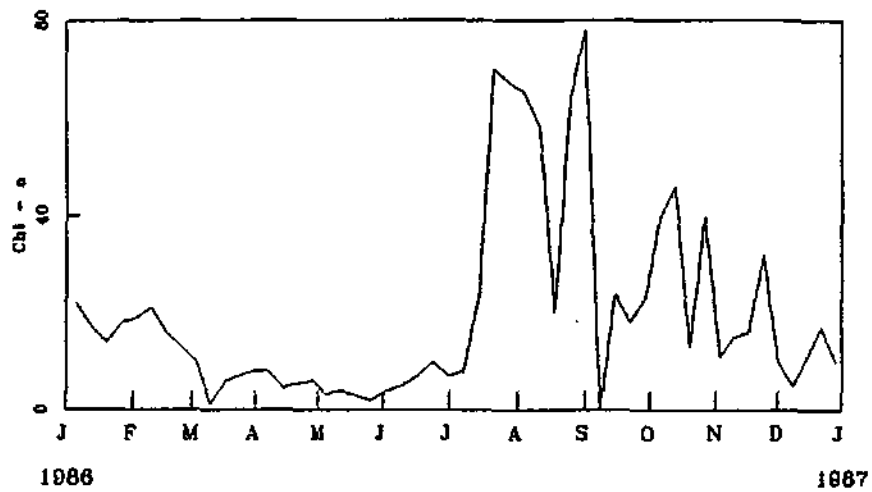


Figure 3.7: Chlorophyll-*a* profile for the year 1986 at the Stilfontein site.

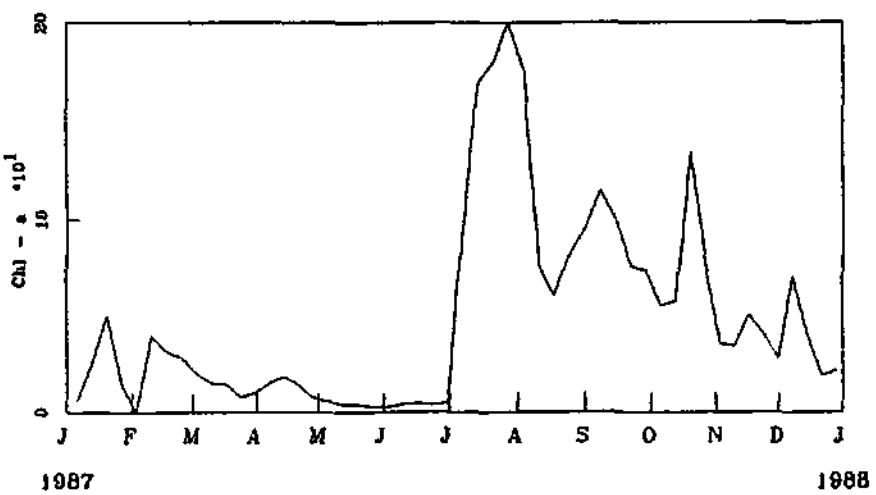


Figure 3.8: Chlorophyll-*a* profile for the year 1987 at the Stilfontein site.

parameter values are shown in Table 3.3. Input data for the model were temperature and turbidity values measured at Stilfontein, as shown in Figures 3.9 through 3.11.

| | 1985 | | 1986 | | 1987 | |
|---|---|---|---|---|---|---|
| Parameter | Alga 1 | Alga 2 | Alga 1 | Alga 2 | Alga 1 | Alga 2 |
| $k_G$ | 1.43 | 1.65 | 1.28 | 1.46 | 1.70 | 1.65 |
| $k_D$ | 0.15 | 0.15 | 0.15 | 0.15 | 0.15 | 0.15 |
| $I_{opt}$ | 0.12 | 0.075 | 0.12 | 0.08 | 0.09 | 0.045 |
| $T_{opt}$ | 11 | 15 | 10 | 13 | 9 | 12 |
| $T_{min}$ | 0 | 5 | 0 | 5 | 0 | 5 |

Table 3.3: Calibrated parameters for the light-temperature model

The simulated chlorophyll-*a* values are displayed in Figures 3.12 through 3.14. There is a reasonable agreement between actual and simulated values, suggesting that the basic light-temperature model described in this chapter describes the response of Vaal River algae to variations in under water light climate and temperature fairly well.

Since the model distinguishes between different types of algae, even though it was calibrated on total algal biomass, it is also possible to see from the model output what contribution each of the two algal groups made to the various winter blooms. This is shown graphically in Figures 3.15 and 3.16.

In the following chapters the addition to this model of other modules is described, making it possible to simulate algal growth over longer periods, and making useful predictions of future levels of algal biomass.

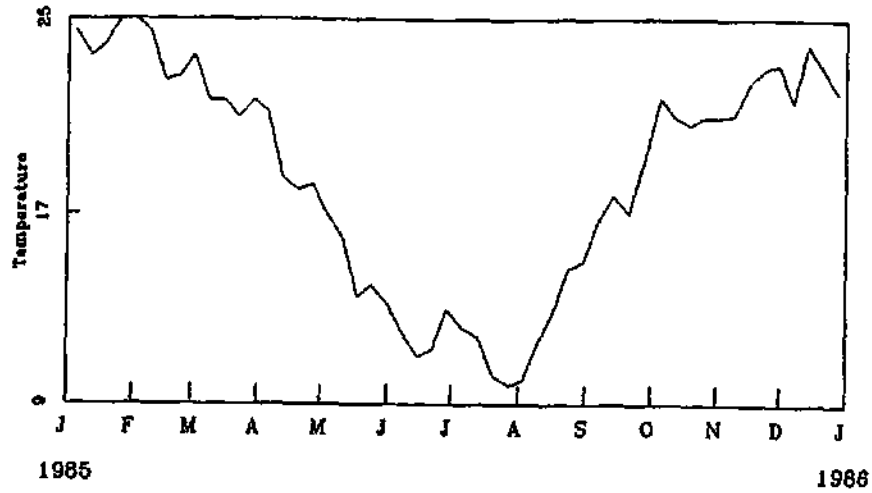


(a)

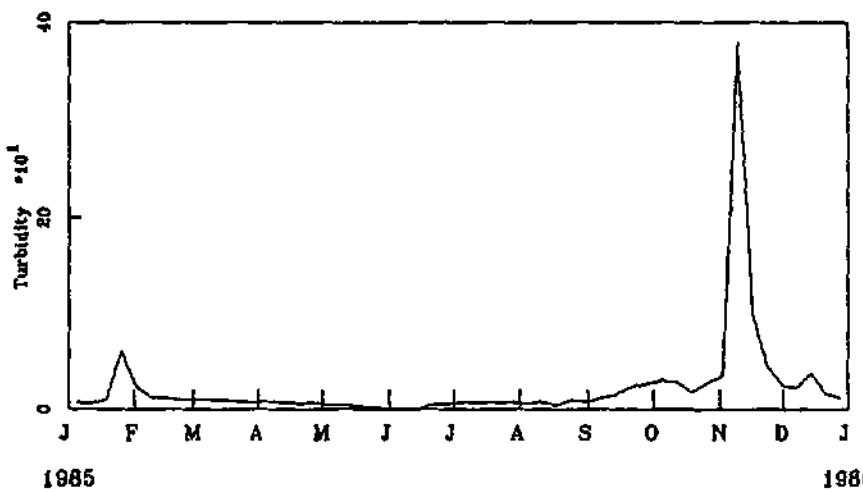


(b)

Figure 3.9: Recorded values of the water temperature (a) and turbidity (b) at the Stilfontein site for 1985.

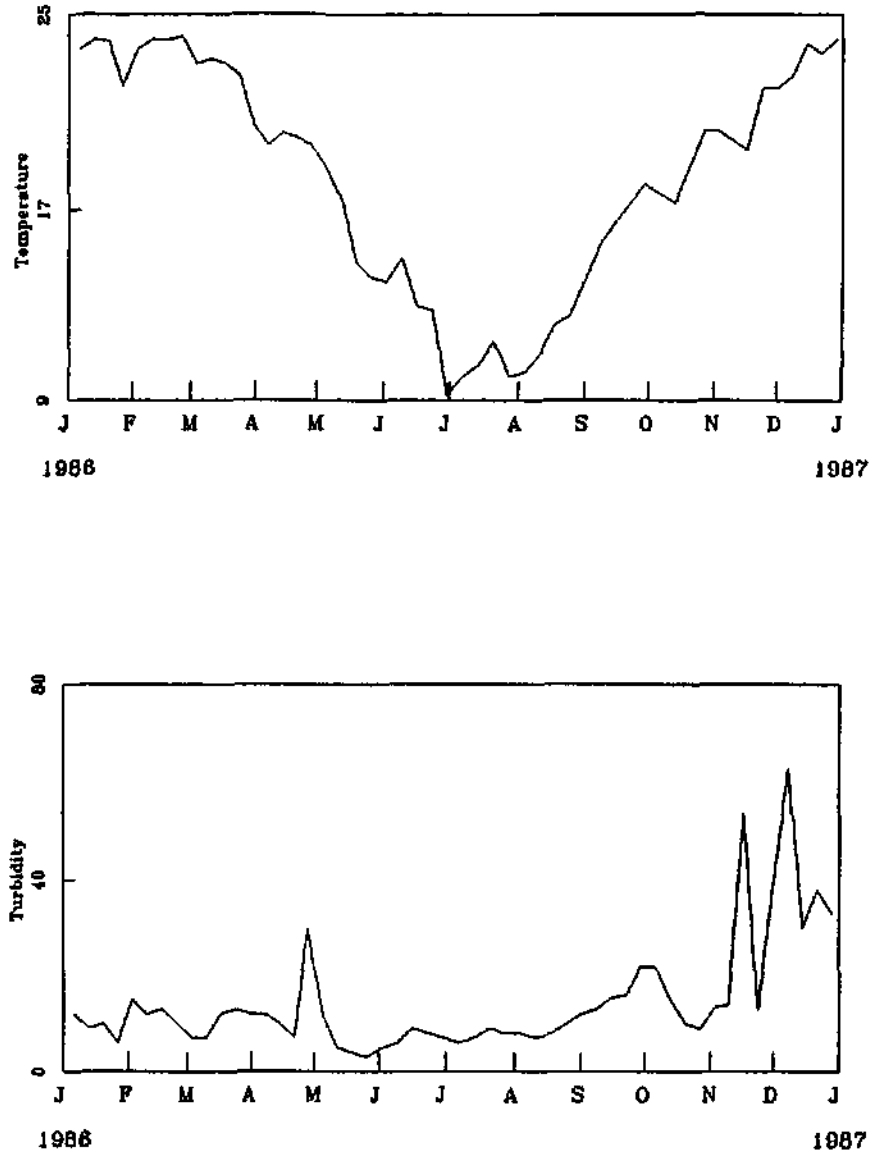


Figure 3.10: Recorded values of the water temperature (a) and turbidity (b) at the Stilfontein site for 1986.

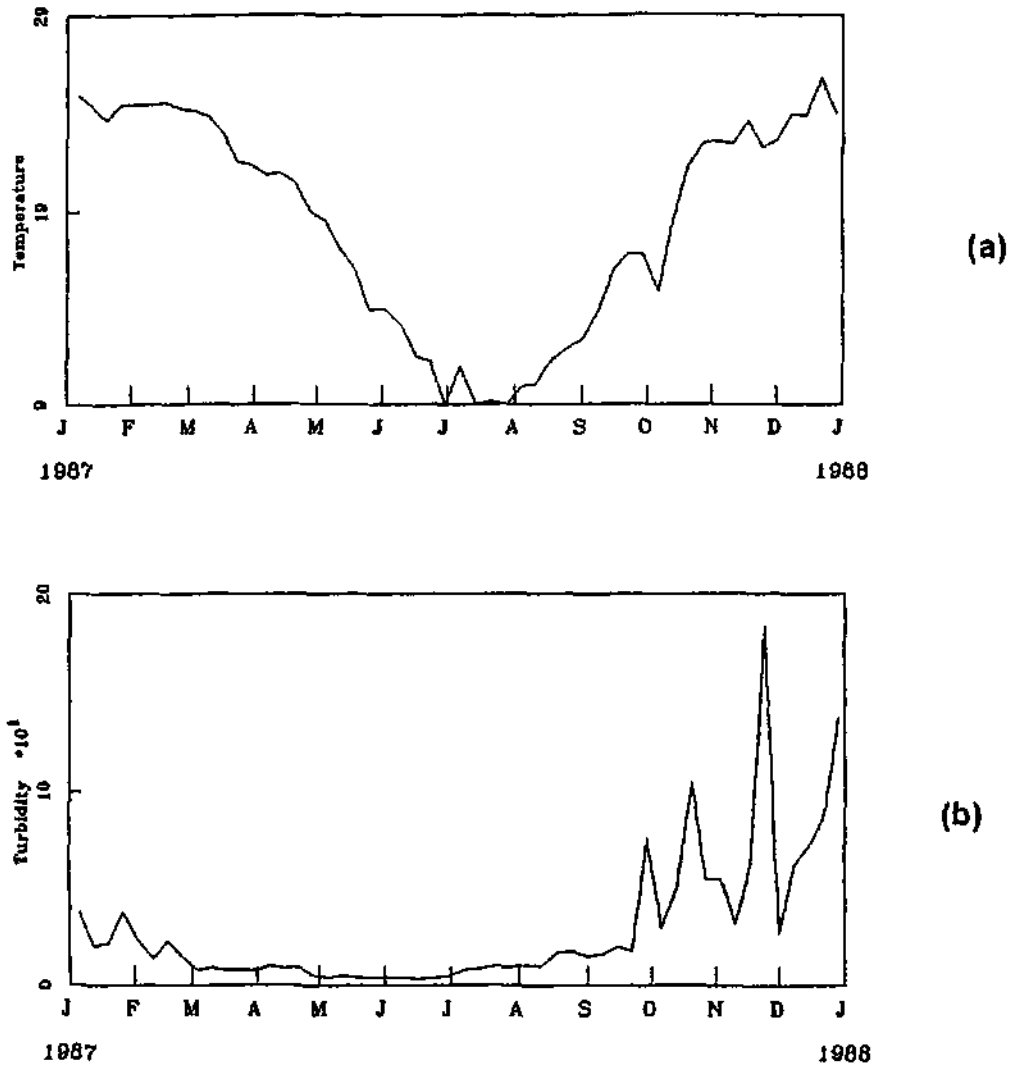


Figure 3.11: Recorded values of the water temperature (a) and turbidity (b) at the Stilfontein site for 1987.

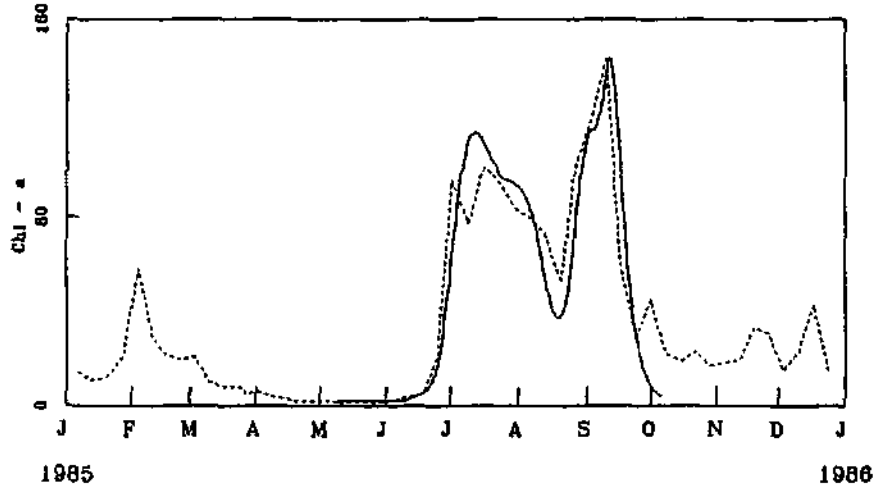


Figure 3.12: Comparison between observed values (dashed curve) and numerically computed values (solid curve), for the total chlorophyll-*a* during the winter period of 1985.

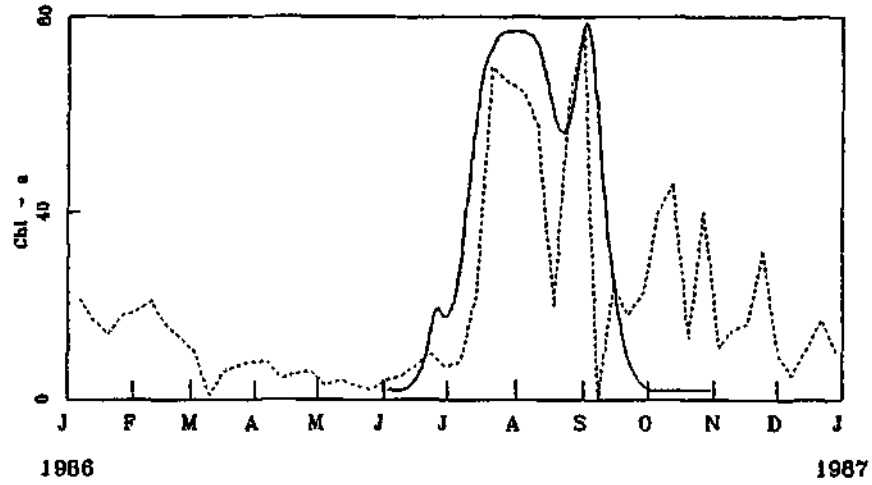


Figure 3.13: The same as Fig. 3.12, but for the total chlorophyll-*a* during the winter period of 1986.

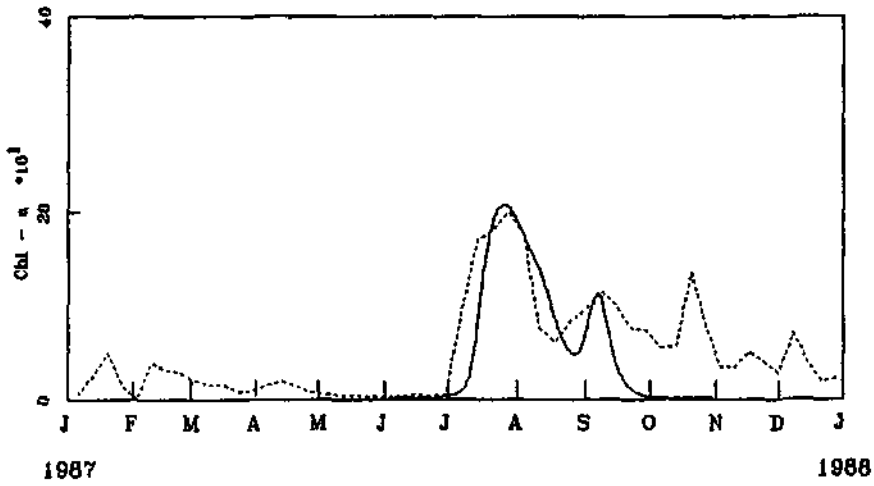


Figure 3.14: The same as Fig. 3.12, but for the total chlorophyll-*a* during the winter period of 1987.

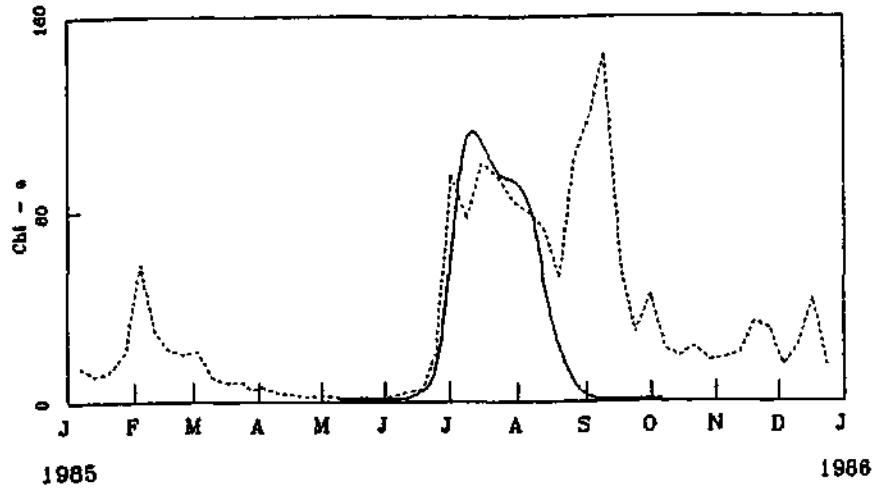


(a)

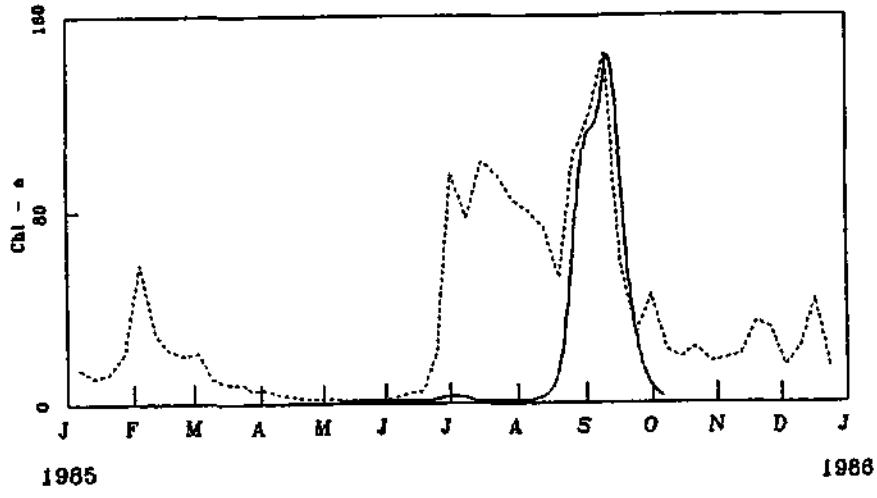


(b)

Figure 3.15: Analysis of the contribution of the two algal groups to the formation of the (computed) total biomass for the winter period 1985: (a): alga 1; (b) alga 2.

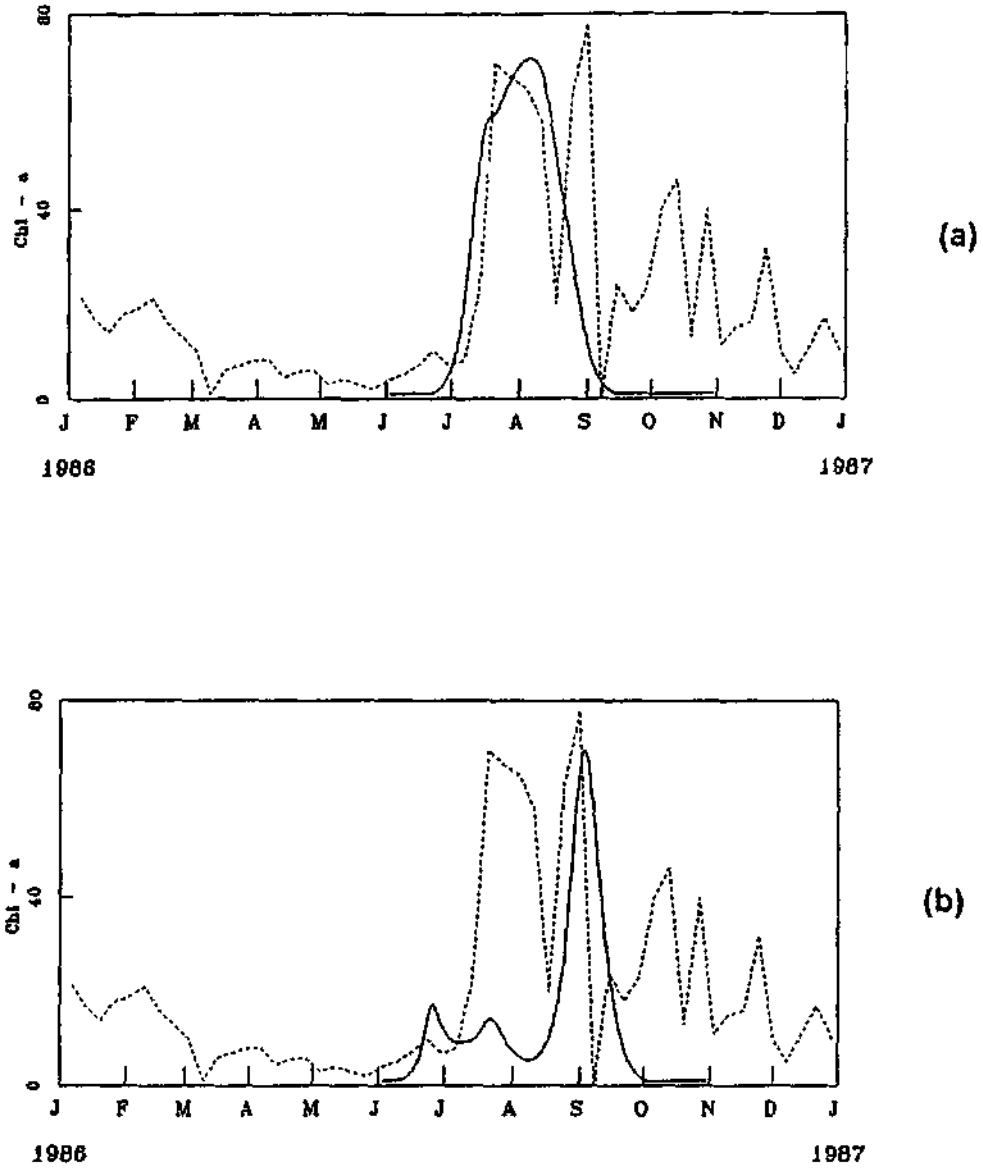


Figure 3.16: The same as Fig. 3.15 but with the results for the winter period of 1986.

# Chapter 4

# Improving the basic model: The silicon effect

When studying the simulations reported in the previous chapter of the winter algal blooms during 1985 and 1986 at Stilfontein, it will be noticed that the simulations do not correspond so well to measured values in the case of the first algal blooms than they do for the second blooms. This can be attributed to the fact that the first bloom was caused mainly by diatoms in both 1985 and 1986, and the second mainly by green algae (Roos, 1992). Unlike other algae, diatoms need to take dissolved silicon from the water in the form of orthosilicic acid $Si(OH)_4$ (see Werner (1992)), and this mechanism was not accounted for in the basic model of chapter 3.

Diatoms need the element silicon during the formation of the frustules of their cells, which protect them against predators and parasites as well as mechanical disturbances (Eppley, 1977). Low levels of dissolved silicon in the water have a significant adverse effect on diatom growth and development.

Since the only algae able to absorb silicon from the water are diatoms, a very elegant and powerful method to find out *a posteriori* to which extent diatoms took part in an algal bloom, is to study dissolved silicon measurements before, during and after the bloom. In fact, dissolved silicon levels are more suitable as an indicator of the presence of diatoms than any other nutrient in the water.

For this reason the first module to be added onto the basic light-temperature model was the interaction between diatoms and dissolved silicon in the water. Figure 4.1 shows a schematic representation of the basic light-temperature model with the interaction between dissolved silicon and diatoms added. There are actually two mechanisms involving silicon which have to be modelled: First the chemical and mechanical processes determining the dissolved silicon concentration in the water in the absence of diatoms, and then the actual uptake of silicon by diatoms and the effect of this on their growth rate and dissolved silicon concentration.

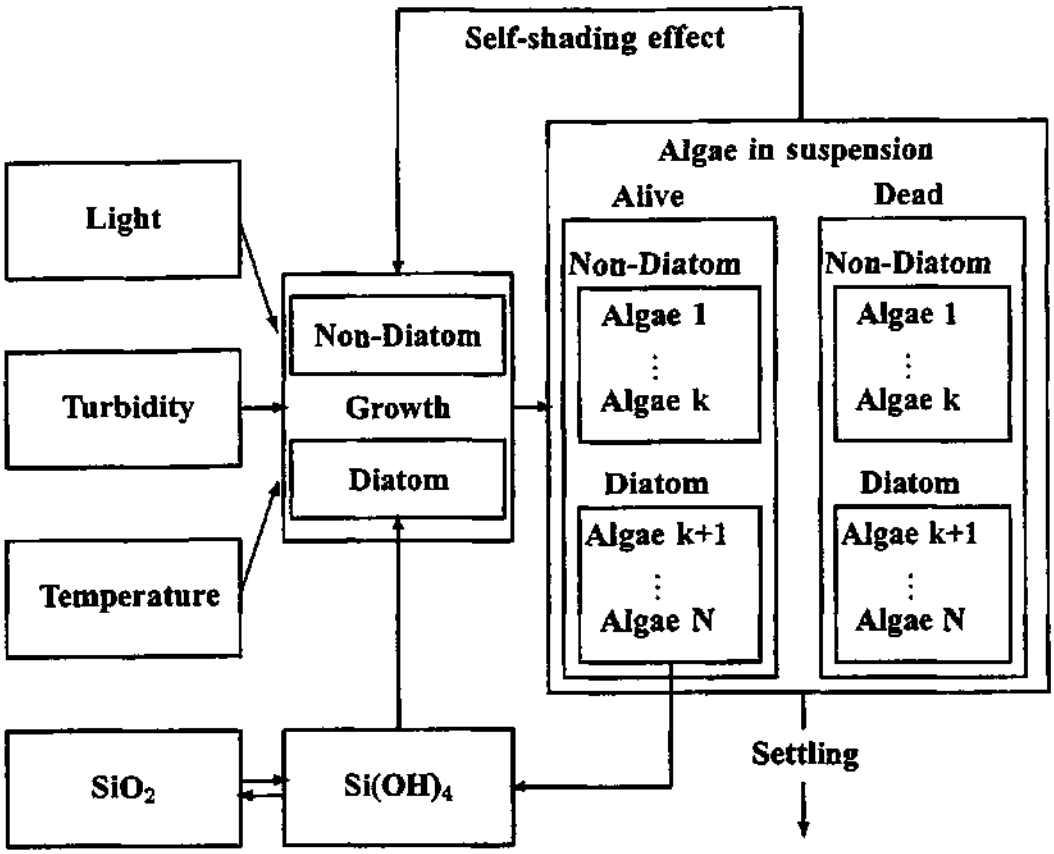


Figure 4.1: Schematic representation of the N-algal growth model including the dissolved silicon effect.

## 4.1 Dissolved silicon content of the water due to mechanical and chemical processes

Diatoms absorb silicon in the form of orthosilisic acid, $Si(OH)_4$ (Werner, 1992), which in its turn is formed mainly from the amorphous $SiO_2$ in the water. The equilibrium constant

$$K(T)|_{am} = \frac{[Si(OH)_4]}{[SiO_2][H_2O]} \tag{4.1}$$

of the chemical reaction

$$SiO_2|_{amorphous} + 2H_2O \rightleftharpoons Si(OH)_4 \tag{4.2}$$

may, under the hypothesis of infinite dilution, be reduced to

$$K(T) \sim [Si(OH)_4] \tag{4.3}$$

According to the literature (Stumm and Morgan, 1970) $K$ is insensitive to pH variations up to a pH of about 9, and independent of pressure variations below pressures of 1000

atmospheres. Like most chemical reaction constants, however, it does depend on the (absolute) temperature $T$, and this temperature dependence satisfies an Arrhenius relation

$$K(T) = Ae^{-\frac{\Delta H_f}{RT}} \tag{4.4}$$

where $\Delta H_f$ is the enthalpy of formation of $Si(OH)_4$ with a value of 5500 cal/mol , $R$ is the universal gas constant, $T$ is the temperature (expressed in degrees Kelvin), while $A$ is a constant.

In view of (4.3) it would be reasonable to use the formula

$$Si_S(T) = A\exp[-\frac{\Delta H_f}{RT}] \tag{4.5}$$

for the temperature dependence of the saturation concentration $Si_S(T) = [Si(OH)_4]$ of orthosilicic acid in the water.

Under controlled laboratory conditions, $A$ should be a constant, as mentioned above. However, in a river water movement and turbidity as well as other chemical processes in the water might very well perturb the properties of the chemical equilibrium described by (4.3), and a value for $A$ should be found from actual measurements of dissolved silicon and temperature for various levels of turbidity (TUR) and the flow discharge $Q$ of the river at times when no significant diatom biomass is present. Table 4.1 shows such data, measured at various dates during 1986 and 1987 in the Vaal River at Balkfontein.

| T (° C) | Si $(10^{-3}Mol/L)$ | A $(Mol/L)$ | Q $(m^3/sec)$ | TUR $(NTU)$ | $Si^{proj}$ $(10^{-3}Mol/L)$ |
|---|---|---|---|---|---|
| 14 | 0.1204 | 1.856 | 15 | | 0.1234 |
| 23 | 0.17643 | 2.029 | 4 | 11 | 0.1654 |
| 20 | 0.14536 | 1.839 | 0.7 | 12 | 0.1503 |
| 10 | 0.112143 | 1.982 | 20 | 4 | 0.1076 |
| 20 | 0.14786 | 1.871 | 13 | 52 | 0.1503 |
| 24 | 0.168214 | 1.875 | 32 | 41 | 0.1707 |
| 26 | 0.17786 | 1.862 | 136 | 57 | 0.1816 |

Table 4.1: Values of $A$ calculated from Balkfontein measurements

In this table, Si is the measured orthosilisic acid concentration, $T$ the temperature, $Q$ the discharge, and TUR the turbidity. For each set of values of $T$ and Si, $A$ was calculated by means of the formula

$$A = \frac{\text{Si}}{\exp[-\Delta H_f/RT]}. \tag{4.6}$$

These results suggest that turbidity and flow do not have a significant influence on the value of $A$, and for the purposes of the model $A$ was therefore kept constant at the average value of the values shown in Table 4.1, namely

$$A(Q) = A = 1.902 \text{ Mol/L}. \tag{4.7}$$

Finally, using this value of $A$, the values $Si^{proj}$ were calculated by means of equation (4.5). These agree well with the measured values $Si$ in the first column of the table.

## 4.2 Modelling the diatom silicon absorption mechanism

According to numerous studies during the last two decades, the rate at which an individual diatom cell absorbs silicon, depends on the particular algal species, as well as the orthosilisic acid concentration in the immediate vicinity of the cell. This rate is usually a nonlinear increasing function of the orthosilisic concentration Si, tending to a constant level beyond a saturation value $Si^{cr}$ of Si. The growth rate drops to zero below a certain threshold value $Si^{min}$ of Si (Jorgensen, 1979).

In the model the rate of absorption of a single cell (or biomass unit) of the i-th (diatom) algal category is represented by the function

$$V_i = \begin{cases} V_{max_i} & \text{if } Si \geq Si_i^{cr} \\ V_{max_i} L(Si, Si_i^{cr}, Si_i^{min}) & \text{if } Si_i^{cr} > Si \geq Si_i^{min} \\ 0 & \text{if } Si < Si_i^{min} \end{cases} \tag{4.8}$$

where $V_{max_i}$ represents the maximum rate of silicon absorption for a particular diatom group, and where

$$L(Si, Si_i^{cr}, Si_i^{min}) = \frac{1 - e^{-\chi(Si - Si_i^{min})}}{1 - e^{-\chi(Si_i^{cr} - Si_i^{min})}}.$$

The tuning parameter $\chi$ is determined by fitting the expression for $V_i$ on actual experimental data.

The behaviour of the function $V_i$ is shown in Figure 4.2 for a realistic choice of the parameters (Werner, 1992).

Little information is available in the literature about the orders of magnitude of the parameters in the transfer function $L$. An overall estimate for the range of the maximum absorption rate is

$$V_{max_i} \in [10^{-1} - 10^{-5}] \quad \text{mg Si}(\mu\text{g chl-a.h})^{-1}.$$

Furthermore, field data seems to indicate that the following orders of magnitude for the remaining parameters would be acceptable (Roos, 1993):

$$\begin{aligned} Si^{cr} &\sim 2 \text{ mg Si/L} \\ Si^{min} &\sim 0.5 \text{ mg Si/L}. \end{aligned} \tag{4.9}$$

It should be noted that these values were extracted from a rather small set of experimental data and that a more intensive study is called for. In particular, the suggested order of magnitude of 0.5 mg Si/L for the threshold Si concentration is rather high and should probably be treated as an upper bound.

During model calibration, values of the parameters within these bounds are assigned by fitting the model output to experimental data.

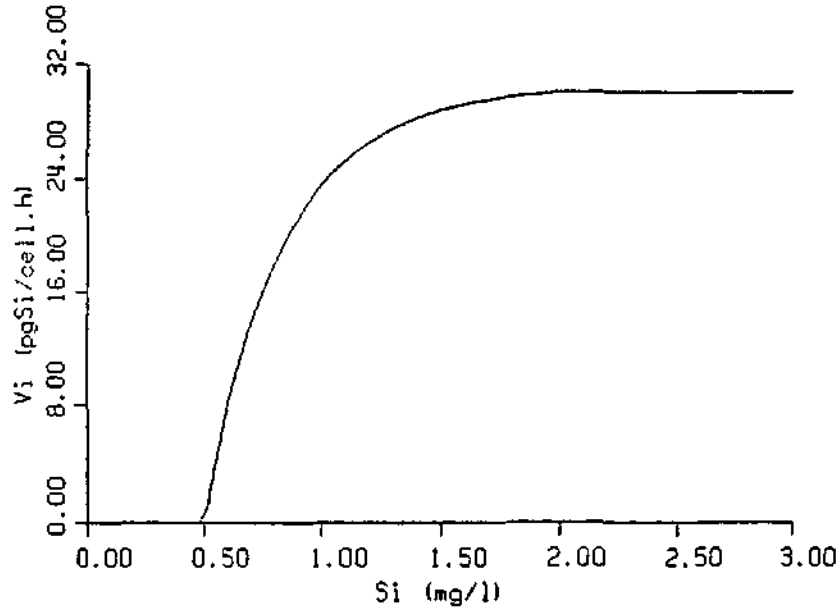


Figure 4.2: The absorption function $V_i$ with $V_{max_i}$ = 30 pg Si/(cell.h), $\mathrm{Si}_i^{cr}$ = 2 mg/L, $\mathrm{Si}_i^{min}$ = 0.5 mg/L and $\chi = 3$.

Equations (4.5) and (4.8) are now used in the following differential equation which models the variation of Si, the orthosilisic acid concentration in the water, due to both chemical processes in the water and absorption of silicon by diatoms:

$$\frac{d\mathrm{Si}}{dt} = k_{\mathrm{Si}}(\mathrm{Si}_S(T) - \mathrm{Si}) - \sum_{i=diatom} V_i x_{1i} \tag{4.10}$$

where only diatom algal groups are involved in the summation. The parameter $k_{\mathrm{Si}}$ is the inverse of the characteristic time of restitution for the orthosilisic acid concentration when no diatoms are present, and turns out to have a value of about 1/7 per day in the case of the Vaal river (i.e. a restitution time of about one week).

The final modification to model to include the effect of dissolved silicon, is to modify the expression for the growth rate $k_{G_i}$ defined in (3.10) in chapter 3 in the case of diatoms. Since metabolic activities and cell divisions are correlated, it was reasonable to make the assumption that the response of diatom growth rate would be similar to silicon absorption rate. Thus , when the i-th algal group consists of diatoms, the following modified formula is used for the growth rate:

$$k_{G_i}(I,T,\mathrm{Si}) = \begin{cases} k_{G_i}(I,T)L(\mathrm{Si},\tilde{\mathrm{Si}}_i^{cr},\tilde{\mathrm{Si}}_i^{min}) & \text{if } \tilde{\mathrm{Si}}_i^{cr} \geq \mathrm{Si} > \tilde{\mathrm{Si}}_i^{min} \\ k_{G_i}(I,T) & \text{if } \mathrm{Si} \geq \tilde{\mathrm{Si}}_i^{cr} \\ 0 & \text{if } \mathrm{Si} \leq \tilde{\mathrm{Si}}_i^{min}. \end{cases} \tag{4.11}$$

This function is quite similar to relation (4.8), with $k_{G_i}(I,T)$ the light-temperature growth rate defined in (3.10) in the previous chapter. The barred parameters in this formula are allowed to differ (usually only slightly) from the similar parameters in (4.8) to take into account the ability of most diatom species to absorb excess silicon and keep it in reserve for periods of silicon depletion (Werner, 1992).

## 4.3 Simulations with the updated model

With the modifications for silicon absorption by diatoms in place, the model at this stage consists of $2N+1$ coupled nonlinear differential equations, namely

$$\begin{aligned} \dot{x}_{1_i} &= [-k_{D_i} + k_{S_i}) + k_{G_i}(I,T,\mathrm{Si})]x_{1_i} \\ \dot{x}_{2_i} &= k_{D_i}x_{1_i} - k_{S_i}x_{2_i} \\ \dot{\mathrm{Si}} &= k_{\mathrm{Si}}(\mathrm{Si}_S(T) - \mathrm{Si}) - \sum_{i=diatom} V_i x_{1i} \end{aligned} \tag{4.12}$$

where the dots indicate differentiation with respect to time.

In order to show the effect of the added module, the simulations of the winter algal blooms at Stilfontein during 1985 and 1986, reported in chapter 3, were repeated with the updated model. As mentioned earlier, the first winter blooms are usually caused by diatoms, and the later ones by green algae. Thus, in the model, one algal category was assumed to consist of diatoms (i.e. requiring silicon) and the other to consist of other algae. Table 4.2 shows the calibrated values of the parameters in the model. Note that

| | 1985 | | 1986 | |
|---|---|---|---|---|
| Parameter | diatom | non-diat. | diatom | non-diat. |
| $k_G$ | 1.43 | 1.68 | 1.28 | 1.40 |
| $k_D$ | 0.15 | 0.15 | 0.15 | 0.15 |
| $I_{opt}$ | 0.12 | 0.075 | 0.12 | 0.08 |
| $T_{opt}$ | 11 | 15 | 10 | 13 |
| $T_{min}$ | 0 | 5 | 0 | 5 |
| $Si_{up}^{cr}$ | 2 | | 2 | |
| $Si_{up}^{min}$ | 0.5 | | 0.5 | |
| $V_{max}$ | 0.007 | | 0.01 | |
| $Si_G^{cr}$ | 1 | | 1 | |
| $Si_G^{min}$ | 0.5 | | 0.5 | |

Table 4.2: Calibrated parameters for the light-temperature-silicon model

the light-temperature parameters are exactly the same as in Table 3.3.

The results of the simulations are shown in Figure 4.3a-b for the winter periods of 1985 and 1986, respectively. Comparison with the results of the previous simulations shown in Figures 3.12 and 3.13, shows a significant improvement in the correspondence between simulated and measured values.

Figure 4.4a-b shows the diatom growth rate, and Figure 4.5a-b the dissolved silicon concentration, both computed by the model, during the 1985 and 1986 winter algal blooms. Note that at low levels of the diatom biomass, dissolved silicon depletion due to diatom absorption is more or less balanced by silicon production, so that the dissolved silicon concentration remains at or slightly above the saturated value, and the diatom growth rate is the same than when calculated without the silicon mechanism. At higher diatom concentrations, the balance can no longer be maintained, and silicon depletion occurs to such an extent that it becomes a limiting factor for growth.

Thus the silicon module seems to perform adequately. However, the simulations reported in this chapter still show some discrepancies between simulated and measured values of chlorophyll-*a* concentration which can not be explained solely by the silicon effect.

In the following chapters it will be shown how the addition of more modules, involving other factors, will further improve model performance.

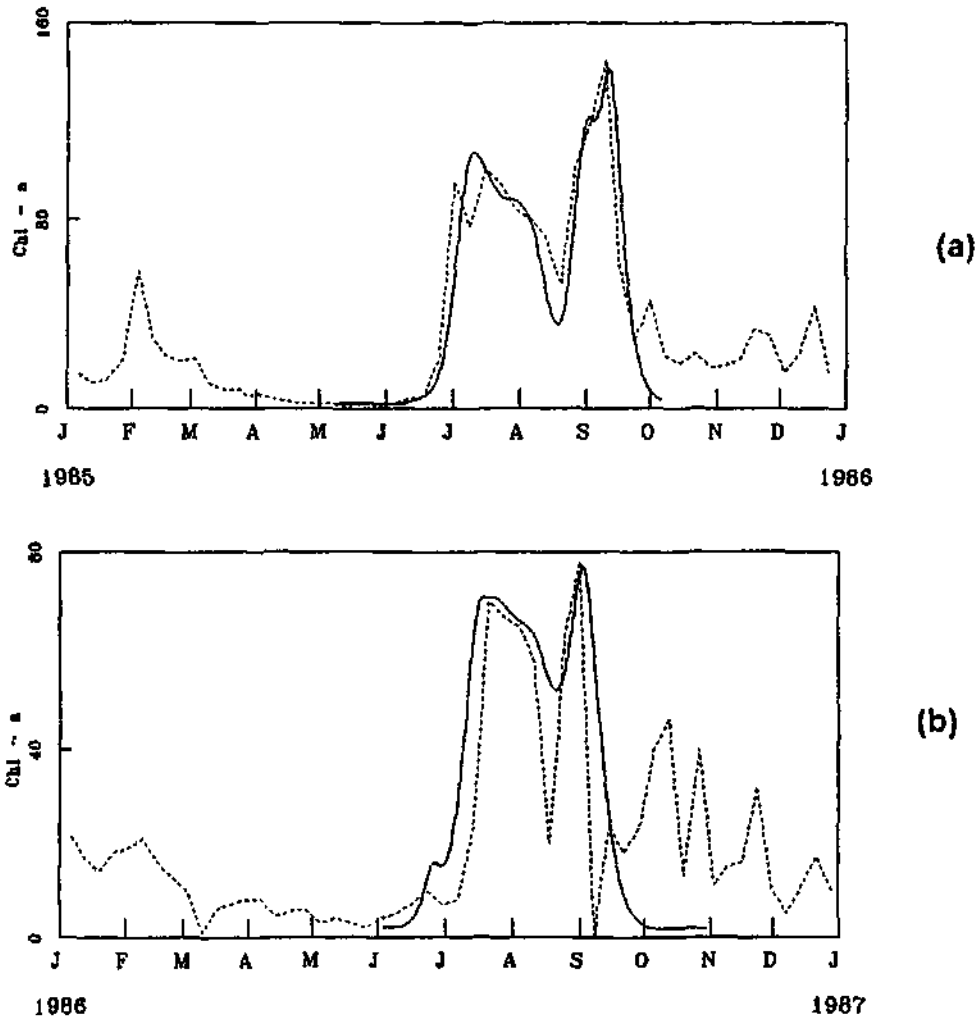


Figure 4.3: Comparison between computed (solid line) and observed data (dashed line) for the winter period: (a) 1985; (b) 1986, when the silicon absorption by diatoms is taken into account.

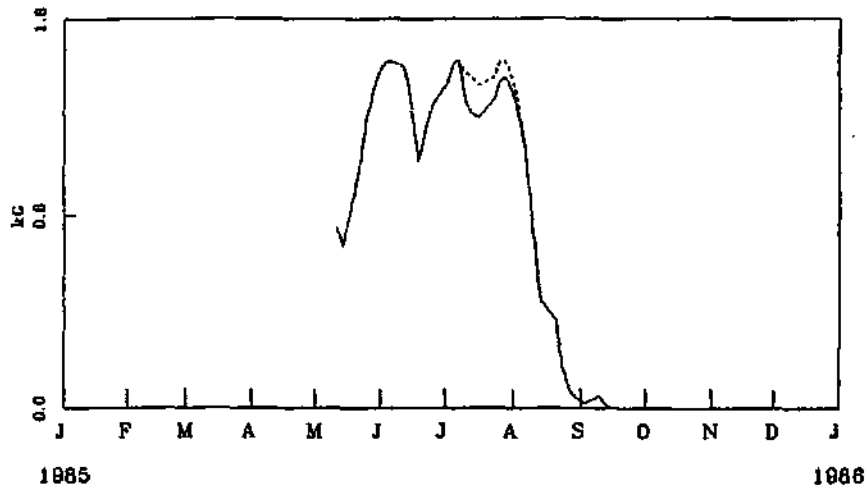


(a)

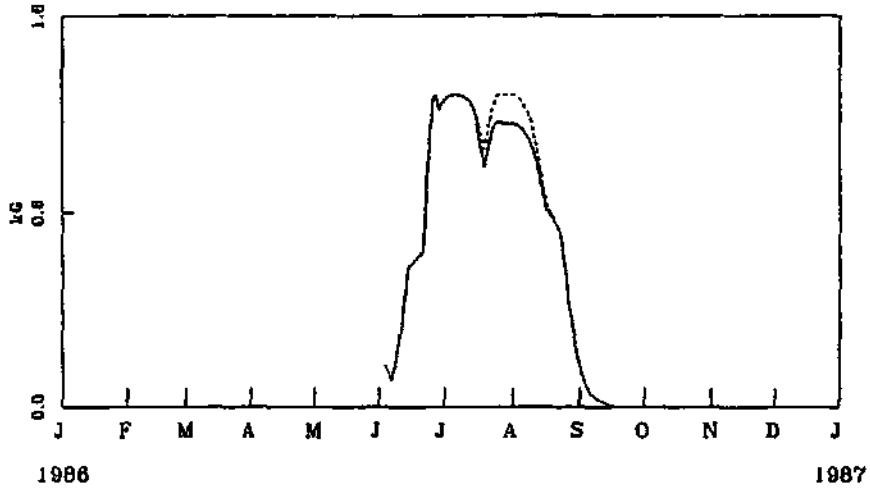


(b)

Figure 4.4: Computed values of the growth coefficient of the diatoms for the years (a): 1985; (b): 1986, assuming that either Si does not affect this coefficient (dashed line) or otherwise (solid line). Note that most of the time solid (Si) and dashed lines (no Si) overlap.

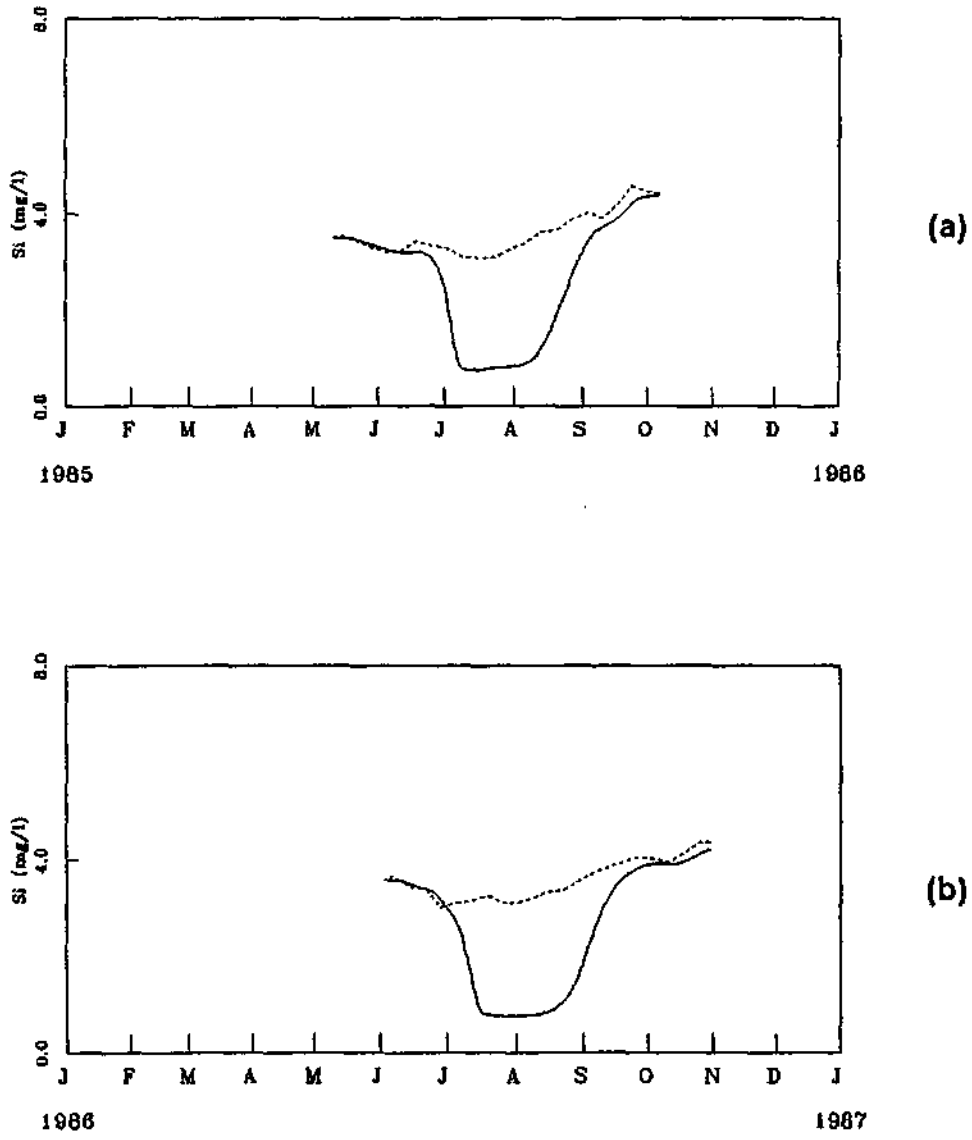


Figure 4.5: Values of dissolved Si concentration during the winter algal blooms as computed by the model: (a): 1985; (b): 1986. The dashed line represents the saturation concentration reachable in absence of diatom growth while, the solid line represents dissolved Si curve as computed by the model.

# Chapter 5

# The interaction between algae and basic nutrients

In this chapter it is shown how the effect of nutrient levels (besides dissolved silicon, which was discussed in the previous section) on algal growth is incorporated in the model. Only macro-elements were considered, under the assumption that since algae need very small amounts of the micro-elements (or trace elements), these will never be limiting factors.

The most significant macro-elements necessary for algal growth in the Vaal river context, are nitrogen and phosphorus in the form of chemical compounds such as ammonium, nitrates and phosphates. These nutrients are vital requirements for the photosynthetic process inside algal cells, which in its turn produces energy and the basic materials necessary for algal development and growth.

Thus the next module to incorporate in the model is one which describes the mechanism by which nutrient levels affects photosynthesis and algal growth. This will be described in the rest of this chapter, and some attention will also be given to an analysis of the effect which algal photosynthesis could have on nutrient levels in its turn.

## 5.1 The effect of nutrient levels on photosynthesis and algal growth

The process of photosynthesis of algae in a river can be viewed at a macro level (i.e. the behaviour of an assemblage of algae rather than individual algal cells), in which case the following equation would be appropriate to describe the process:

$$106CO_2 + 16NO_3^- + HPO_4^{2-} + 122H_2O + 18H^+$$

$$+TraceElements \xrightarrow{I,T} C_{106}H_{263}O_{110}N_{16}P + 138O_2 \qquad (5.1)$$

The rate of photosynthesis do not only depend on dissolved nitrate and phosphate concentrations in the water, but also on under water light climate and water temperature. In chapter 3 the effect of light and temperature on algal growth was described mathematically, but this still has to be done for photosynthetic activity. Some studies on the effect of light and temperature on photosynthetic activity is reported in Wetzel (1983), and some of the results of these are reproduced in Figure 5.1a-b.

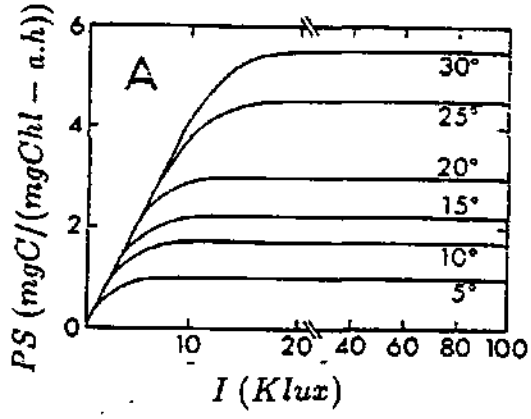


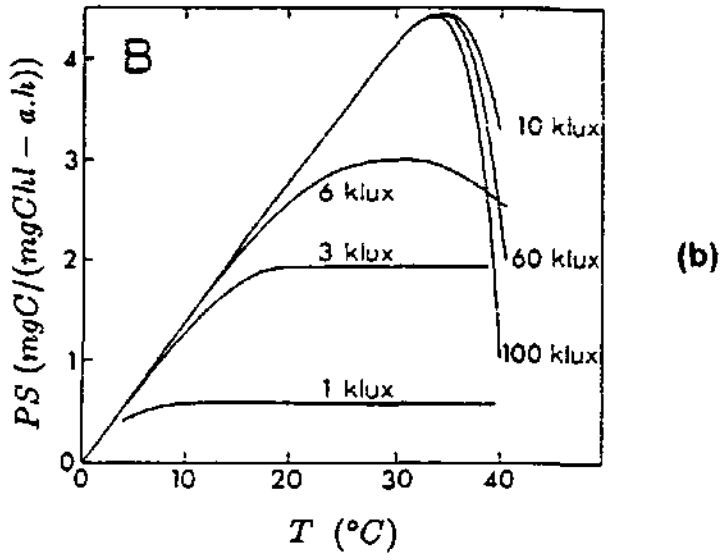


Figure 5.1: The dependence of photosynthetic activity on (a) variations in under water light intensity at constant temperatures, and (b) variations in water temperature at constant under water light intensities (from Wetzel (1983)).

This figure shows that the response of photosynthetic activity to variations in light and temperature is not unlike that of the growth rate $k_G$, discussed in the previous two chapters. However, unlike the growth rate, the initial slope of the graph of photosynthesis *versus* light intensity does not depend on the temperature. The following formula for the rate of photosynthesis $PS(I,T)$ was devised:

$$PS(I,T) = PS_{max} f(T)(1 - e^{-\frac{\chi_{PS} I}{f(T)}}) Inhib(I) \tag{5.2}$$

with

$$f(T) = (\frac{T}{T_{PS}^{opt}})^{1.5} e^{(1-(\frac{T}{T_{PS}^{opt}})^{1.5})}$$

and

$$Inhib(I) = \begin{cases} 1 & \text{if } I < I_{Inhib} \\ g e^{1-g} & \text{if } I \geq I_{Inhib} \end{cases}$$

where

$$g = \frac{I}{I_{Inhib}} .$$

This relation contains four new parameters, namely:

| | | |
|---|---|---|
| $T_{PS}^{opt}$ | : | the optimal temperature for photosynthesis |
| $PS_{max}$ | : | the overall maximum photosynthetic rate |
| $I_{Inhib}$ | : | the inhibiting light intensity for photosynthesis |
| $\chi_{PS} = \frac{1}{PS_{max}} \frac{dPS}{dI}\|_{I=0}$ | : | the slope of the photosynthetic rate vs. light intensity curve at the origin. |

The relation (5.2) is graphed in Figures 5.2 and 5.3 for various values of temperature and light intensity, and with realistic values for the parameters in the formula. A comparison with the measured values displayed in Figure 5.1 shows that (5.2) is able to simulate the response of photosynthetic activity to light and temperature variations quite well.

As stated above, both photosynthetic rate and growth rate also depend on concentrations of dissolved nutrients. When these concentrations are sufficiently high, they are not limiting factors for algal growth. Under such conditions the light-temperature-silicon model described in the previous sections would be quite effective. However, when the nutrient concentrations drop below certain levels (which vary from algal species to algal species) both growth and photosynthetic rates decrease. It should also be noted that it is not only concentrations of phosphates and nitrates which have to be taken into account. The ratio between nitrate and phosphate concentrations (henceforth referred to as the $N/P$ ratio, or simply as $N/P$ in formulas) is an important parameter in its own right. In fact, a typical algal species would have a particular optimal value of this ratio, $(N/P)^{opt}$, for which growth and photosynthetic rates are optimal.

To include the effects of nutrients, the photosynthetic rate (5.2) as well as the growth rate $k_{G_i}(I,T,\mathrm{Si})$ defined in (4.11) are multiplied by a transfer function $r_i(N,P,N/P)$ to yield the updated rates

$$k_{G_i}(I,T,\mathrm{Si},N,P,N/P) = r_i(N,P,N/P) k_{G_i}(I,T,\mathrm{Si}) \tag{5.3}$$

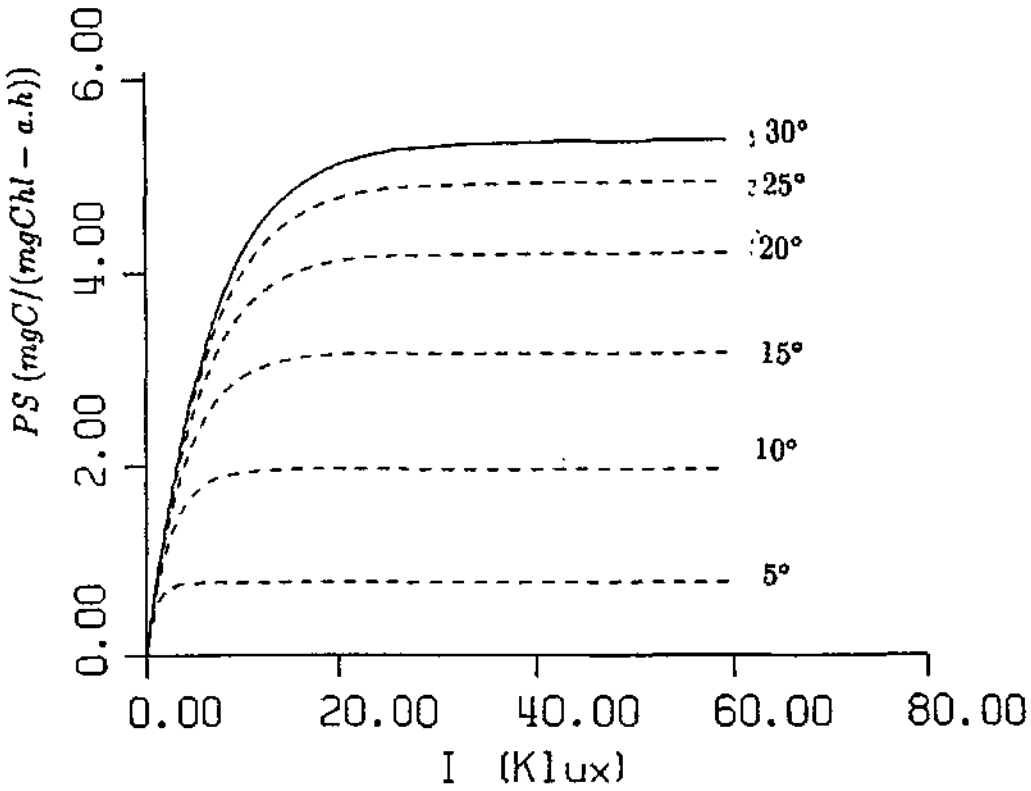


Figure 5.2: Relation between rate of photosynthesis and variations in light intensity for different constant temperatures, calculated with (5.2).

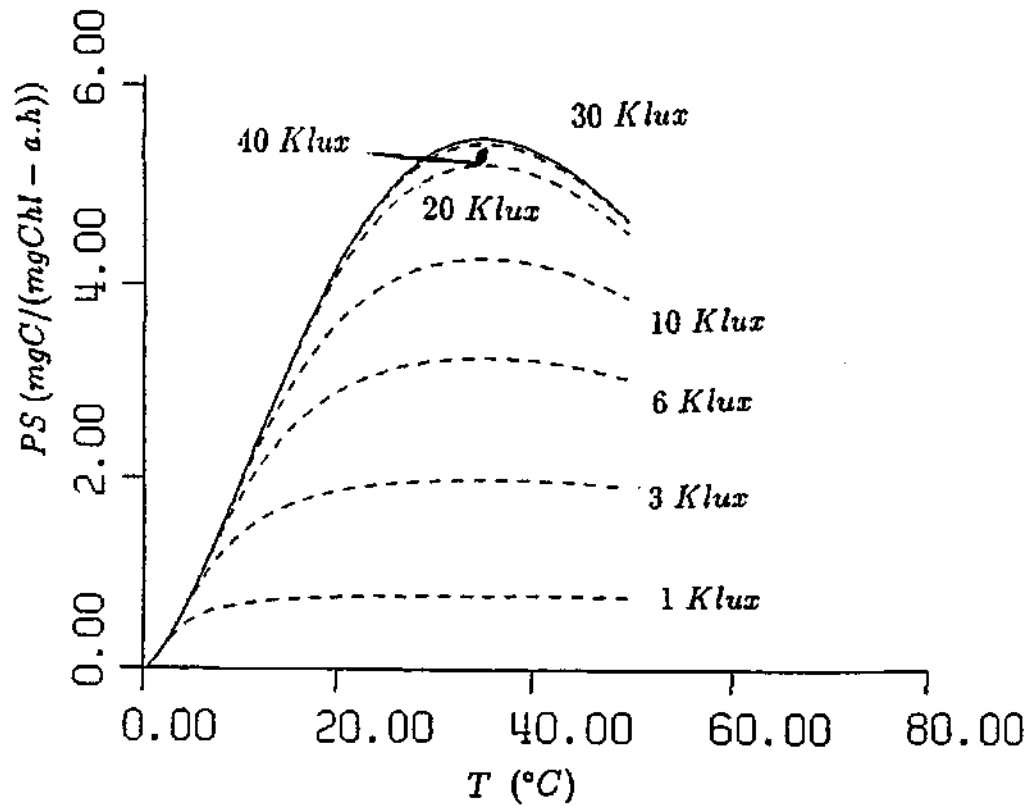


Figure 5.3: Relation between rate of photosynthesis and variations in temperature for different constant light intensities, calculated with (5.2).

and

$$PS_i(I,T,N,P,N/P) = r_i(N,P,N/P)PS(I,T) \tag{5.4}$$

where

$$r_i(N,P,N/P) = (1-e^{-\chi_{N_i}[N]})(1-e^{-\chi_{P_i}[P]})f_i(N/P)\frac{(1-e^{-\frac{\chi_{(N/P)_i}}{f_i(N/P)}})}{(1-e^{-\chi_{(N/P)_i}})} \tag{5.5}$$

with

$$f_i(N/P) = (\frac{N/P}{(N/P)_i^{opt}})^n e^{1-(\frac{N/P}{(N/P)_i^{opt}})^n} \tag{5.6}$$

As usual, the subscript $i$ refer to properties of the i-th algal group, $(N/P)_i$ is the optimal $(n/P)$ ratio, $n$ is a tuning parameter, and $\chi_{N_i}$ and $\chi_{P_i}$ are dispersion factors of the form

$$\chi_{N_i} = \frac{4}{N_{sat_i}}, \quad \text{and} \quad \chi_{P_i} = \frac{4}{P_{sat_i}} \tag{5.7}$$

where $N_{sat_i}$ and $P_{sat_i}$ are saturation concentrations for nitrates and phosphates above which these nutrients are not limiting factors for growth. $[N]$ and $[P]$ are of course the nitrate and phosphate concentrations respectively, and $N/P$ the $N/P$ ratio. The parameter $\chi_{(N/P)_i}$ is a dispersion coefficient for the $N/P$ ratio. It is one of the free parameters in the model, which is assigned a value when fitting model output on to algal biomass data. It is interesting to note also that though $\chi_{(N/P)_i}$ is algae specific, i.e. varies significantly for different algal categories, this does not really seem true for $\chi_{N_i}$ and $\chi_{P_i}$ (although we left open the possibility).

A three dimensional representation of the transfer function (5.5) is shown in Figure 5.4.

The model equations (4.12) are thus now updated to (5.4) together with the coupled system of differential equations:

$$\begin{aligned}
\dot{x}_{1_i} &= [-k_{D_i} + k_{S_i}) + k_{G_i}(I,T,\mathrm{Si},N,P,N/P)]x_{1_i} \\
\dot{x}_{2_i} &= k_{D_i}x_{1_i} - k_{S_i}x_{2_i} \\
\dot{\mathrm{Si}} &= k_{\mathrm{Si}}(\mathrm{Si}_S(T) - \mathrm{Si}) - \sum_{i=diatom} V_i x_{1i}.
\end{aligned} \tag{5.8}$$

A schematic representation of the model up to this point is shown in Figure 5.5.

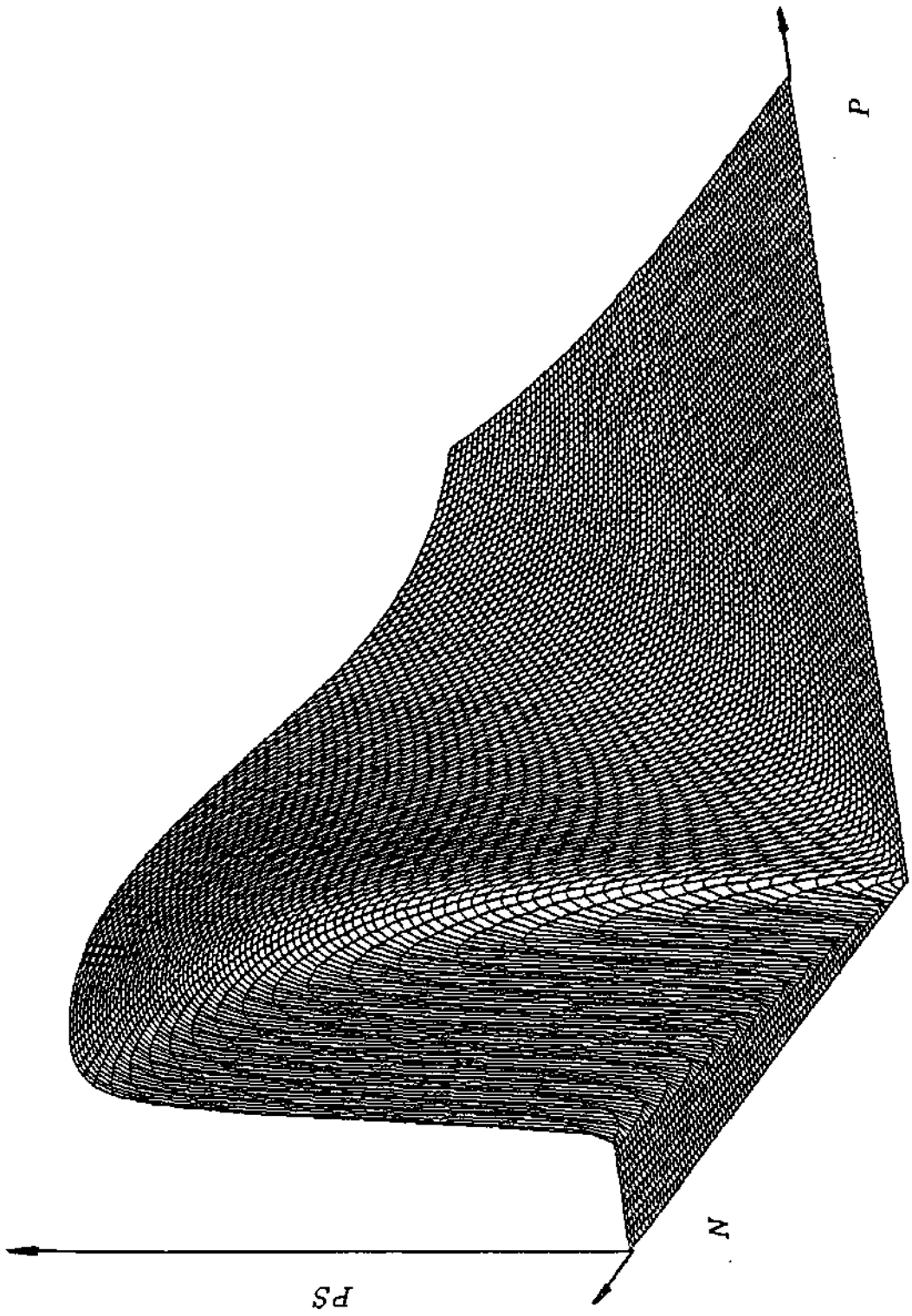


Figure 5.4: The transfer function (5.5), with $N^{sat} = 0.17mg/L$, $P^{sat} = 0.026mg/L$ and $(N/P)^{opt} = 4$.

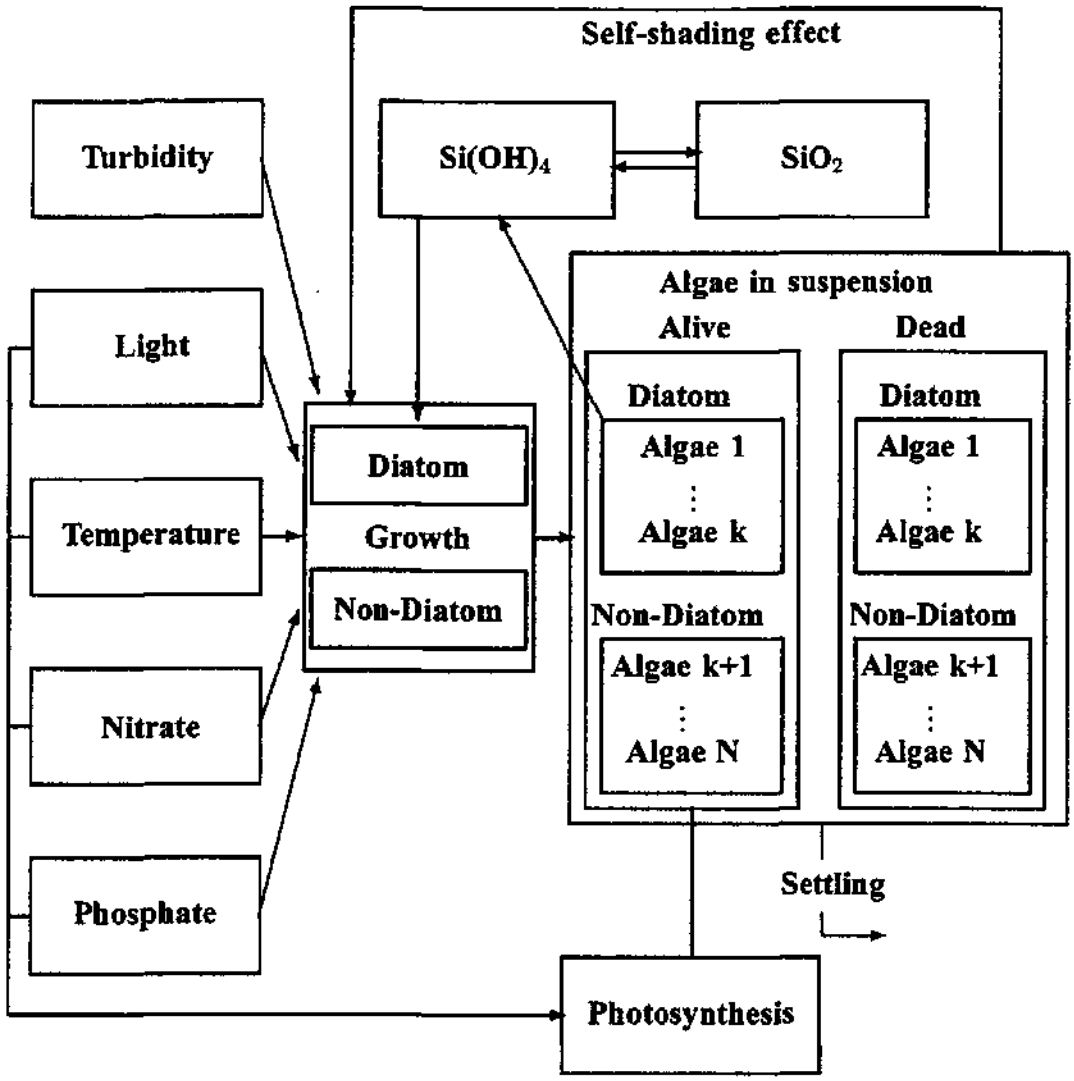


Figure 5.5: Schematic representation of the model including the effects of light, temperature, dissolved silicon and dissolved nutrient concentrations.

## 5.2 Simulating the Stilfontein winter algal blooms with nutrient effects included.

At this point the reader is referred back to Figure 4.3a, showing the simulation of the winter algal blooms of 1985 at Stilfontein, using the light-temperature-silicon model (henceforth referred to as the LTS model). The first major bloom, with a duration from late June to about middle August, has an oscillation in the measured values which the LTS model was unable to simulate. This failure of the LTS model was due to the fact that it was based on the assumption that the river is eutrophic at all times, i.e. that nutrients are never limiting factors to growth.

Figures 5.6 through 5.8 show the concentration levels for dissolved nitrogen (nitrates and ammonium) and phosphates, as well as the $N/P$ ratio measured at Stilfontein during 1985. In the Vaal River, average saturation values for dissolved nitrogen and phosphates were found to be 0.18 mg/L and 0.026 mg/L (Pieterse and Toerien, 1978). Figure 5.6 and 5.7 show concentration levels of these nutrients well above this. This makes it unlikely that the sharp deviation between observed and simulated chlorophyll-*a* values was caused by a shortage of the nutrients as such. However, Figure 5.8 shows very sharp variations of the $N/P$ ratio, which seems to be the cause of the discrepancy. In fact, it can be observed that the $N/P$ ratio has an oscillation during the first winter algal bloom which corresponds with the oscillation in the chlorophyll-*a* profile which the LTS model failed to simulate. A careful study of Figure 5.8 suggested that the first algal bloom should not be seen as due to one diatom group of algae, but rather by two, which respond similarly to variations in light, temperature and dissolved silicon concentration, but have optimal $N/P$ rations which differ significantly.

This hypothesis was tested by resimulating the 1985 winter algal blooms, using the updated model (5.8) with three algal groups, of which two were considered to be diatoms. The two diatom groups were assigned the same light, temperature and silicon parameters, but the optimal $N/P$ ratios were taken to be equal to $(N/P)_{opt} = 20$ and 13 for algal (diatom) groups 1 and 2 respectively. The other parameters were basically those displayed in Table 4.2. Figure 5.9 shows the results of this simulation, which does now pick up the oscillation in chlorophyll-*a* which the LTS-simulation couldn't. This oscillation was indeed due to a nutrient effect.

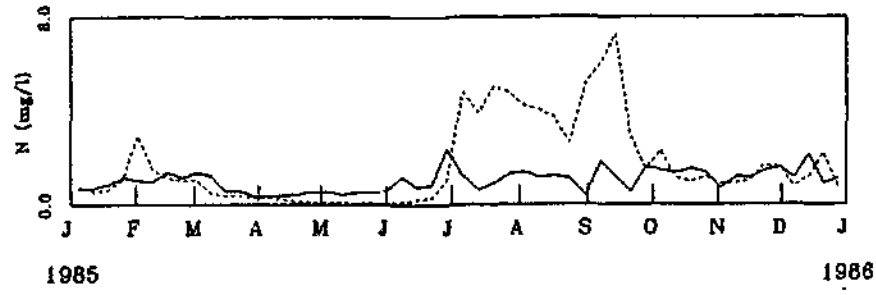


Figure 5.6: Total nitrogen concentrations measured at Stilfontein during 1985 (solid line). The chlorophyll-*a* profile (dashed line) is also shown for comparison purposes (values are not to scale).

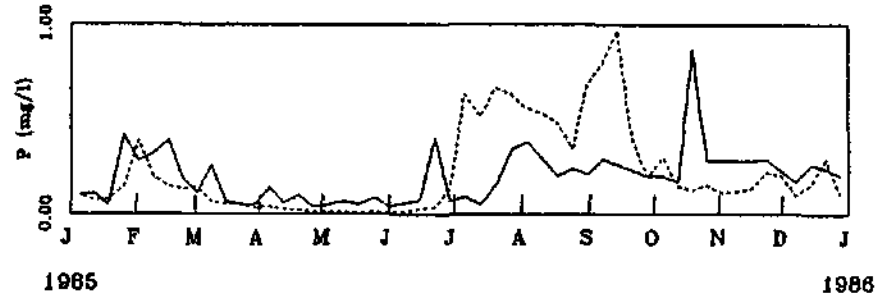


Figure 5.7: Dissolved phosphate concentrations measured at Stilfontein during 1985 (solid line). The chlorophyll-*a* profile (dashed line) is also shown for comparison purposes (values are not to scale).

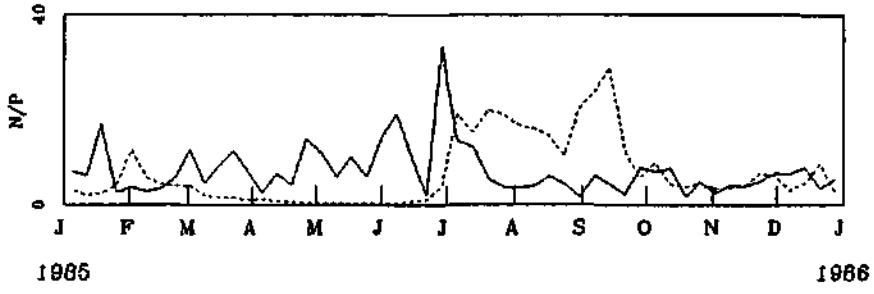


Figure 5.8: The $N/P$ ratio at Stilfontein during 1985 (solid line). The chlorophyll-*a* profile (dashed line) is also shown for comparison purposes (values are not to scale).

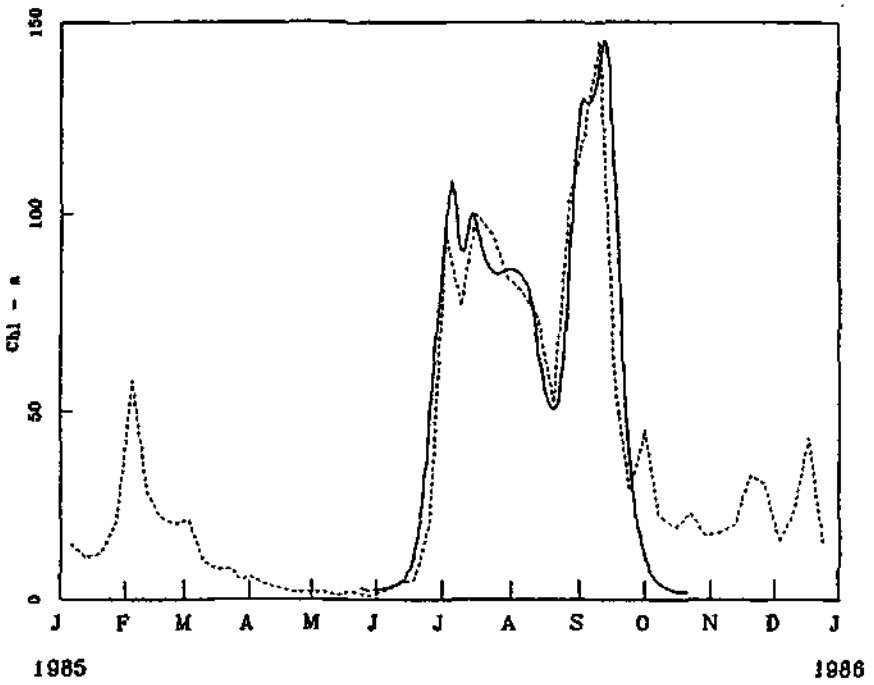


Figure 5.9: Comparison between simulated values (solid line) and on site measurements (dashed line) for the winter algal blooms at Stilfontein, 1985. The effects of variations in light, temperature, silicon and nutrient availability are all taken into account.

## 5.3 Simulating algal growth over one full year

Even though the updated model (5.8) is still based on the hypothesis that river flow is steady, it is sufficiently sophisticated to simulate algal growth over periods of more than a few weeks. This subsection describes a simulation of algal growth at Stilfontein over the full year of 1985.

Based on available data for chlorophyll-*a*, water temperature, turbidity, and phosphate and nitrogen concentration, six algal groups were identified, with parameter values as shown in Table 5.1.

The results of this simulation are shown in Figures 5.10 through 5.16. Figure 5.10 shows a comparison between measured and simulated chlorophyll-*a* values, and in Figures 5.11 through 5.16 a breakdown is given of the extent to which each algal group contributed to the total algal biomass.

The first three algal groups are those which were used in the simulation of the winter blooms described in subsection 5.2. Figures 5.11 through 5.13 show to which extent each of these were involved in those blooms.

| | Alga 1 | Alga 2 | Alga 3 | Alga 4 | Alga 5 | Alga 6 |
|---|---|---|---|---|---|---|
| $k_{G_{opt}}$ $(Day^{-1})$ | 1.4 | 1.4 | 1.54 | 1.8 | 1.5 | 1.8 |
| Opt. temperature $(°C)$ | 11 | 11 | 15 | 25 | 20 | 25 |
| Min. temperature $(°C)$ | 0 | 0 | 5 | 10 | 10 | 10 |
| Opt. light $(cal.(cm^2.min)^{-1})$ | 0.115 | 0.115 | 0.075 | 0.22 | 0.06 | 0.01 |
| Sat. N $(mgN)$ | 0.17 | 0.17 | 0.17 | 0.17 | 0.17 | 0.17 |
| Sat. P $(mgP)$ | 0.026 | 0.026 | 0.026 | 0.026 | 0.026 | 0.026 |
| Opt. N/P $(mgN.(mgP)^{-1})$ | 20 | 13 | 5 | 5 | 3 | 5 |

Table 5.1: Basic parameter set for the 6 algal categories.

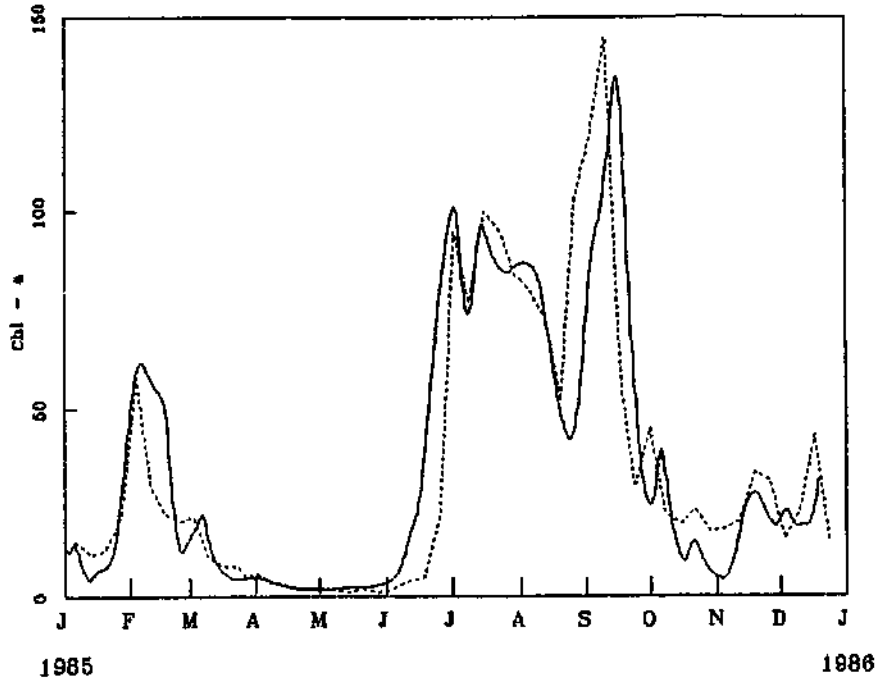


Figure 5.10: Comparison between simulated (solid line) and measured (dashed line) chlorophyll-*a* values for the full year of 1985, at Stilfontein.

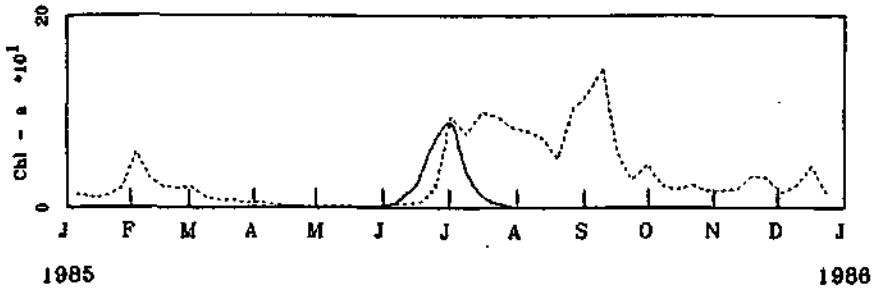


Figure 5.11: Computed contribution of algal group 1 (solid line) towards the total chlorophyll-*a* profile for 1985, at Stilfontein. The measured total chlorophyll-*a* is also shown as a dashed line.

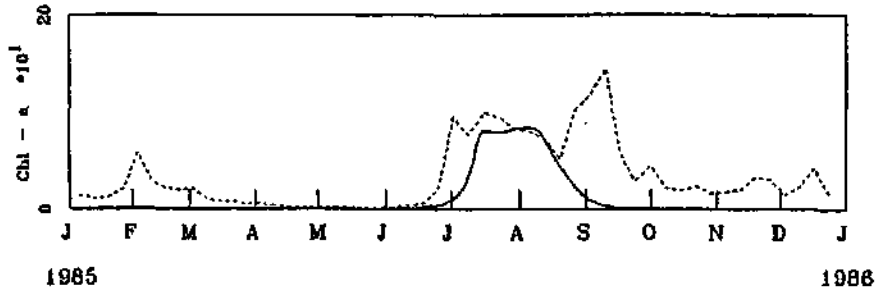


Figure 5.12: Computed contribution of algal group 2 (solid line) towards the total chlorophyll-*a* profile for 1985, at Stilfontein. The measured total chlorophyll-*a* is also shown as a dashed line.

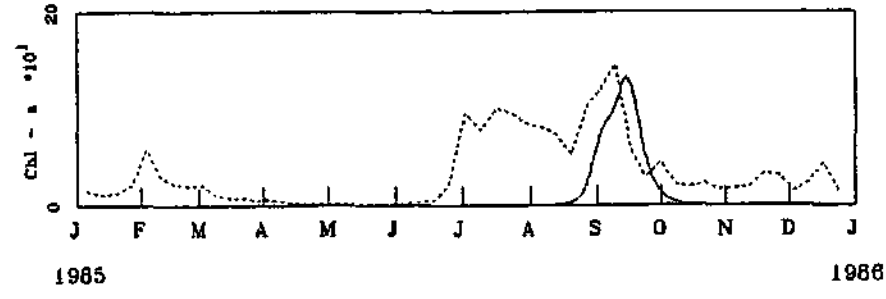


Figure 5.13: Computed contribution of algal group 3 (solid line) towards the total chlorophyll-*a* profile for 1985, at Stilfontein. The measured total chlorophyll-*a* is also shown as a dashed line.

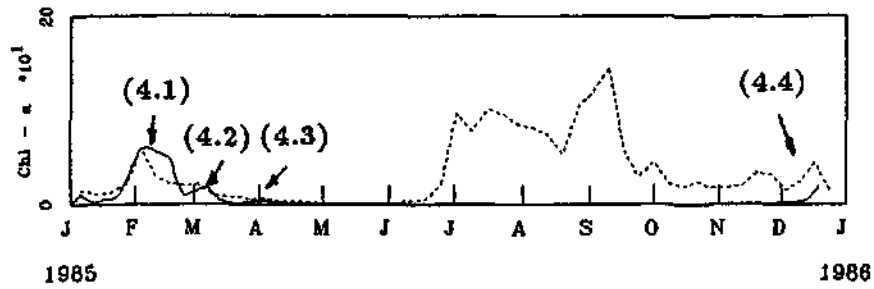


Figure 5.14: Computed contribution of algal group 4 (solid line) towards the total chlorophyll-*a* profile for 1985, at Stilfontein. The measured total chlorophyll-*a* is also shown as a dashed line.

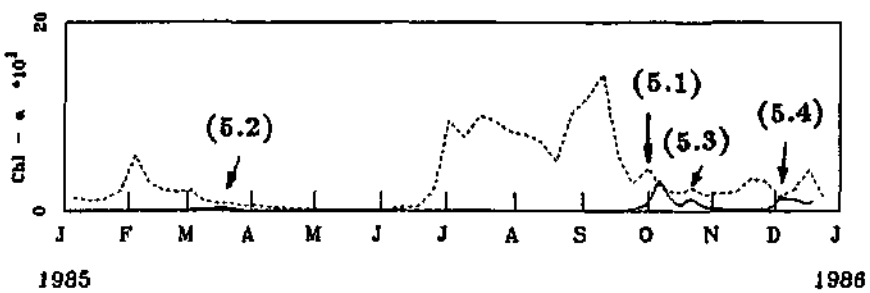


Figure 5.15: Computed contribution of algal group 5 (solid line) towards the total chlorophyll-*a* profile for 1985, at Stilfontein. The measured total chlorophyll-*a* is also shown as a dashed line.

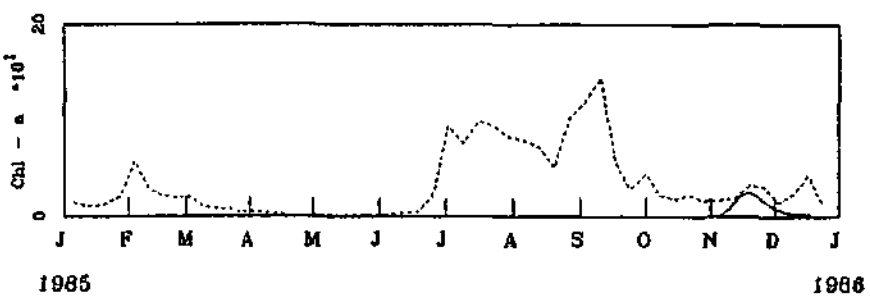


Figure 5.16: Computed contribution of algal group 6 (solid line) towards the total chlorophyll-*a* profile for 1985, at Stilfontein. The measured total chlorophyll-*a* is also shown as a dashed line.

Figure 5.14 shows the contribution of the fourth algal group. It is seen to be strongly involved in three blooms in summer (see points 4.1, 4.2 and 4.3) as well as a bloom in the early summer period (point 4.4). In Figure 5.15 it is seen that the fifth algal group was involved in the algal bloom in September/October (point 5.1), and was also responsible for the smaller peak in October (point 5.3). This algal group also showed up in March (5.2). It combined with the fourth algal group during the bloom in the early summer (5.4). The sixth algal group was only involved during an algal bloom in November, and was never present at significant levels at any other time during the year (Figure 5.16).

So far the effect of algal growth and photosynthesis on the concentrations of nutrients in the water have not been taken into account. The rest of this chapter is devoted to a discussion of some aspects of the influence of algal activities on the environment.

## 5.4 Elementary analysis of the influence of algal blooms on the composition of the water body

In chapter 4 the effect of silicon absorption by diatoms on the dissolved silicon concentration was modellled by equation (4.10). In this section the effect of any type of algae on its environment will be modelled.

Referring again to the chemical equation (5.1) describing photosynthesis, it is fairly obvious that this process would be inclined to change the concentrations of certain chemical substances in the water, as well as the ratios between such substances. In the rest of this section we will first model the effect of photosynthesis on the concentrations of dissolved carbon dioxide and oxygen, and after that we will consider the interaction between photosynthesis and dissolved macro nutrients.

### 5.4.1 The effect of photosynthesis on concentrations of dissolved carbon dioxide and oxygen.

The photosynthetic activity of a given algal species is most often quantified by measuring its rate of $CO_2$ absorption. It would therefore be reasonable to expect that in a river the concentration of dissolved $CO_2$ in the water would be a fundamental parameter to be measured in order to monitor algal photosynthesis. Unfortunately such measurements are not readily available, and as far as we know, this is also true for the Vaal River. One way to get around this, is to consider the effect which dissolved $CO_2$ might have on other, more accessible factors. One possibility is to consider the $pH$ of the water. In general it is very difficult to model the $pH$ of the water in a natural system like a river accurately. However, it is usually possible to make certain simplifying assumptions which would still enable a useful simulation of $pH$ variations. In the case of the Vaal River, studies like those reported by Roos (1992) have indicated that the ionic composition of the water is dominated by sulfate ions ( $SO_4^{2-}$) and calcium ions ( $Ca^{2+}$). A graph of

*pH* values against the sulfate concentration at Stilfontein for the years 1985 through 1987 does not reveal a significant correlation between these two factors (Figure 5.17), and it seems reasonable to disregard, at least as a first approximation, the effect of sulfate ions on pH variations (at least for this site, and for the time period 1985-1987).

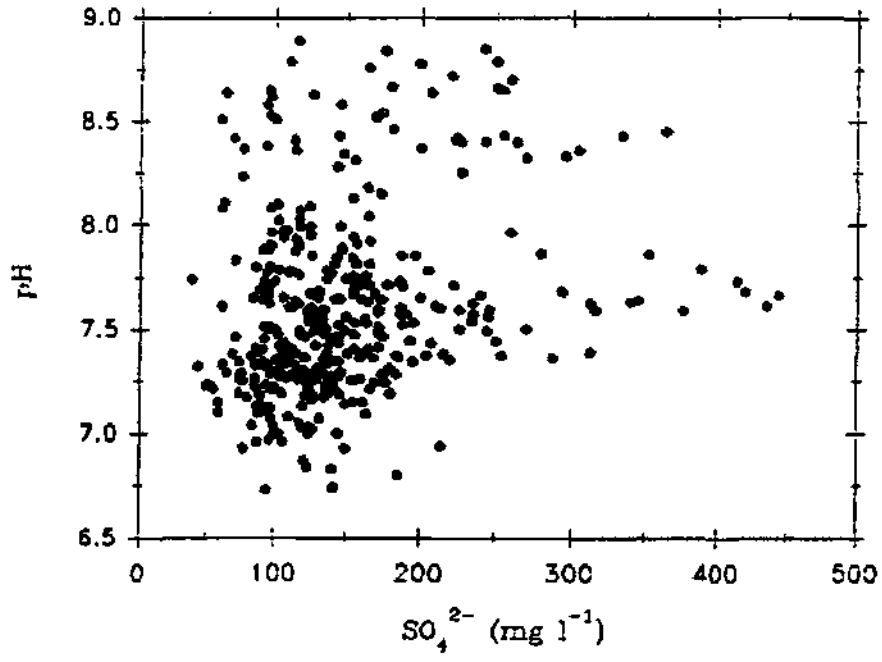


Figure 5.17: *pH versus* sulfate concentration for the years 1985-87 at Stilfontein.

Thus the following calcium-carbonate system was considered in order to model *pH* variations:

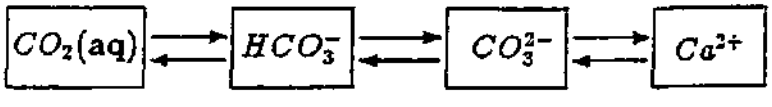


Figure 5.18: The calcium-carbonate system considered in this report.

In this scheme each arrow represents a chemical reaction with a characteristic equilibrium

which is temperature dependent. More precisely, we have:

$$\begin{array}{lcll} CO_{2_{aq}} & \rightleftharpoons & H_2CO_3 & K_{H_2CO_3}(T) = \frac{[H_2CO_3]}{[CO_{2_{aq}}]} \\ H_2CO_3 & \rightleftharpoons & H^+ + HCO_3^- & K_{HCO_3^-}(T) = \frac{[H^+][HCO_3^-]}{[H_2CO_3]} \\ HCO_3^- & \rightleftharpoons & H^+ + CO_3^{2-} & K_{CO_3^{2-}}(T) = \frac{[H^+][CO_3^{2-}]}{[HCO_3^-]} \\ CaCO_{3_S} & \rightleftharpoons & Ca^{2+} + CO_3^{2-} & K_{Ca2+}(T) = [Ca^{2+}][CO_3^{2-}] \\ H_2O & \rightleftharpoons & H^+ + OH^- & K_{H^+}(T) = [H^+][OH^-] \end{array} \tag{5.9}$$

where $K_x(T)$ denotes the equilibrium associated with $x$ and $[x]$ denotes the concentration of substance $x$. The specific values for the different equilibrium constants may be found in Stumm and Morgan (1970), Garrels and Christ (1965). Furthermore, if we make use of the ionic balance

$$2[Ca^{2+}] + [H^+] = [HCO_3^-] + 2[CO_3^{2-}] + [OH^-]$$

we end up at the following relation between pH and dissolved $CO_2$ concentration

$$h^4 + a_0 h^3 + a_1 h = a_2 \tag{5.10}$$

where

$$\begin{aligned} a_0 &= 0.0003\alpha \frac{\gamma_{Ca^{2+}}}{\gamma_{H^+}^2} e^{(7.45 - \frac{11422}{RT})}, \\ a_1 &= -0.0003\alpha \frac{\gamma_{Ca^{2+}}}{\gamma_{H^+}^3} \left(\frac{\alpha}{\gamma_{HCO_3^-}} + e^{(13.04 - \frac{11338}{RT})} \frac{1}{\gamma_{OH^-}}\right) e^{(24.54 - \frac{13838}{RT})}, \\ a_2 &= -0.0003\alpha^2 \frac{\gamma_{Ca^{2+}}}{\gamma_{CO_3}^2 \gamma_{H^+}^4} e^{(27.96 - \frac{17953}{RT})}, \end{aligned} \tag{5.11}$$

and where

$$\begin{aligned} h &= 10^{8.5}[H^+] \\ \alpha &= 10^5[CO_2] \end{aligned}$$

A parameter $\gamma_i$ denotes the activity of chemical substance $i$, and is defined by

$$-\log_{10} \gamma_i = \frac{A z_i^2 \sqrt{I}}{1 + B b_i \sqrt{I}},$$

where

$$\begin{aligned} A &= 0.81325 e^{-\frac{278}{RT}} \\ B &= 0.37467 e^{-\frac{78.6}{RT}}, \end{aligned} \tag{5.12}$$

and $z_i$ is the number of electrical charges carried by the ion $i$. $I$ is the ionic strength of the solution, defined by

$$I = \frac{1}{2}\{4[Ca^{2+}] + [H^+] + 4[CO_3^{2-}] + [HCO_3^-] + [OH^-]\},$$

and the coefficients $b_i$ are characteristic of the chemical substances concerned. Explicit values of these coefficients may be found in Garrels and Christ (1965). Thus, for a given value of the dissolved concentration of $CO_2$, the algebraic relation (5.10) can be solved for a value of $h$ which, in its turn, can be easily converted into the following approximation of the $pH$ value:

$$pH = -\log_{10} h + 8.5 \ .$$

We now return to a model of variations of $CO_2$ concentration. For this we used the differential equation

$$\frac{d}{dt}CO_2 = \underbrace{K_{CO_2}(CO_{2s}(T) - CO_2)}_{A} - \underbrace{\sum_i PS_i x_{1i}}_{B} + \underbrace{\sum_i Resp_i x_{1i}}_{C} + \underbrace{\frac{d}{dt}CO_2|_{othersources}}_{D} \tag{5.13}$$

In this equation, term A represents the restitution of $CO_2$ concentration, in the absence of any algae, to a saturation value $CO_{2_S}$, which in its turn depends on the $CO_2$ concentration in the atmosphere via the equilibrium relation

$$CO_{2_S} = 4.902\ 10^{-3} \exp^{\frac{5220}{RT}} P_{CO_{2_g}}$$

where $P_{CO_{2_g}}$ is the partial pressure of $CO_{2_g}$ in the atmosphere.

Term B represents the effect of algal photosynthesis on the dissolved $CO_2$ concentration. The transfer function $PS_i$ was defined previously in equations (5.2) and (5.4).

Term C represents the contribution to dissolved $CO_2$ in the water as a result of algal respiration. The respiration rate, $Resp_i$ is here assumed to be the following function of the temperature only (Wetzel, 1983):

$$Resp_i = a_{R_i} \exp^{\chi_{R_i} T} \tag{5.14}$$

The coefficients $a_{R_i}$ and $\chi_{R_i}$ are characteristic of a specific algal group. Figure 5.19 shows how well the function (5.14) can be fitted onto measured values taken from Wetzel (1983).

The last term, $D$ represent effects like the decomposition of dead organic material, chemical reactions and other sources of $CO_2$ which have not been included in the model at this stage.

Variations in dissolved oxygen concentration in the water can be modelled in a quite similar way, using the differential equation

$$\frac{d}{dt}O_2 = K_{O_2}(O_{2s}(T) - O_2) + \sum_i PS_{O_2 i} x_{1i} - \sum_i Resp_{O_2 i} x_{1i} + \frac{d}{dt}O_2|_{othersources} \ . \tag{5.15}$$

Here $O_{2S}$ is the saturation concentration of dissolved oxygen in the water, given approximately (Cole, 1975) by the formula

$$O_{2_S} = \frac{414}{31.6 + T}.$$

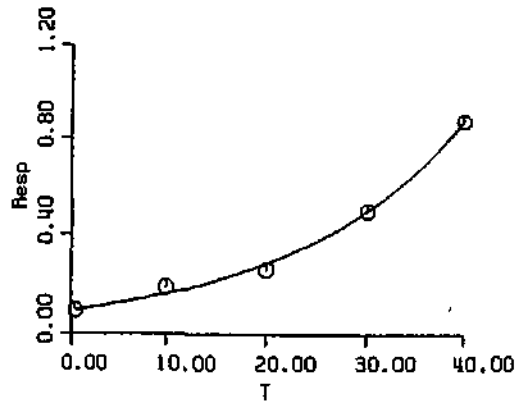


Figure 5.19: Fitting of the transfer function for respiration on experimental data from Wetzel (1983).

$PS_{O_2 i}$ is defined by an equation which differs from (5.2) and (5.4) only in that other values are assigned to some of the parameters. $Resp_{O_2 i}$ is also quite similar to (5.14), but with other parameter values.

The algal growth model can now be updated to the following system of equations:

$$\begin{aligned}
\dot{x}_{1_i} &= [-k_{D_i} + k_{S_i}) + k_{G_i}(I, T, \mathrm{Si}, N, P, N/P)]x_{1_i} \\
\dot{x}_{2_i} &= k_{D_i}x_{1_i} - k_{S_i}x_{2_i} \\
\dot{\mathrm{Si}} &= k_{\mathrm{Si}}(\mathrm{Si}_S(T) - \mathrm{Si}) - \sum_{i=diatom} V_i x_{1i} \qquad (5.16) \\
\dot{CO_2} &= K_{CO_2}(CO_{2s}(T) - CO_2) - \sum_i PS_i x_{1i} + \sum_i Resp_i x_{1i} \\
\dot{O_2} &= K_{O_2}(O_{2s}(T) - O_2) + \sum_i PS_{O_2 i} x_{1i} - \sum_i Resp_{O_2 i} x_{1i} \\
a_2 &= h^4 + a_0 h^3 + a_1 h. \qquad (5.17)
\end{aligned}$$

A schematic representation is shown in Figure 5.20.

In order to show how the model (5.17) could be used to investigate changes in oxygen and $CO_2$ concentrations in the water, the chlorophyll-*a* profile for 1985 at Stilfontein was resimulated with the updated model. Since experimental evidence in the literature (see (Cole, 1975)) suggests that the optimal temperature for photosynthesis for a specific algal species could be from 5 to 15 degrees Centigrade higher than the optimum temperature for growth of that species, the assumption was made during this simulation that the optimal temperature for photosynthesis is equal to the optimal temperature for algal growth plus a correction factor of 10° C.

In Figures 5.21 and 5.22 the simulated effect of algae on dissolved carbon dioxide and oxygen is shown. It is interesting to note that algal photosynthesis has a marked effect on dissolved oxygen concentrations, increasing these to levels up to around 40% above the saturation value in the absence of algae.

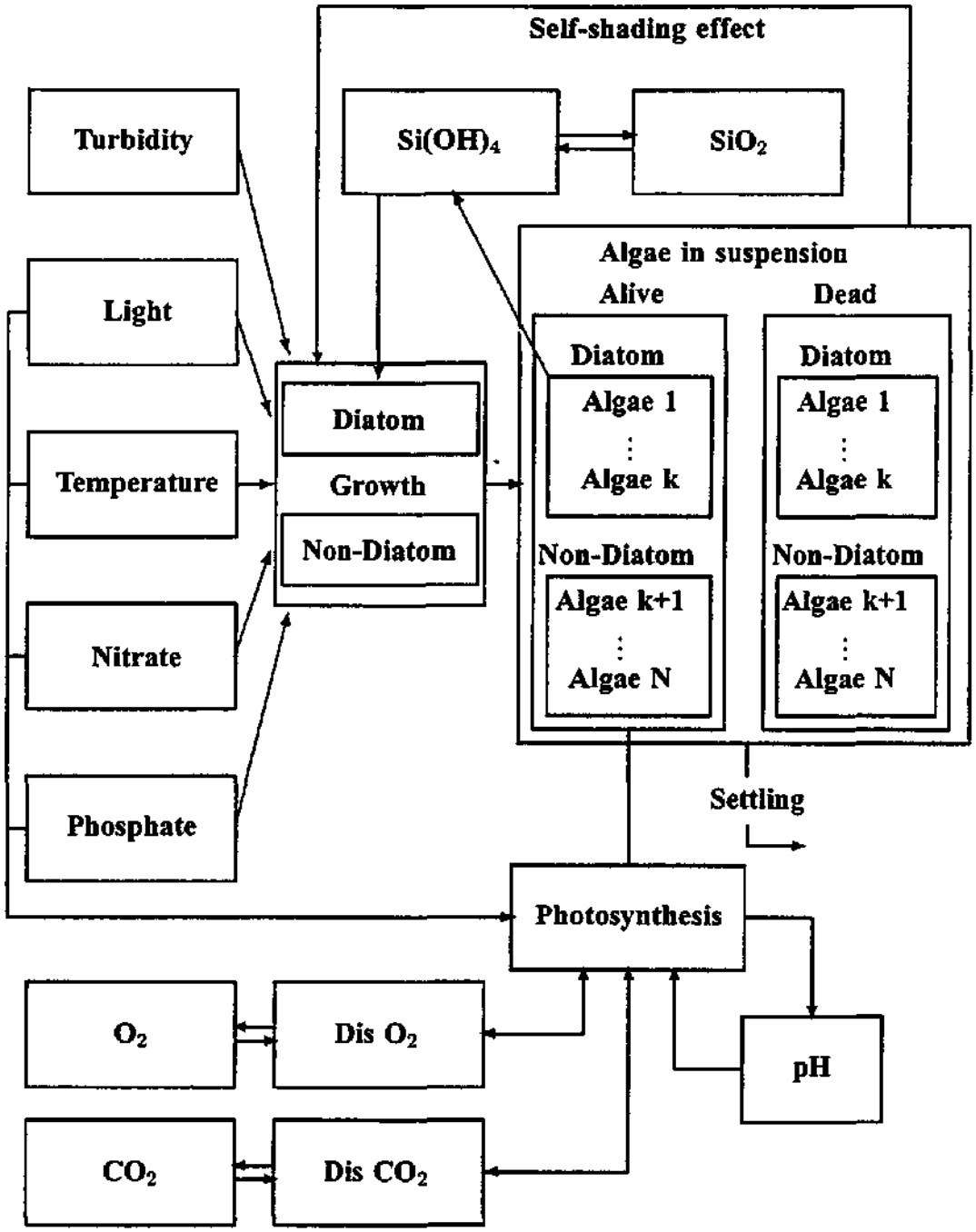


Figure 5.20: Schematic representation of the mathematical model (5.17).

These results are difficult to test against measurements due to lack of such data. However, they can be validated indirectly by using them to calculate $pH$ variations, and comparing these with measured $pH$ values. Such a comparison is shown in Figure 5.23.

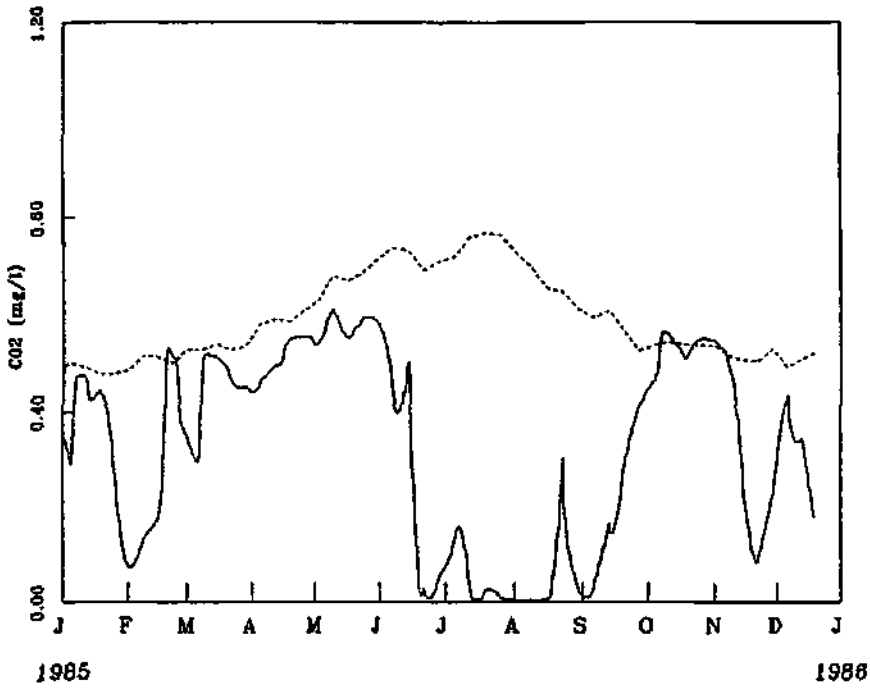


Figure 5.21: Variations in dissolved carbon dioxide concentration as simulated by the model. Saturation concentration is represented by a dashed line while algae-perturbed concentration is represented by a solid line.

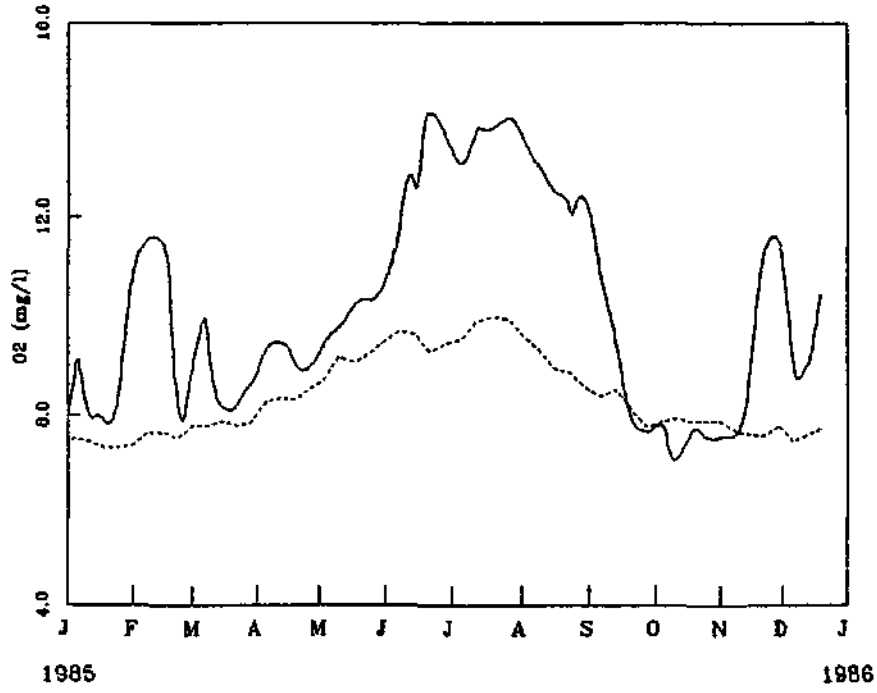


Figure 5.22: Variations in dissolved oxygen concentration as simulated by the model. Saturation concentration is represented by a dashed line while algae-perturbed concentration is represented by a solid line.

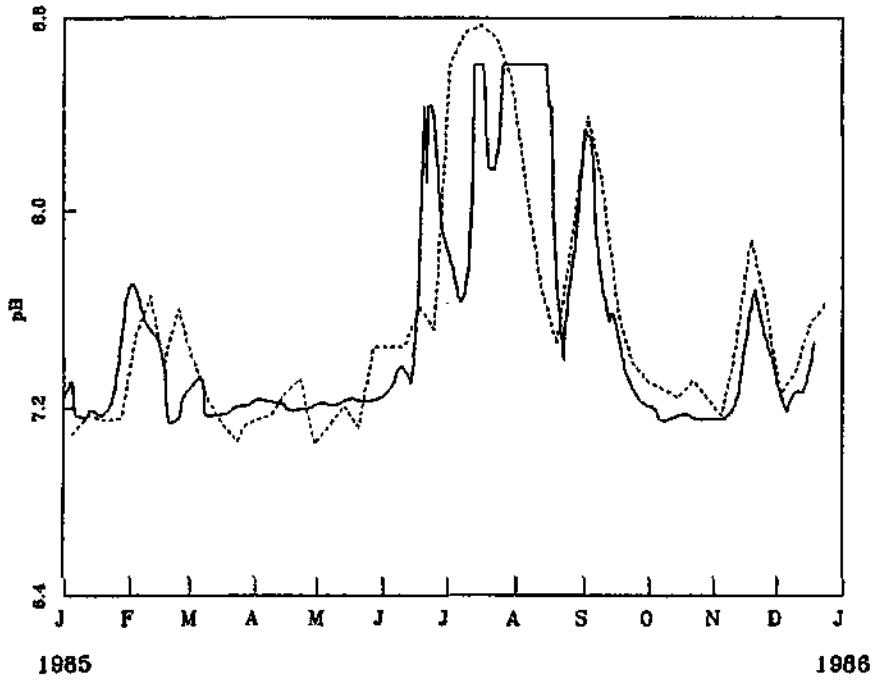


Figure 5.23: Comparison between computed (solid line) and measured (dashed line) values for the *pH* at the Stilfontein site for the period 1985.

Considering that quite severe simplifying assumptions were made, the correspondence between simulated and measured $pH$ values are quite satisfactory. The model also shows quite clearly that the algal population, as a result of photosynthesis, is actually causing the $pH$ to increase, thereby creating more favourable conditions for an algal bloom. This feedback effect shows that rivers should be considered as biochemical systems, in which biological and chemical processes interact.

### 5.4.2 The effect of algal activity on dissolved nitrogen concentration

We next turn to a mathematical description of the effect of algae on dissolved nutrients in the water, starting with dissolved nitrogen.

Modelling the effect of algal activity on dissolved nutrients is a much more complex matter than the case of dissolved carbon dioxide and oxygen. Some of the reasons for this are:

1. There are many components which must be modelled simultaneously.
2. Some very significant interactions are of unnatural origin, and can not easily be quantified.
3. There are time delayed actions in some of the processes in the system.

Figure 5.24 is a possible interaction network for nitrogen which we do not claim to be complete, but is still sufficient for the purposes of this study.

As suggested in Figure 5.24, it is assumed that nitrogen is absorbed by algae in two different forms, namely Ammonium ($NH_4$) and nitrate ($NO_3$). For this reason the modelling of variations in dissolved nitrogen concentration is done by means of two differential equations: One for ammonium and one for nitrate.

The following equation was formulated for ammonium:

$$\frac{d[NH_4]}{dt} = \underbrace{\frac{d[NH_4]}{dt}|_{Source}}_{A} + \underbrace{\frac{d[NH_4]}{dt}|_{Dec.}}_{B} + \underbrace{\frac{d[NH_4]}{dt}|_{Ex.}}_{C} - \underbrace{\frac{d[NH_4]}{dt}|_{Nit.}}_{D} - \underbrace{\frac{d[NH_4]}{dt}|_{Phot.}}_{E}, \tag{5.18}$$

Term A describes the rate of increase of dissolved ammonium due to any action unrelated to algal activities, such as industrial and mining discharges, rain, agricultural activities, chemical reactions, etc. By its very essence, this term can not be calculated by the model, and must be provided as input data for the model.

Term B represents the rate by which ammonium is formed and recirculated by the decomposition of dead algae in suspension and on the river bottom. Because this process of decomposition could take from a few minutes to a few days, depending on the ambient

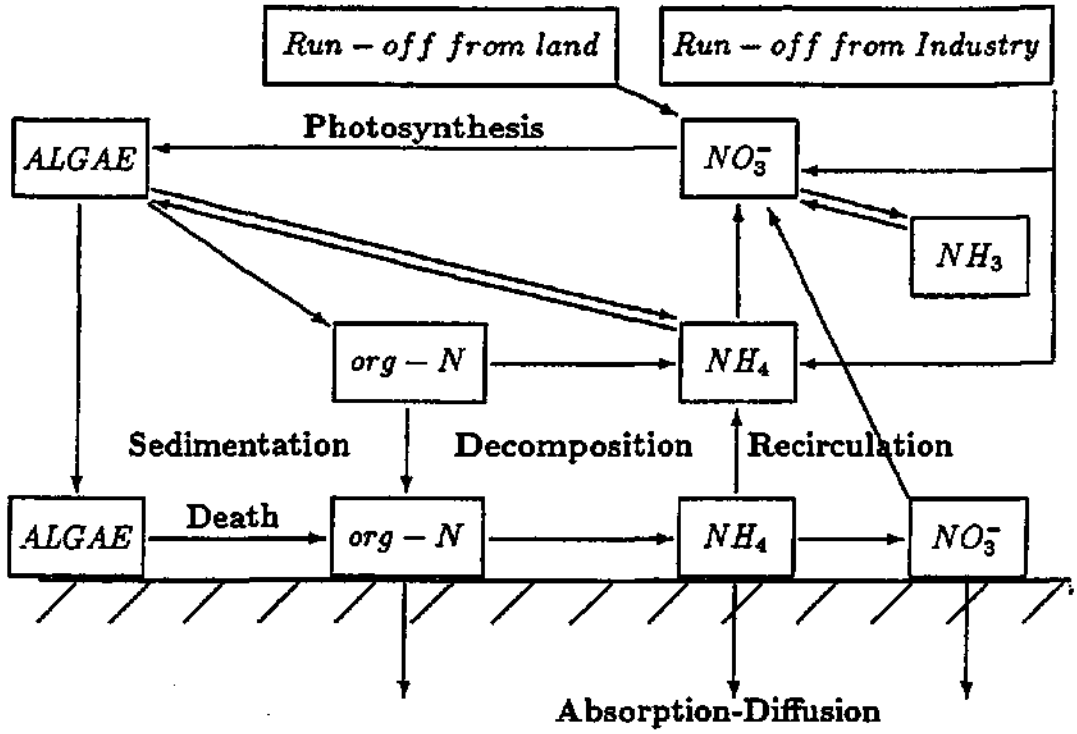


Figure 5.24: Interaction network describing the relation between algae and dissolved nitrogen as implemented in the model.

temperature and the particular algal group, this source of ammonium is modelled by the following time delayed term:

$$\frac{d[NH_4]}{dt}|_{Dec.} = \sum_{i=algae} ksed_i x_{i_2}(t - \tau_{D_i}) Inh^N_{algae_i} \text{kef}_i \tag{5.19}$$

where $\tau_{D_i}$ is the time period necessary for the release, at time $t$, of $NH_4$ from organic dead material originating from algae of the $i$-th group, while $ksed_i x_{i_2}$ is the concentration of dead algae of the $i$-th group which sedimented at time $t - \tau_{D_i}$. The parameter $Inh^N_{algae_i}$ is the ratio, per weight, between chlorophyll-$a$ and nitrogen content for the cells of the $i$-th algal group. The coefficient $\text{kef}_i$ is an efficiency coefficient included to make provision for the fact that all sedimented algae will not be made available for decomposition and recirculation.

Term C represents the rate at which ammonium is formed in the water from low molecular weight nitrogen compounds excreted by living algae. From these compounds a polycondensation process produces soluble inorganic nitrogen, which can be reabsorbed by algae (Wetzel, 1983). This transformation process takes about one day, so that this term should also contain a time delay. It is furthermore known that the amplitude of this source term is correlated to the algal respiration rate (USEPA Report, 1985). Thus the following expression was used to model term C:

$$\frac{d[NH_4]}{dt}|_{Ex.} = \sum_{i=algae} Resp_i x_{i_1}(t - \tau_E) R_{C-N_i}. \tag{5.20}$$

Here $\tau_E$ is the time period necessary for material excreted at time $t - \tau_E$ to be converted, at time $t$, into $NH_4$. $Resp_i x_{i_1}$ is the production rate of carbon dioxide by algae of the $i$-th group , through respiration, at time $t - \tau_E$. $R_{C-N_i}$ is a conversion factor.

Term D is the rate at which ammonium is decreased by a chemical reaction which transforms it into nitrate ($NO_3$). This nitrification process actually takes place in two steps, namely:

Step 1: The oxidation of ammonium into nitrite

$$NH_4^+ + \frac{3}{2}O_2 \rightarrow NO_2^- + 2H^+ + H_2O$$

Step 2: The transformation of nitrite into nitrate

$$NO_2^- + \frac{1}{2}O_2 \rightarrow NO_3^- .$$

However, the reaction which transforms nitrite into nitrate is extremely fast, with a characteristic time of the order of a fraction of a second. This is negligible in comparison with the time step used when solving the model equations numerically, which is about 5 minutes. Thus it would be acceptable, within the context of the model, to treat the reaction as the single step

$$NH_4 + 2O_2 \rightarrow NO_3^- + 2H^+ + H_2O. \tag{5.21}$$

Therefore the rate of decrease of ammonium by means of a nitrification reaction is modelled by

$$\frac{d[NH_4]}{dt}|_{Nit.} = -k(T, pH)_{Nit.}[NH_4^+], \tag{5.22}$$

where $k(T, pH)_{Nit.}$ is the speed of nitrification which, in general, depends on the temperature and the $pH$.

As Figure 5.25 shows, the nitrification rate increases with temperature up to approximately $30°C$. Beyond this temperature, the nitrification rate is inhibited and starts decreasing with increasing temperature values.

Since water temperatures of above 25° are seldom observed in the Vaal River, we did not attempt to design a transfer function for $k(T, pH)_{Nit.}$ which would fit the whole experimental curve in Figure 5.25. Instead we used the following function, which describes only the ascending part of the curve:

$$k(T, pH)_{Nit.} = k_{Nit.}^{max}(pH)1 - e^{0.2(T-4)} \tag{5.23}$$

The correspondence between (5.23) and the experimental data is shown in Figure 5.26. On this graph we also show the behaviour of the transfer function suggested by an USEPA report (USEPA Report, 1985), namely

$$k(T, pH)_{Nit.} = k_{Nit.}^{20}(pH)\theta^{T-20},$$

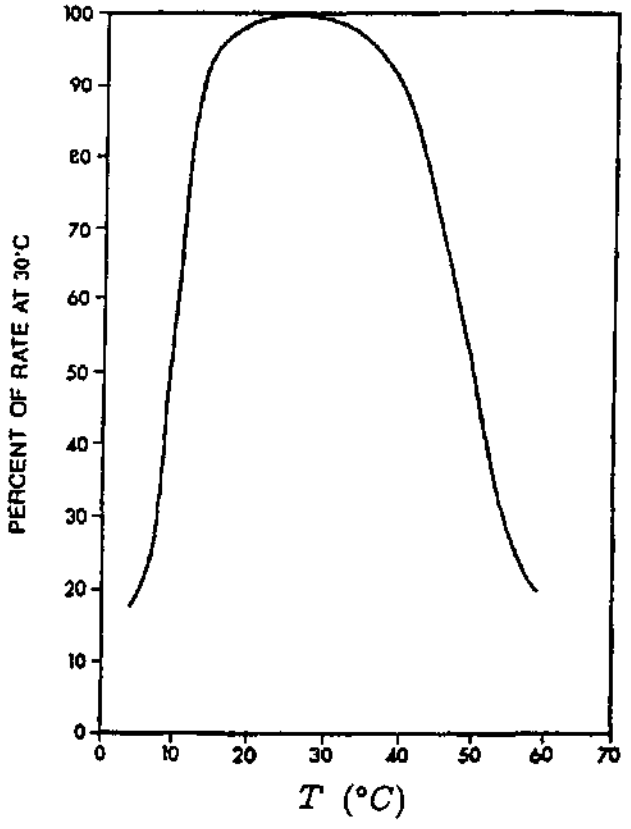


Figure 5.25: Temperature dependence of the nitrification speed (from Steeman Nielsen (1975)).

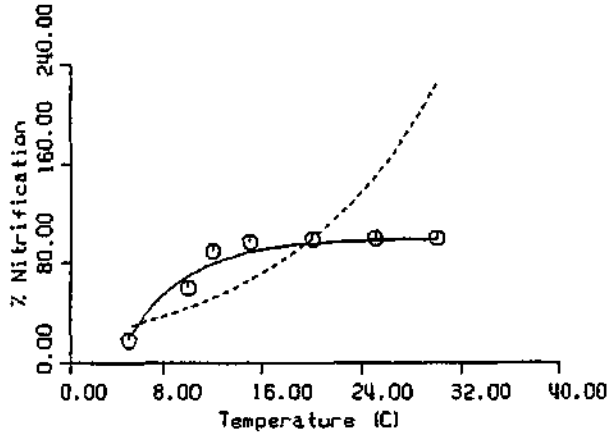


Figure 5.26: Comparison between relation (5.23) (solid line) and experimental data (circles). The USEPA report (1985) transfer function is shown as a dashed line. $k_{Nit.}^{max}(pH)$ and $k_{Nit.}^{20}(pH)$ have been scaled to 1 while $\theta = 1.085$ i.e. an average value.

which is clearly unsuitable.

To account for the very important effect of $pH$ , a $pH$ depended factor also needs to be added, so that (5.23) becomes

$$k(T,pH)_{Nit.} = k_{Nit.}^{max}(1 - e^{0.2(T-4)})f_{Nit}^{pH}, \tag{5.24}$$

where the factor $f_{Nit}^{pH}$ is given by

$$f_{Nit}^{pH} = g^3 e^{(1-g^3)} \tag{5.25}$$

where

$$g = \frac{pH - 4.5}{8.5 - 4.5} = \frac{pH - 4.5}{4}.$$

Figure 5.27 shows a fit of (5.25) onto experimental data.

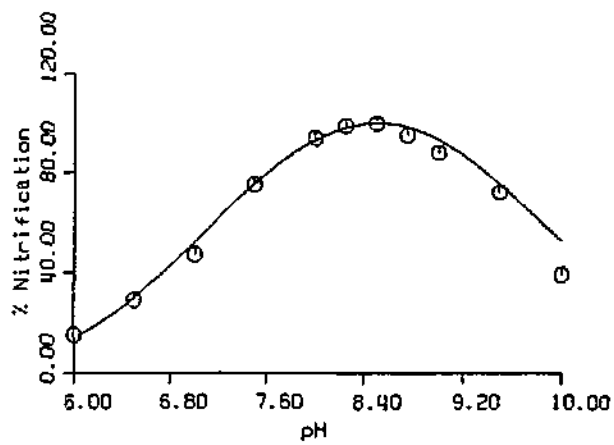


Figure 5.27: Effect of $pH$ on nitrification rate: The dashed line refers to experimental data and the solid line represents relation (5.25).

The last term in (5.18), E, represents the rate at which ammonium is absorbed by algae during photosynthesis. This is modelled by the expression

$$\frac{d[NH_4]}{dt}|_{Phot.} = \sum_{i=algae} PS_i x_{i_1} R_{NH_4-C} Pref_{NH_4} \tag{5.26}$$

where $PS_i$ is the photosynthetic rate defined in (5.2) and (5.4)), and $R_{NH_4-C}$ is a conversion factor , which has a value of about 0.176 for algal photosynthesis. Since it is known that algae are able to absorb nitrogen as either ammonium or nitrate, with a preference for ammonium, the preference factor $Pref_{NH_4}$ was also added. More precisely, algae tend to absorb nitrogen primarily as ammonium, until nitrogen absorption exceeds 75% of the total ammonium pool. After that nitrogen absorption switches to dissolved nitrate. Thus we first calculated the total ammonium pool by means of

$$Pool_{NH_4} = [NH_4] + (\frac{d[NH_4]}{dt}|_{Source} + \frac{d[NH_4]}{dt}|_{Dec.} + \frac{d[NH_4]}{dt}|_{Ex.} - \frac{d[NH_4]}{dt}|_{Nit.}) * \Delta t,$$

where $\Delta t$ is the time step for numerical integration. The factor $Pref_{NH_4}$ is equal to 1, until nitrogen absorption by photosynthesis (calculated in the model by multiplying the right hand side of (5.26) by $\Delta t$) exceeds 75% of $Pool_{NH_4}$, after which it becomes zero.

We next turn to modelling variations in dissolved nitrate concentration. For this the following differential equation is used:

$$\frac{d[NO_3]}{dt} = \underbrace{\frac{d[NO_3]}{dt}|_{Source}}_{A} + \underbrace{\frac{d[NO_3]}{dt}|_{Nit.}}_{B} - \underbrace{\frac{d[NO_3]}{dt}|_{Phot.}}_{C}. \tag{5.27}$$

In equation(5.27) term A represents the rate at which dissolved nitrate concentration is increased by factors unrelated to algal activity, such as industrial and mining discharge, rain, etc. It is similar to term A in (5.18), and must also be provided as model input data.

Term B represents the rate of nitrate production by the nitrification reaction (5.21), and it is described by the expression

$$\frac{d[NO_3]}{dt}|_{Nit.} = k(T, pH)_{Nit.}[NH_4^+], \tag{5.28}$$

where $k(T, pH)_{Nit.}$ is the nitrification speed given by (5.24).

Term C is the rate of nitrate absorption during photosynthesis. It is closely related to term E in (5.18), and is given by the expression

$$\frac{d[NO_3]}{dt}|_{Phot.} = \sum_{i=algae} PS_i x_{i_1} R_{NO_3-C}(1 - Pref_{NH_4}) \tag{5.29}$$

where $R_{NO_3-C}$ is the conversion factor relevant for nitrate absorption. For reasons explained above, term C is zero whenever term E in (5.18) is not, and vice versa.

Although nitrogen is a very important nutrient for algae and other organisms, there are certain nitrogen compounds, such as un-ionised ammonia ($NH_3$) which could be toxic to such organisms. Un-ionised ammonia is in fact toxic to fish at fairly low concentrations. Since it is easy to obtain $NH_3$ concentrations once those of ammonium is known, it make sense to have the model calculate these concentrations as well.

The key to this is the equilibrium reaction

$$NH_3 + H_2O \rightleftharpoons NH_4^+OH^-. \tag{5.30}$$

Assuming we have equilibrium at all times we can write down the equilibrium constant

$$K_{NH_3} = \frac{[NH_4^+][OH^-]}{[NH_3]} = \frac{[NH_4^+]K_W}{[NH_3][H^+]}$$

where $K_W$ is the dissociation constant for water. After taking the logarithm of this relation, and performing some simple algebra, we end up with the desired formula

$$[NH_3] = [NH_4^+]10^{(pH-pK_H)}, \tag{5.31}$$

where

$$\begin{aligned} pK_H &= \log_{10} K_{NH_3} - \log_{10} K_W \\ &= 0.09018 + \frac{2729.2}{T} \end{aligned}$$

with $T$ the temperature expressed in degrees Kelvin.

### 5.4.3 The effect of algal activity on dissolved phosphorus concentration

The mechanisms governing changes in dissolved phosphorus concentrations and dissolved nitrogen concentrations are fairly similar.

Figure 5.28 shows an interaction network for the phosphorus cycle that would be sufficient for the purposes of the model.

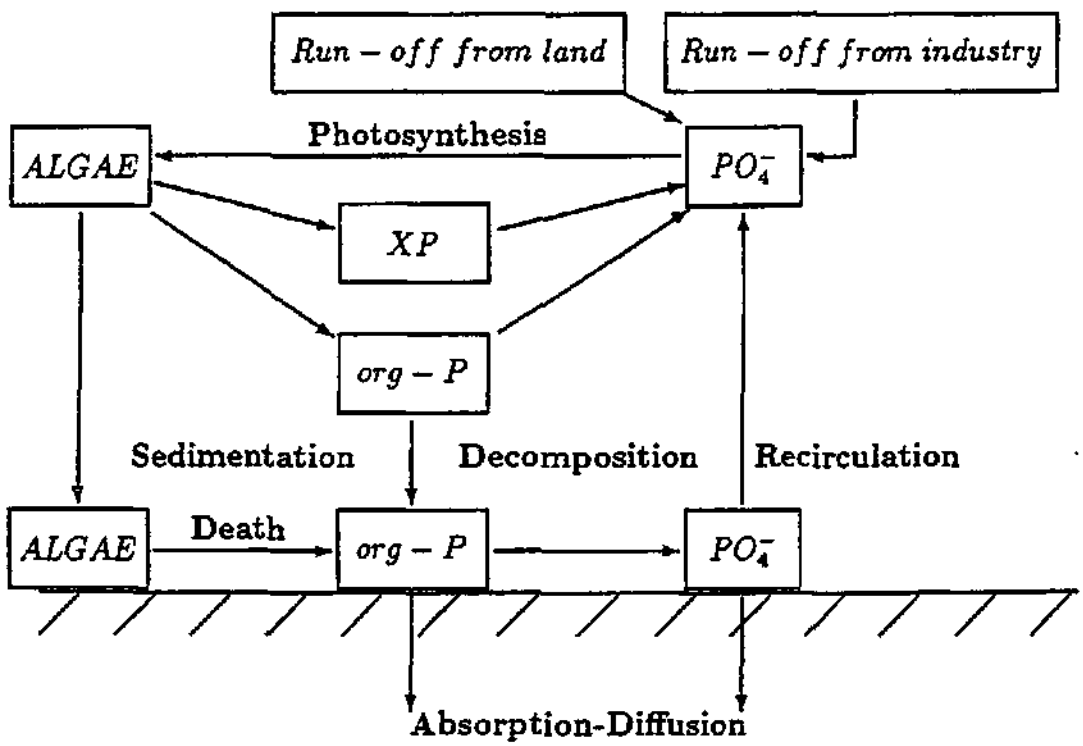


Figure 5.28: A basic interaction network describing the relation between algae and dissolved phosphorus as implemented in the model.

As indicated in this scheme, it is assumed that phosphorus is absorbed by algae during photosynthesis mainly as orthophosphate ($PO_4$). This is modelled by the following

differential equation:

$$\frac{d[PO_4]}{dt} = \underbrace{\frac{d[PO_4]}{dt}|_{Source}}_{A} + \underbrace{\frac{d[PO_4]}{dt}|_{Dec.}}_{B} + \underbrace{\frac{d[PO_4]}{dt}|_{Ex.}}_{C} - \underbrace{\frac{d[PO_4]}{dt}|_{Phot.}}_{D}, \tag{5.32}$$

In this equation term A represents model input data. Similarly as in previous cases, this is the rate by which dissolved phosphate concentration is increased by external factors such as industrial and mining discharges, etc.

Term B is given by time delay expression

$$\frac{d[PO_4]}{dt}|_{Dec.} = \sum_{i=algae} ksed_i x_{i_2}(t - \tau_{D_i}) Inh^P_{algae_i} kef_i , \tag{5.33}$$

which is quite similar to (5.19). This term is the rate at which dissolved phosphate is added by a process of decomposition of dead algae. Note that the same parameters are used here as in (5.19), except that $Inh^N_{algae_i}$ is replaced by $Inh^P_{algae_i}$, which is now the ratio, per weight, between chlorophyll-*a* and phosphorus content in algal cells of group $i$.

Term C is given by the expression

$$\frac{d[PO_4]}{dt}|_{Ex.} = \sum_{i=algae} Resp_i x_{i_1}(t - \tau_E) R_{C-P_i} , \tag{5.34}$$

and represents the rate at which $PO_4$ is added by means of a polycondensation process acting on low molecular weight phosphorus compounds excreted by living algae. This is a quite similar process as that modelled by term C of (5.18), and , in fact, (5.34) differs from (5.20) only in that the conversion factor $R_{C-N_i}$ is now replaced by $R_{C-P_i}$.

Term D is the rate of absorption of phosphate by algae during photosynthesis. Following the same reasoning as in the case of the last term in (5.18), it is described by the following expression:

$$\frac{dPO_4}{dt}|_{Phot.} = \sum_{i=algae} PS_i x_{i_1} R_{P-C} . \tag{5.35}$$

Here $R_{P-C}$ is a conversion factor with a value of about 0.0244.

Since the first source terms in each of nutrient equations (5.18, 5.27, 5.32) represent external sources of nutrients, and no data about these were available, we left them out for a first approximation, and considered only nutrient variations due to algal activities. Thus we added the following three equations to the other model equations:

$$\begin{aligned}
\frac{d[PO_4]}{dt} &= \frac{d[PO_4]}{dt}|_{Dec.} + \frac{d[PO_4]}{dt}|_{Ex.} - \frac{d[PO_4]}{dt}|_{Phot.} \\
\frac{d[NH_4]}{dt} &= \frac{d[NH_4]}{dt}|_{Dec.} + \frac{d[NH_4]}{dt}|_{Ex.} - \frac{d[NH_4]}{dt}|_{Nit.} - \frac{d[NH_4]}{dt}|_{Phot.} \\
\frac{d[NO_3]}{dt} &= \frac{d[NO_3]}{dt}|_{Nit.} - \frac{d[NO_3]}{dt}|_{Phot.} .
\end{aligned}$$

The updated model was then used , once again , to simulate the chlorophyll-*a* profile at Stilfontein during 1985. Computed values of the rates $\frac{d[PO_4]}{dt}$ and $\frac{dN}{dt} = \frac{d[NH_4]}{dt} + \frac{d[NO_3]}{dt}$ are shown in Figures 5.29 and 5.30.

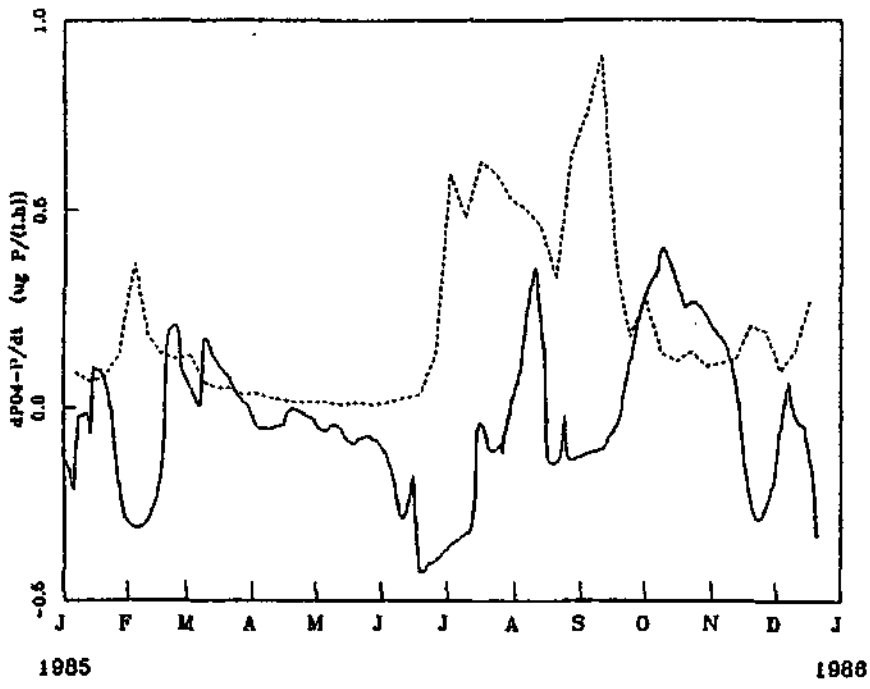


Figure 5.29: The rate $\frac{dPO4-P}{dt}$, computed by the model for 1985 at the Stilfontein site (solid line). The measured chlorophyll-*a* profile is also shown for comparison purposes (dashed line).

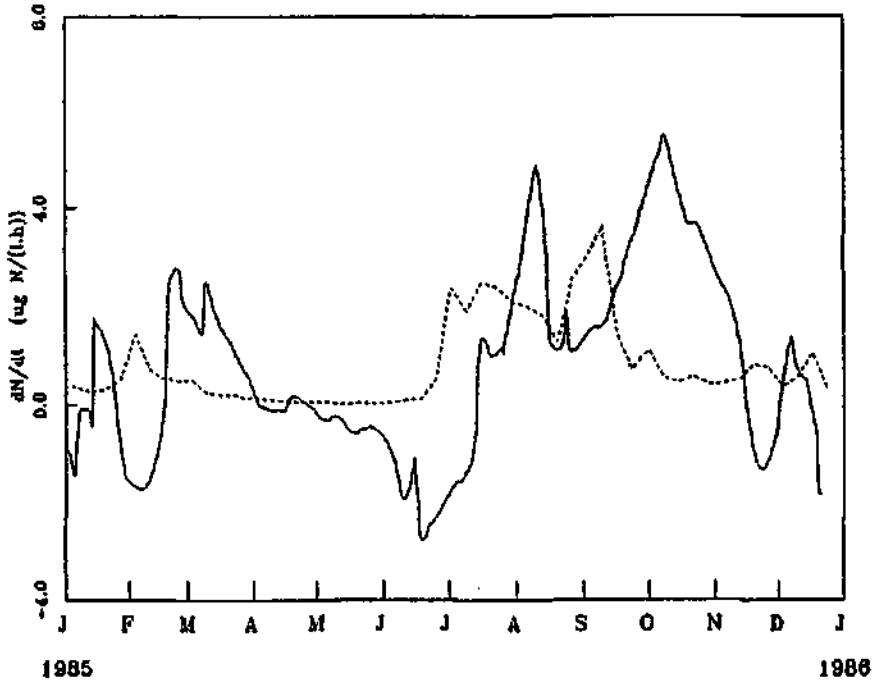


Figure 5.30: The rate $\frac{dN}{dt}$ , computed by the model for 1985 at the Stilfontein site (solid line). The measured chlorophyll-*a* is also shown for comparison purposes (dashed line).

These figures show that algae can either add nutrients to the water (positive rates) or remove them (negative rates). That algae should remove nutrients is not surprising, but their role as a source of nutrients need to be explained in biological terms: When the algal biomass stay high for a long period of time, decomposition of dead algae could add dissolved nutrients to the water at such a rate higher than the rate of absorption because of photosynthesis, thus leading to a nett increase of dissolved nutrients in the water. For such long lasting algal blooms it is therefore unlikely that the bloom would end because of a lack of nutrients.

Figures 5.31 and 5.32 show comparisons between the computed rates of change and the measured concentrations of dissolved nitrogen and phosphorus. There is clearly a correlation between the observed changes in nutrient concentrations and the computed ones, in which only algal activities were taken into account. The correlation is stronger in the case of phosphorus (Figure 5.31) than nitrogen (Figure 5.32).

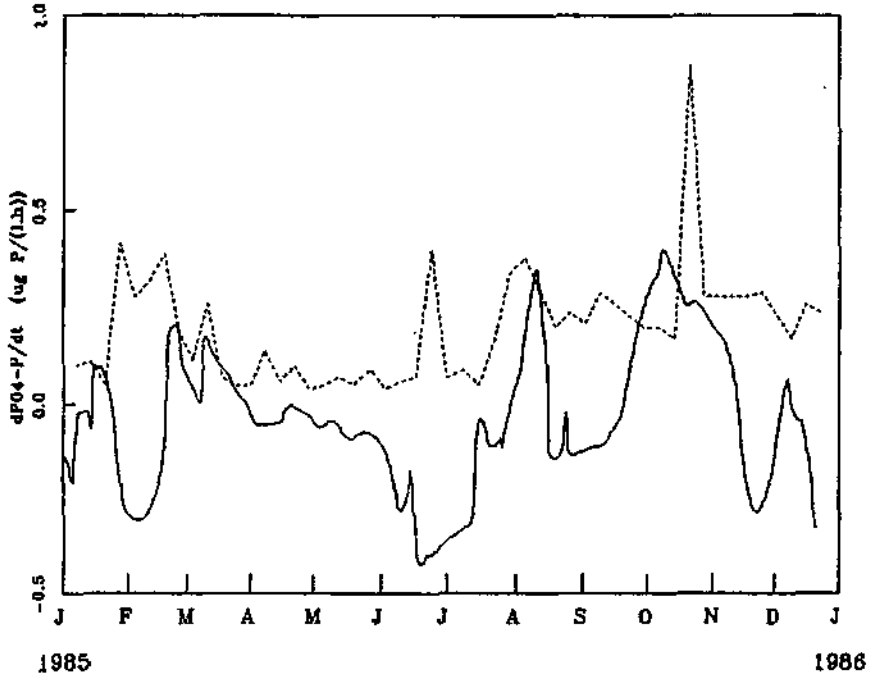


Figure 5.31: Comparison between the rate $\frac{dPO4-P}{dt}$ computed by the model (solid line) and the measured concentration of dissolved $P$, at Stilfontein during 1985 (dashed line).

However, the correlations are far from perfect. As may be expected, algal activities, though having a nonnegligible effect on nutrient availability in the water, do not govern, as such, the levels of dissolved nitrogen and phosphorus in the river. A realistic model of changes in concentration of these nutrients would require that other environmental factors, represented in equations (5.18), (5.27) and (5.32) ) by the first "source" terms, be taken into account explicitly. This could be done by combining the present model with a water quality module, describing all relevant chemical aspects of the water. This is no easy task, however, and would require a separate research project.

However, in the next subsection it will be shown how this problem could be largely

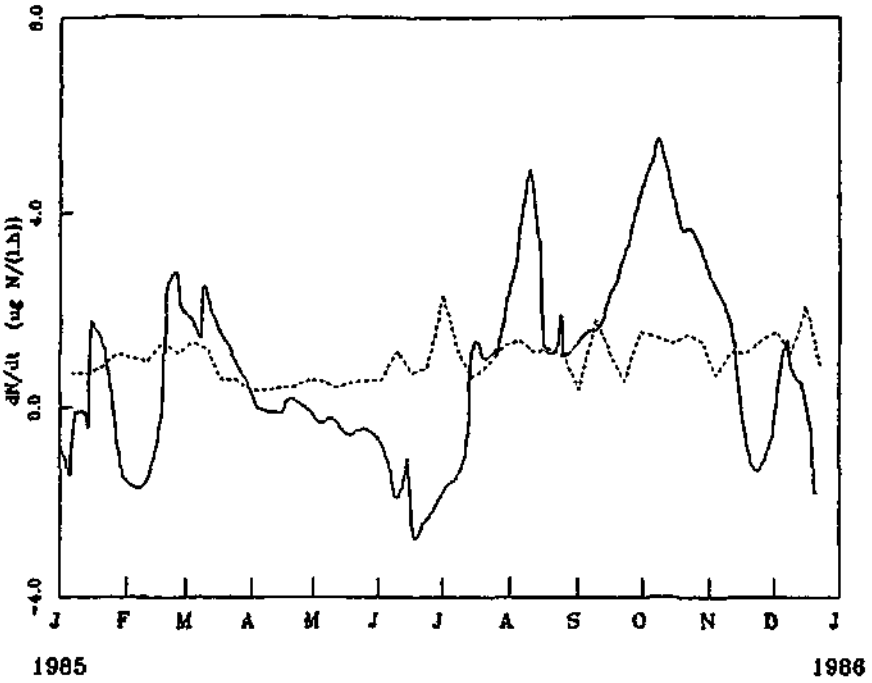


Figure 5.32: Comparison between the rate $\frac{dN}{dt}$ computed by the model (solid line) and the measured concentration of dissolved $N$, at Stilfontein during 1985 (dashed line).

overcome in the case of phosphorus (at least at the Stilfontein site) by assuming a relation between the calcium-carbonate system and the (maximum) dissolved concentration of (ortho) phosphate in the river.

### 5.4.4 Possible relationship between the calcium-carbonate system and dissolved phosphorus concentration

It is reasonable to assume that, in the absence of algae, changes in the dissolved phosphate concentration are governed by the equation

$$\frac{d[PO4]}{dt}|_{Source} = K_{PO_4}([PO_{4s}] - [PO_4]), \tag{5.36}$$

in which $[PO_{4s}]$ is a saturation concentration determined by chemical aspects, while $K_{PO_4}$ is a restitution constant. The value of this saturation concentration is expected to be related to equilibria for other dissolved elements. It was therefore decided to couple $[PO_{4s}]$ to the calcium-carbonate equilibrium system *via* the solubility product of hydroxylapatite ($Ca_5(PO_4)_3OH$),

$$[Ca^{2+}]^5[PO_4^{3-}]^3[OH^-] = K_{apatite}. \tag{5.37}$$

The concentration $[PO_4^{3-}]$ was assumed to be the same as the desired saturation concentration $[PO_{4s}]$.

This decision was based on the following facts:

a) The calcium-carbonate system already proved to be important for an explanation of the interaction between the algal population and the $pH$ of the water. b) There is a strong correlation between measured values of dissolved calcium and phosphate concentrations in the river at Stilfontein during the time period 1986-1989. (See Figure 5.33). c) A similar relation between calcium and phosphate concentration *via* the solubility product of apatite has been established in the case of other river systems (such as the Rhine river).

Figure 5.34 shows a schematic representation of the phosphate cycle, updated to include these additional aspects.

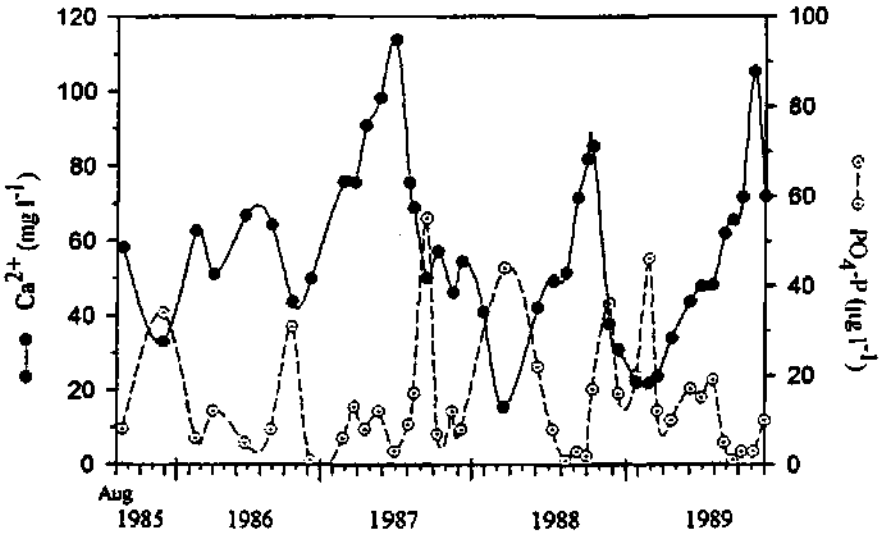


Figure 5.33: Correlation between dissolved calcium and phosphate concentrations at the Balkfontein site (from Roos (1992)).

To get a rough idea of the implications of the additional assumptions made so far in this section, the interactions shown in Figure 5.34 were simplified as much as possible. Thus it was assumed that all parameters, except the dissolved carbon dioxide and phosphate concentrations, remain constant during computations, and that only direct interactions between algae and these two substances are taken into account. Furthermore, since we were not interested at this point in the effect of $CO_2$ and $PO_4$ concentrations on the algae, but rather the other way around, changes of the total algal biomass, calculated from the rest of the model or taken from available measurements, are assumed to be available *a priori*. Under these simplifying assumptions we get a rather simple dynamical system of the form

$$\begin{aligned} \frac{d}{dt}CO_2 &= K_{CO_2}(CO_{2s} - CO_2) - PS\,x(t) + Resp\,x(t) \\ \frac{d}{dt}PO_4 &= K_{PO_4}(PO_{4s}(CO_2) - PO_4) - PS_{PO_4}\,x(t)\,, \end{aligned} \tag{5.38}$$

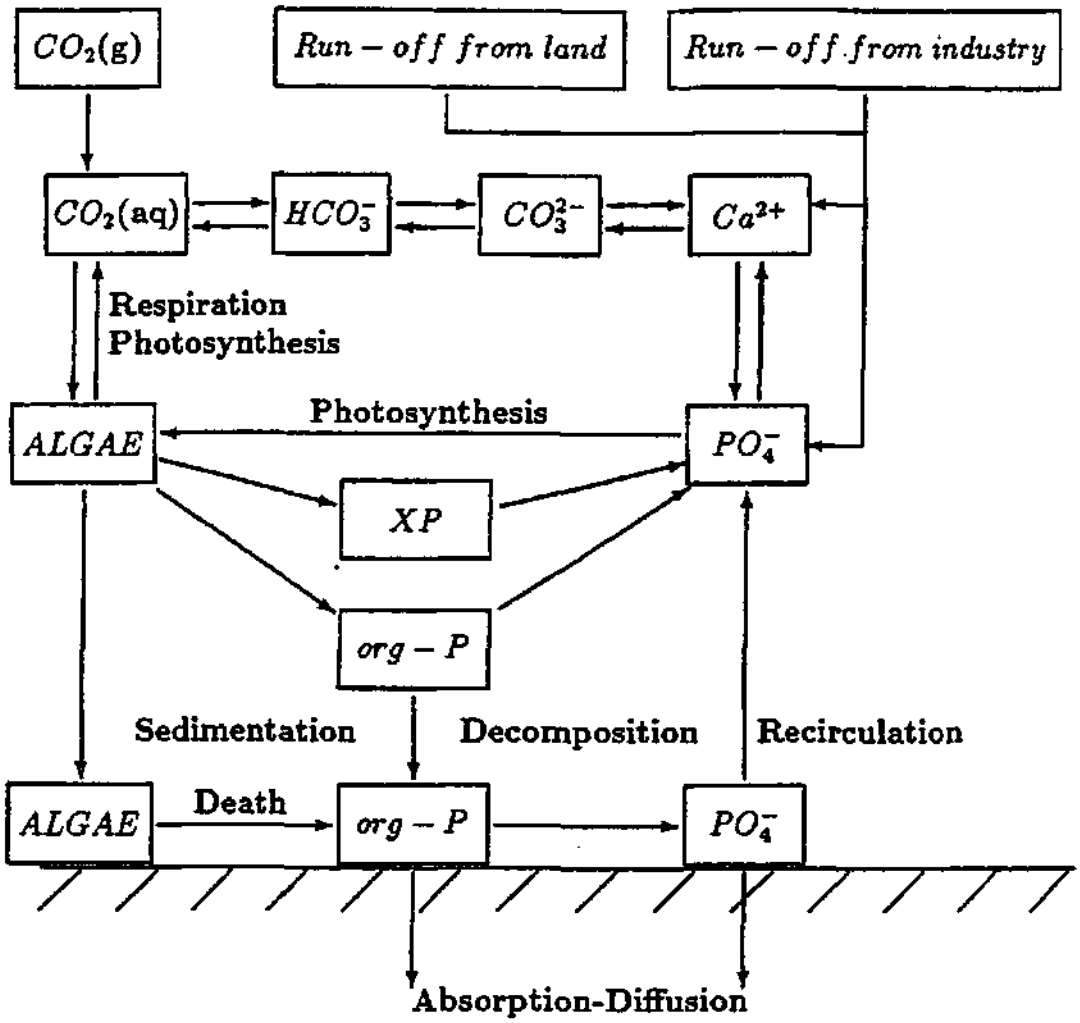


Figure 5.34: Updated basic interaction network describing the relation between algae and dissolved phosphorus.

where $PO_{4s}(CO_2)$ is calculated by means of (5.37) as well as equation (5.10) and its associated equations and relations described earlier in this chapter.

This system models the two mechanisms by which photosynthesis affects the dissolved phosphate concentration. The first is a decrease of the dissolved phosphate concentration due to absorption by algae during photosynthesis. The second mechanism is the reduction of carbon dioxide in the water due to the same photosynthetic reaction. As mentioned before, a decrease in the carbon dioxide concentration increases the $pH$, i.e. the concentration $[OH^-]$, but it also decreases the calcium concentration $[Ca^{2+}]$. From (5.37) it is clear that the concentration $[PO_4^{3-}]$, and therefore also $PO_{4s}$, is much more sensitive to changes in the calcium concentration than to changes in $[OH^-]$, so that a decrease in $CO_2$ concentration would lead to a nett increase in the saturated concentration $PO_{4s}$.

In general, the total chlorophyll-$a$ concentration varies in the range $8\mu g.l^{-1}$ to $360\mu g.l^{-1}$, with an average of about $70\mu g.l^{-1}$. Therefore three different simulations were done with

the system (5.38), each with a different value of the maximum chlorophyll-*a* concentration $x_{max}$. These values were (a) $x_{max} = 25\mu g.l^{-1}$, representing a low intensity algal bloom, (b) $x_{max} = 50\mu g.l^{-1}$, i.e. a bloom of average intensity and (c) $x_{max} = 120\mu g.l^{-1}$ which represents a strong algal bloom. Figures 5.35 through 5.37 show the results of these simulations.

In the case of a low intensity algal bloom the chemical effects (i.e. increase of $PO^{4s}$ due to a decrease in $CO^2$) are dominant, and a nett increase in dissolved phosphate concentration could be expected (see figure 5.35). For a strong algal bloom, a nett increase is again expected during the early stages of the bloom, but when the total chlorophyll-*a* passes beyond a certain critical value $x_{crit}$, the decreasing effect of dissolved phosphate concentration due to algal absorption starts to dominate, leading to a nett decrease in dissolved phosphate. At the end of the bloom the balance between the two mechanisms will again reverse, so that dissolved phosphate increases once more. These effects can be seen clearly in Figure 5.37. When the peak algal biomass during an algal bloom corresponds more or less with the critical value $x_{crit}$, the two mechanisms are reasonably in balance, and the dissolved phosphate concentration should remain constant through most of the bloom (see Figure 5.36).

The dynamics of this simple model shows once again that algae are living in "symbiosis" with their environment.

Of course it still remains to be shown that: (a) The behaviour simulated by the simplified mathematical model agrees with the real behaviour observed in nature and (b) the integration of equation (5.32) together with the source term (5.36) provides simulated values of the dissolved phosphate concentrations that are in agreement with the measured values, *in situ*.

In order to indicate that the dynamics of the simple model show some agreement with actual observations, we refer to Figure 5.38, which shows a comparison between measured values of chlorophyll-*a* and dissolved phosphate at Stilfontein during 1985.

In this figure we first draw attention the summer to autumn period of 1985, and in particular points B, C and D, when the algal blooms were characterised by weak or average chlorophyll-*a* concentrations. Here the dissolved phosphate and chlorophyll-*a* concentrations show a positive correlation, agreeing with the dynamics of model (5.38). We next turn to the first winter algal bloom which was rather strong (point E). Here an increase of dissolved phosphate at the beginning of the bloom (point E1) is followed by a decrease (point E2) and again an increase at the end of the algal bloom (point E3). This is also in agreement with the behaviour of model (5.38). The second winter bloom (point F) is even stronger than the first, and we would have expected the dissolved phosphate concentration to show a similar behaviour. However, it does not–the phosphate concentration increases with chlorophyll-*a* concentration where it should have decreased.

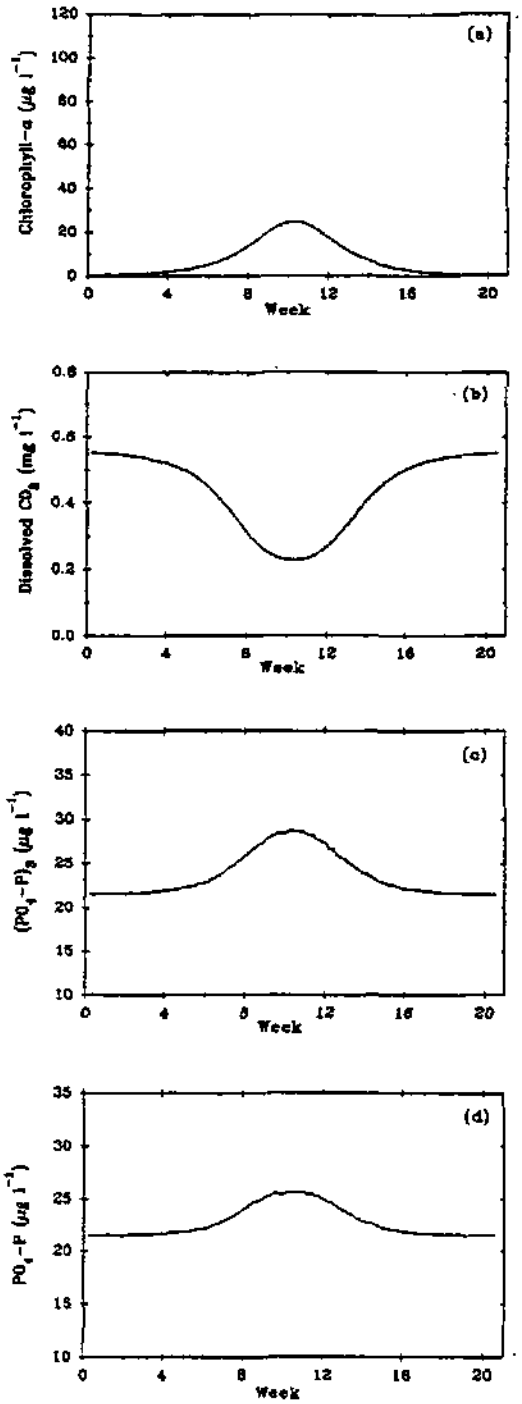


Figure 5.35: Values computed by the model (5.38), with $x_{max} = 25\mu$ g Chl-$a$.l$^{-1}$.

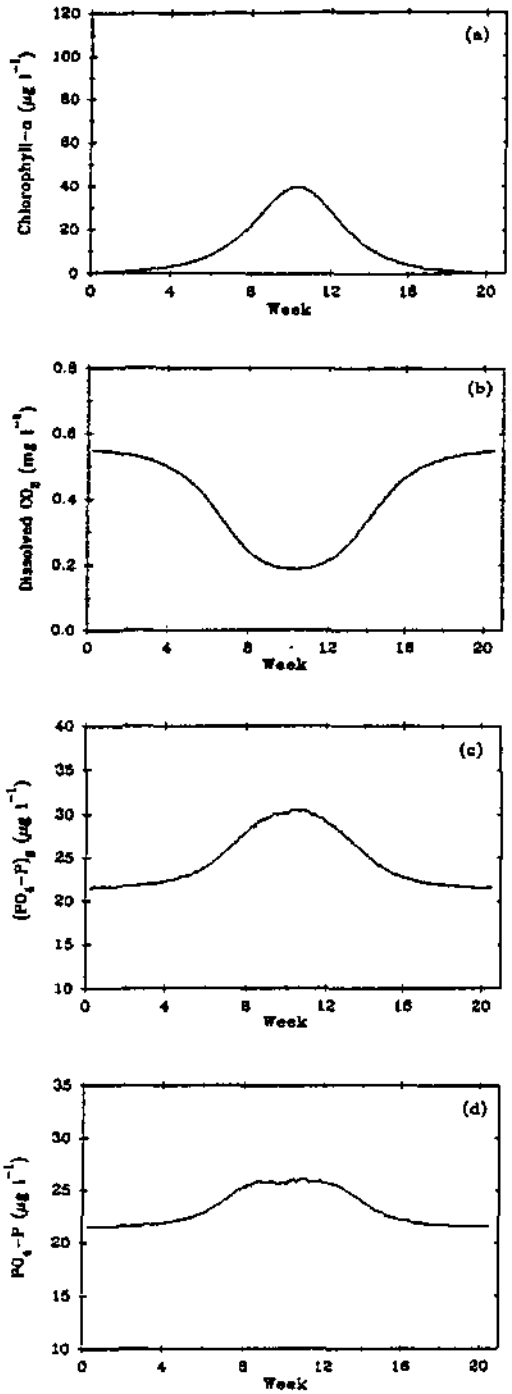


Figure 5.36: The same as Figure 5.35, but with $x_{max} = 50\mu g$ Chl-$a.l^{-1}$.

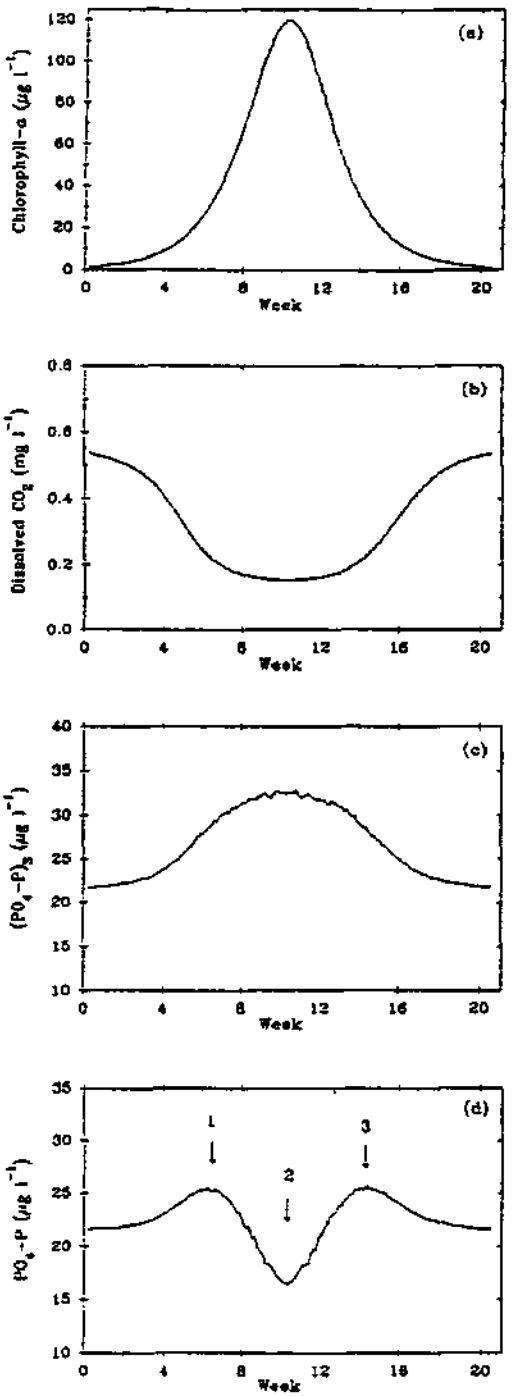


Figure 5.37: The same as Figure 5.35, but with $x_{max} = 120\mu g$ Chl-$a$.$l^{-1}$.

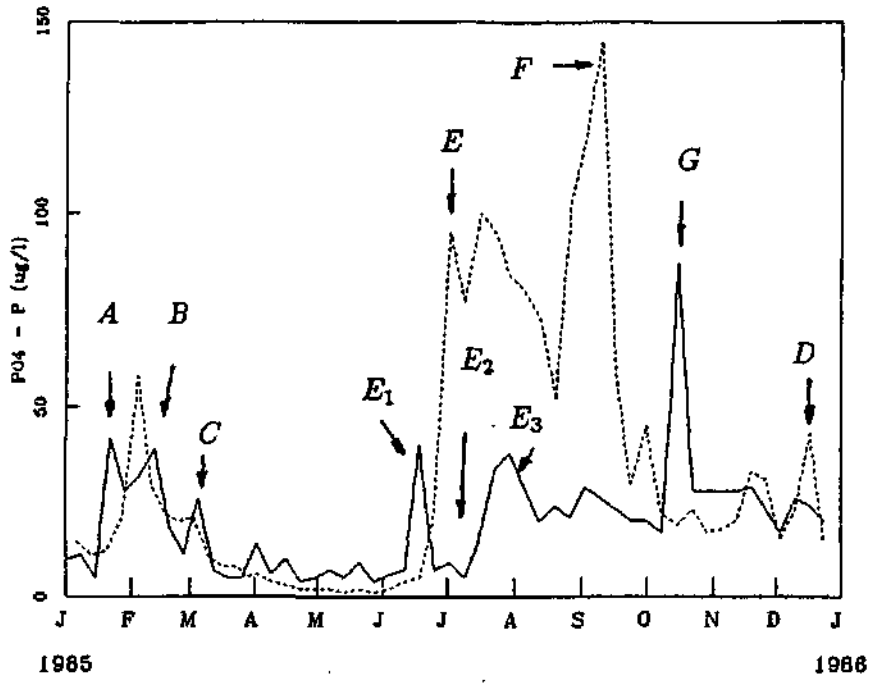


Figure 5.38: Comparison between measured chlorophyll-*a* (dashed line) and dissolved phosphate concentration (solid line) data from Stilfontein, 1985.

Possible explanations for this anomaly could be:

1. The second algal bloom involved green algae, which contain more chlorophyll-*a* per cell than the diatoms involved in the first bloom. Thus the second algal bloom was probably not really stronger than the first in terms of biomass.

2. The second algal bloom followed directly after the diatom bloom, and it is quite possible that a large amount of dead organic material would still have been in suspension, creating a rather unfavourable under water light climate for photosynthesis.

The phosphate peaks at A and G can not be explained in terms of the simple model (5.38), however.

To show how simulated and measured values of dissolved phosphate concentration compare, we simulated the 1985 data at Stilfontein once again, using the updated model with the nutrient equations, and with the source term (5.36) inserted into the differential equation (5.32). The computed dissolved phosphate values are displayed together with the measured values in Figure 5.39. Considering how many simplifying approximations were made, the agreement between the computed and measured values is fairly good. Note that the computed phosphate concentration also show a an increase around the point G in Figure 5.38. A careful analysis of the model output revealed that this peak was caused by the decomposition of dead organic material (see Figure 5.40).

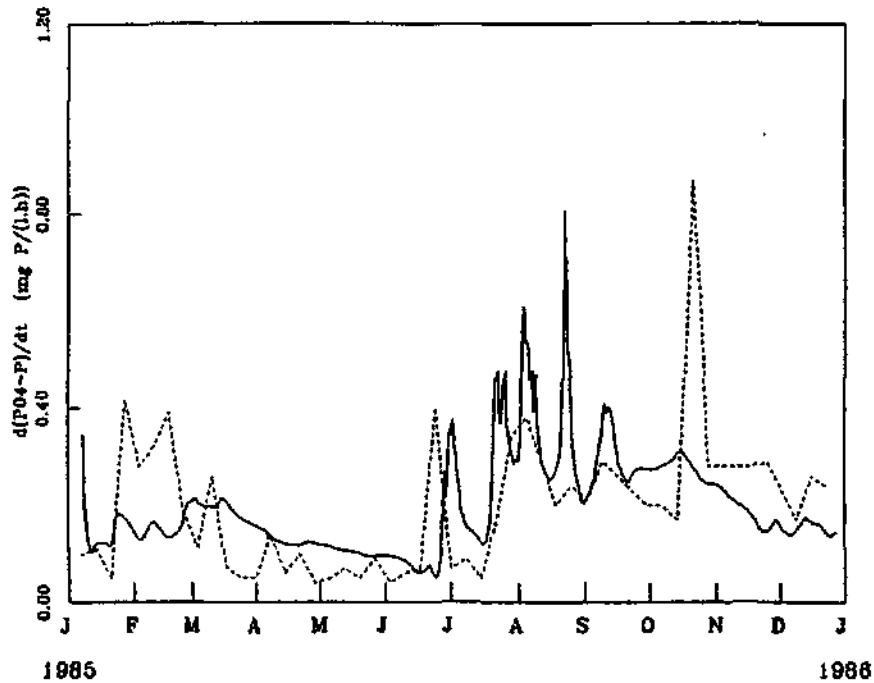


Figure 5.39: Comparison between computed (solid line) and measured (dashed line) phosphate concentrations at the Stilfontein site, 1985.

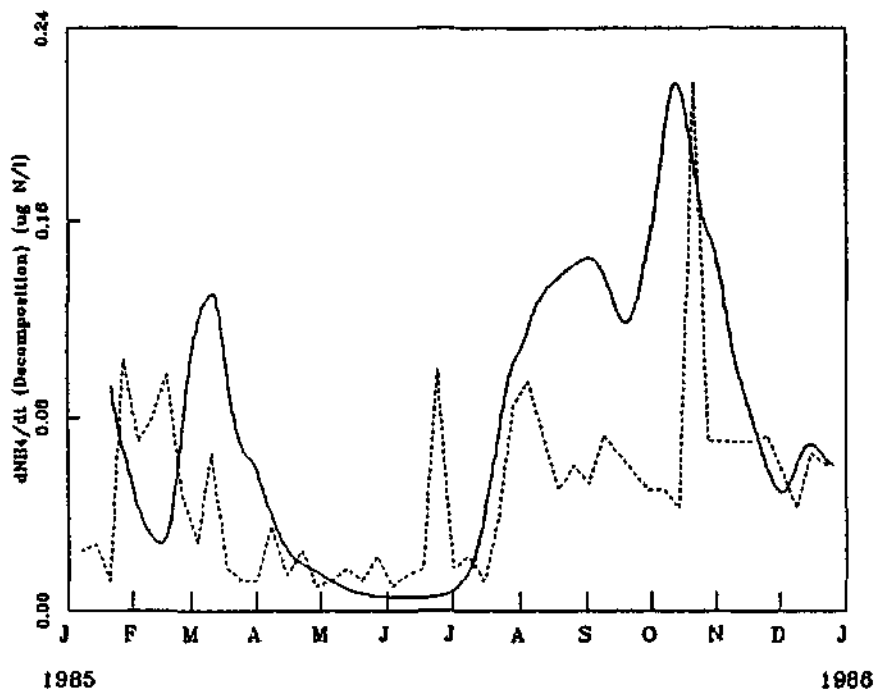


Figure 5.40: values of $\frac{dNH4-N}{dt}|_{Dec.}$ as computed by the model (solid line). The measured $PO_4$ concentration data are shown for comparison purposes (dashed line).

# Chapter 6

# Effect of River Flow on Algal Behaviour

## 6.1 Introduction.

Up to this point it was assumed that the effect of changes in river flow on algal growth is negligible compared to the effects of temperature, light and nutrient concentrations. As agreed before we will refer to the model described in the previous chapters, which was based on this assumption, as the *stationary* model. Since the results of simulations with this stationary model compared well with measured river data, the assumption seems to be justified, at least for the Stilfontein site in the river. One of the reasons for this good correlation is that, even though flow effects were not incorporated explicitly, they were included into the model implicitly during the calibration of many of the parameters (it would be recalled that values were assigned to many parameters during calibration by fitting model output onto measured chlorophyll-*a* concentrations). However, the disadvantage of this is that, whenever flow conditions change significantly, the model would have to be recalibrated.

Thus it was desirable to include flow effects explicitly. To do this, one of two approaches could be followed:

- By running an existing program modelling river flow, and using the flow results as input for the main algal growth model, or
- By developing a flow module which could be included as part of the main algal growth model.

We decided on the second option for a number of reasons. In the first place, modelling the interaction between flow and algal growth could be considerably simplified by not using an external program to calculate the flow. If an external program were to be used, the complete flow profile would first have had to be calculated, stored in a file and then

used as input for the algal growth model. With the flow simulation included as a module in the main model, on the other hand, the flow results obtained at each time step could be used directly by the rest of the model. Secondly, including the flow as a module within the larger model leads to a single complete dynamical system modelling algal growth, which may be easily extended or simplified to suit particular needs.

## 6.2 Basic equations of unsteady flow.

Because of the large number of factors influencing river flow, exact modelling of river discharge is not possible. At best we can, by making various simplifying assumptions, build a mathematical model which idealises the real situation, whilst leading to a system of equations that can be handled numerically. This subject has received much attention in the past, and the theory behind the modelling of river flow is well documented (Mahmood and Yevjevich, 1975; Roache, 1977; Shen, 1977; Garcia-Navarro and Saviron, 1992).

The Vaal River is characterised by the following properties:

- The river can be viewed as an open channel.
- This channel has a slight slope and the channel walls and bottom make only small angles with the channel axis.
- The channel geometry is roughly prismatic.
- The flow in the channel is unsteady, but only slightly so.

In the light of the properties mentioned above, the following simplifying hypotheses can be made regarding the flow:

- The flow is one-dimensional, i.e. the velocity is uniform over the cross section. The centrifugal effect due to channel curvature is negligible.
- The vertical distribution of pressure within the cross section is hydrostatic, i.e. the vertical acceleration is neglected and the density of the fluid is assumed to be constant. This can be expressed mathematically by the relation

$$p = \rho g(h - z), \quad z \leq h$$

  where $z$ is the vertical coordinate, $h$ is the water depth, $\rho$ is the water density and $g$ is the gravitational acceleration.
- The effects of boundary friction and turbulence (which only appear in a thin layer close to the boundary) can be represented by the introduction of a force of resistance.

Under these hypotheses it is possible to describe the flow by means of two equations (see Roache (1977) for more details), namely the continuity equation

$$\frac{\partial A}{\partial t} + \frac{\partial Q}{\partial \xi} = 0 \tag{6.1}$$

and the momentum equation

$$\frac{\partial Q}{\partial t} + \frac{\partial}{\partial \xi}(\frac{Q^2}{A} + \frac{1}{2}gAh) = gA(S_0 - S_f), \tag{6.2}$$

where $\xi$ denotes the coordinate in the direction of the flow, $Q$ the discharge, $A$ the cross-sectional area of the channel, $S_0$ the channel slope and $S_f$ the friction slope. (These equations are also known as the Saint-Venant equations.)

From this system of equations it follows that we are dealing with two dependent variables, namely the discharge, $Q$, in the $\xi$-direction, and the cross-sectional area, $A$. $A$ and $h$ are related through the equation $A = \frac{1}{2}(w_t + w_b)h$, where $w_t$ and $w_b$ denotes the top- and bottom width of the channel, respectively.

In the Saint-Venant equations (6.1, 6.2), the effect of boundary friction and turbulence is represented by the friction slope, $S_f$, which is usually estimated by using Manning's formula:

$$S_f = \frac{Q^2 n^2}{A^2 R^{4/3}} \tag{6.3}$$

where $n$ is Manning's roughness factor and $R$ is the hydraulic radius, defined as the cross-sectional area, $A$, divided by the wetted perimeter. An alternative representation of the friction slope is given by Chezy's formula:

$$S_f = \frac{Q^2}{CA^2R} \tag{6.4}$$

where $C$ is Chezy's coefficient.

## 6.3 Numerical solution of the Saint Venant equations

Even in their simplified versions, the Saint Venant equations (6.1, 6.2) are still a system of nonlinear hyperbolic first order partial differential equations, which cannot be solved analytically except in a few special cases. General solutions, therefore, can only be obtained numerically. Due to the nonlinear nature of the equations, it is known that numerical solutions may lead to spontaneous discontinuities. For this reason the choice of a method of solution for the Saint Venant equations is very important.

Over the years, many numerical schemes have been developed to solve the flow equations (Mahmood and Yevjevich, 1975; Roache, 1977; Shen, 1977; Garcia-Navarro and Saviron, 1992; Lax and Wendroff, 1960). Most of these schemes fall into one of two groups, namely those using the Method of Characteristics (MOC) and those using Finite Difference (FD) methods. Within the group of finite difference schemes, a wide variety of methods can again be found, which can be subdivided into explicit and implicit finite difference schemes.

### 6.3.1 The McCormack scheme

From this vast array of possible numerical solution methods a scheme had to be found which would be best suited to our needs. While there is no general criterion to say which numerical scheme really is the "best", some schemes do seem better suited for certain uses. In the present case the purpose was to find a scheme which is as simple and computationally efficient as possible, while still giving good, stable results under all conditions dictated by the model and its input data. For instance, the flow in the Vaal River is fairly regular, with a gradual slope, and does not necessitate the use of an unconditionally stable, very robust method like an implicit finite difference method. Instead an explicit method can be used which is easier to apply and much cheaper on computational time, whilst still being completely stable under normal flow conditions.

The numerical method chosen for the modelling of flow in the Vaal River, is therefore an explicit finite difference method based on the McCormack scheme (see Garcia-Navarro and Saviron (1992), Lax and Wendroff (1960) and the references therein), which, provided that the Saint Venant equations (6.1,6.2) are written in the compact form

$$\frac{\partial U}{\partial t} + \frac{\partial F(U)}{\partial \xi} = H(U, \xi, t), \tag{6.5}$$

computes the solution at time $t = (n+1)\Delta t$ and position $\xi = i\Delta\xi$ by means of the following predictor-corrector scheme:

$$U_i^{(1)} = U_i^n - \frac{\Delta t}{\Delta \xi}[(1-\epsilon)F_{i+1}^n - (1-2\epsilon)F_i^n - \epsilon F_{i-1}^n] + \Delta t H_i^n \tag{6.6}$$

$$U_i^{n+1} = \frac{1}{2}(U_i^n + U_i^{(1)}) - \frac{\Delta t}{2\Delta\xi}[\epsilon F_{i+1}^{(1)} + (1-2\epsilon)F_i^{(1)} + (\epsilon - 1)F_{i-1}^{(1)}] + \frac{\Delta t}{2} H_i^{(1)} \tag{6.7}$$

The McCormack scheme is second order accurate in space and time and is a shock-capturing technique. Its main advantage is its ability to handle both calculations of slowly varying flows as well as rapidly varying ones. It is also computationally efficient since it uses one-sided differences (forward or backward) to replace the spatial derivative. This has three advantages over the more common techniques using centered differences:

- the program logic is simple because all dependent variables are calculated over the primary mesh points.
- the inclusion of the free term (the friction term) is trivial
- due to its simplicity it can easily be generalised to several space dimensions

The numerical scheme (6.6, 6.8) also contains a variable $\epsilon$ which can take one of the two values $\epsilon = 0$ or $\epsilon = 1$, leading to a forward- ($\epsilon = 0$) or backward ($\epsilon = 1$) difference scheme. Some authors have suggested applying the two versions cyclically permuted to obtain best results, but it was found that for the present application satisfactory results are achieved using only the forward difference scheme.

### 6.3.2 Boundary and initial conditions

Like all finite difference schemes, the McCormack scheme allows the numerical solution of the flow to be advanced from one time-step to the next for all the computational points in a grid row except for the first and last ones. In order to obtain the full solution, boundary conditions must therefore be specified. For a hyperbolic partial differential equation to have a unique solution, a full set of initial conditions, $Q(t = 0, \xi)$ and $A(t = 0, \xi)$, as well as two boundary conditions, need to be specified. In the case of normal river conditions (i.e. sub critical flow), one boundary condition is needed at the upstream end of the channel, while the other must be at the downstream boundary.

Once one of the flow variables, $A$ or $Q$, is specified at the upper boundary, the other can solved for, using the method of characteristics (Jorgensen, 1979). (This method provides a relation between the variables $Q$ and $A$, so that one variable can be uniquely determined once the other is specified.)

A similar situation prevails at the lower end of the reach, i.e. one of the variables $Q$ or $A$ needs to be specified, and the other can be calculated using the MOC. Here the situation is rather more complex however, since in the simulation of river flow, the downstream boundary conditions are generally unknown, and form part of the solution being sought. The only information available at this boundary is the relation between $Q$ and $A$ given by the characteristics. In order to calculate $Q$ and $A$, we thus need another relation between the two variables. This is a general problem for which no "ideal" solution exists.

The strategy used in the current application to overcome this problem was to calculate a relation by means of interpolation between the two variables at a point higher up in the computational reach, far from the lower boundary. Using this relation between $Q$ and $A$, together with the relation obtained from the MOC, it was possible to obtain an equation involving only one of the variables, which could be solved using the Newton-Raphson method. The second variable could then be determined as before using the MOC. The resultant boundary condition obtained in this way was tested for stability, and satisfactory results were obtained even for extreme flow conditions and long time integrations.

## 6.4 Incorporating flow effects into the algal growth model.

For the sake of simplicity, the flow model was first added to the basic light-temperature algal growth model only. This is a much easier exercise than adding the flow to the full growth model, which is very complex in its own right. Once the difficulties in merging the river flow model into the algal growth model were sorted out using the basic model, the flow was finally added to the full stationary growth model.

In order to incorporate flow effects into the stationary growth model, the latter had to be modified to make provision for a space as well as a time coordinate.

The basic equation describing algal growth,

$$\frac{dx}{dt} = (-k_D + F_G(t,x,y))x \tag{6.8}$$

was extended to include the effect of discharge, in the following way:

Consider a control volume $V$ as shown in Figure 6.1. The rate of change in algal biomass in this volume is equal to the rate of change in biomass of algae within the volume (governed by their growth rate and dying rate), plus the biomass flowing per unit time into the volume through the surface $S$, minus that flowing out of the volume per unit time.

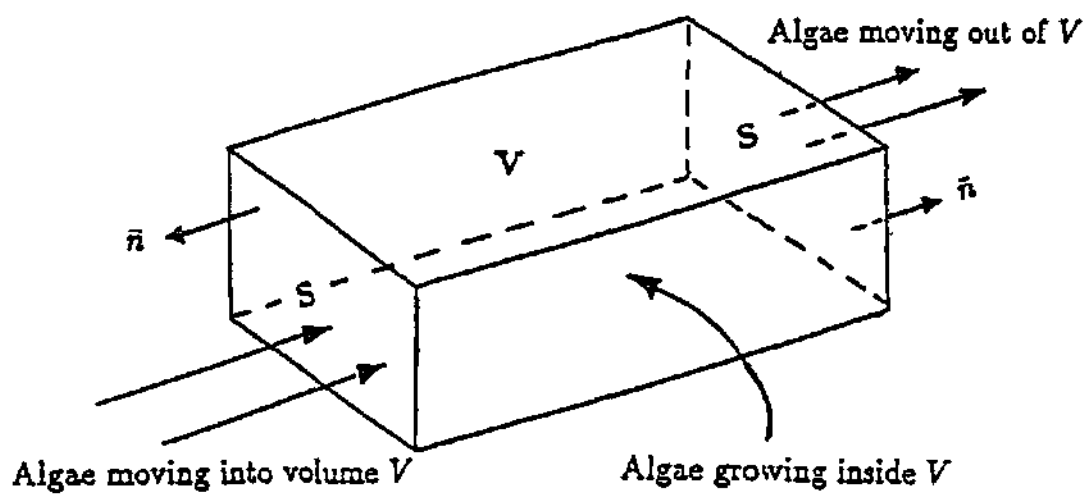


Figure 6.1: Graphic representation of the change in algal concentration due to the flow.

Mathematically, this can be written as

$$\begin{aligned} \text{Rate of change in algal biomass} &= \text{Rate of change within volume due to growth} \\ &\quad + \text{Rate of change due to inflow and outflow} \\ &= \int_V \frac{\partial x}{\partial t} dV + \int_S (x)\underline{U}.\underline{n} dA, \end{aligned}$$

where $\underline{U}$ is the velocity of the flow, and $\underline{n}$ is a unit vector perpendicular to the surface $S$ (see Figure 6.1).

Applying the Divergence theorem to the second term in the above equation, we get

$$\text{Rate of change in algal biomass in } V = \int_V (\frac{\partial x}{\partial t} + \underline{\nabla}.(x\underline{U}))dV$$

The quantity being integrated now represents the local rate of change in algal biomass concentration, and since only one spatial dimension is used, the equation describing algal growth can be rewritten as

$$\frac{\partial x}{\partial t} + \frac{\partial (xU)}{\partial \xi} = (-k_D + F_G(t,x,y))x. \tag{6.9}$$

Similarly, the equation for the dead algae, $y$, in suspension in the water becomes

$$\frac{\partial y}{\partial t} + \frac{\partial (yU)}{\partial \xi} = k_D x - k_S y. \tag{6.10}$$

The term $\partial(xU)/\partial\xi$, which represents the effect of flow, is replaced by a simple second order finite difference approximation in the actual computer program which solves the model equations numerically.

## 6.5 Calculated effects of river flow on algal growth

Various numerical simulations were performed with the new dynamic model. In a first set of experiments, all variables such as light and temperature were kept constant over the whole spatial reach. Thus the environmental conditions at every point in space were identical, and the only condition that was varied was the river flow. In all the experiments flow was taken to be initially constant, with a discharge of 40 $m^3s^{-1}$ and depth of 5 m. The flow channel was specified as having a rectangular cross section, with a width of 40 m. Furthermore the channel was assumed to have zero inclination and to be perfectly smooth ($S_0 = S_f = 0$). Although this simplification is not acceptable in the simulation of real river conditions, such a simplified system can still provide important insights into the basic effect of water flow on algal growth.

All experiments were conducted over a spatial reach of 100 km, and growth was simulated for a time period of 80 days, using two algal groups.

In order to obtain a reference, a first simulation was conducted with the flow discharge kept constant at 40 $m^3s^{-1}$. The result of this is shown in Figure 6.2. As expected, there was no spatial variation in algal growth, since conditions at every point in the spatial reach were identical at all times.

To study the effect of the flow on algal growth, we performed two numerical experiments with the model. In the first, the flow was smoothly oscillated, according to a sine curve, between 20 $m^3s^{-1}$ and 60 $m^3s^{-1}$, with all other variables constant in space (Figure 6.3). In the second, the flow was varied much more drastically. In this case the discharge was kept constant at 40 $m^3s^{-1}$ for some time, and then sharply increased over a very short time to 200 $m^3s^{-1}$. The discharge was kept constant at 200 $m^3s^{-1}$ for the remainder of the computation. This result is shown in Figure 6.4. Both of these figures are virtually identical to the reference case where flow was kept constant.

The results of this first set of simulations may appear surprising at first sight, but can be explained as follows:

If we consider a fixed volume of water in the river, the water flow causes some concentration of algae to flow out of this control volume. At the same time, however, some concentration of algae also move into the volume. Now if all the environmental parameters are constant over the whole reach being modelled, and if the same potential for algal growth is present at each point in space, the concentration of algae flowing out of the control volume will be more or less equal to the concentration of algae moving in, unless the flow varies drastically over a very short space. Therefore, under these circumstances, the direct effect of river flow on algal growth is simply to move the algae along, and so if there is a similar concentration of algae everywhere in the river, this effect will be negligible.

Of course, this can only happen if all significant environmental factors affecting algal growth are constant over the whole reach of the river being modelled (typically a stretch of approximately 100 kilometers). It is well known, however, that in an actual river the concentrations of algae at any given time do show variations from one point to the next. The fundamental reason for this is that, in a river, environmental factors are *not* constant over such a long spatial reach. Temperature variations of a number of degrees Celsius are not uncommon, light availability may vary, and nutrient concentrations most definitely vary. For this reason it is most necessary to also take these variations into account.

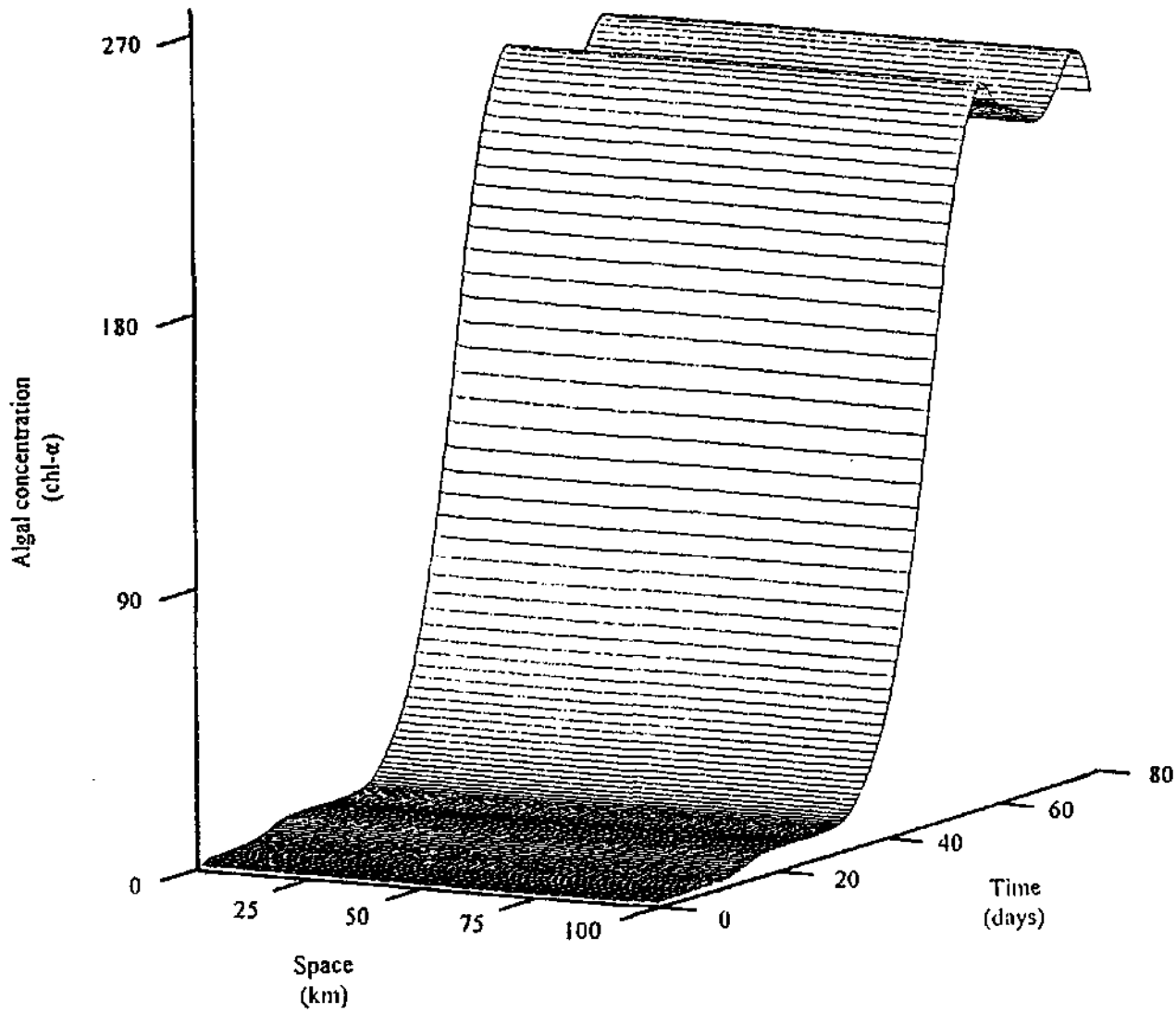


Figure 6.2: Reference algal growth profile. River flow and environmental parameters kept constant in space.

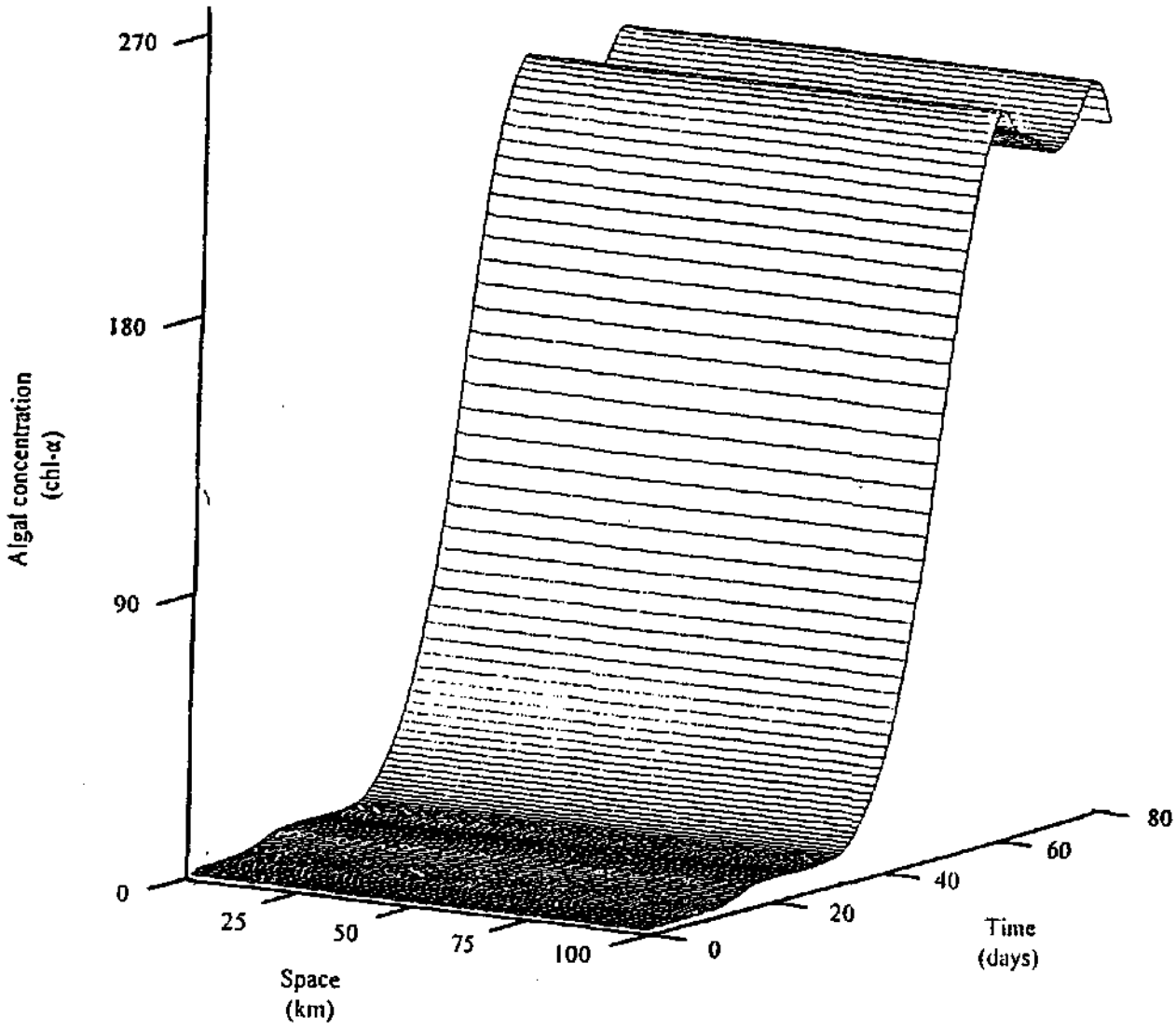


Figure 6.3: Algal growth profile under the influence of gradually varied river flow. All other parameters kept constant in space.

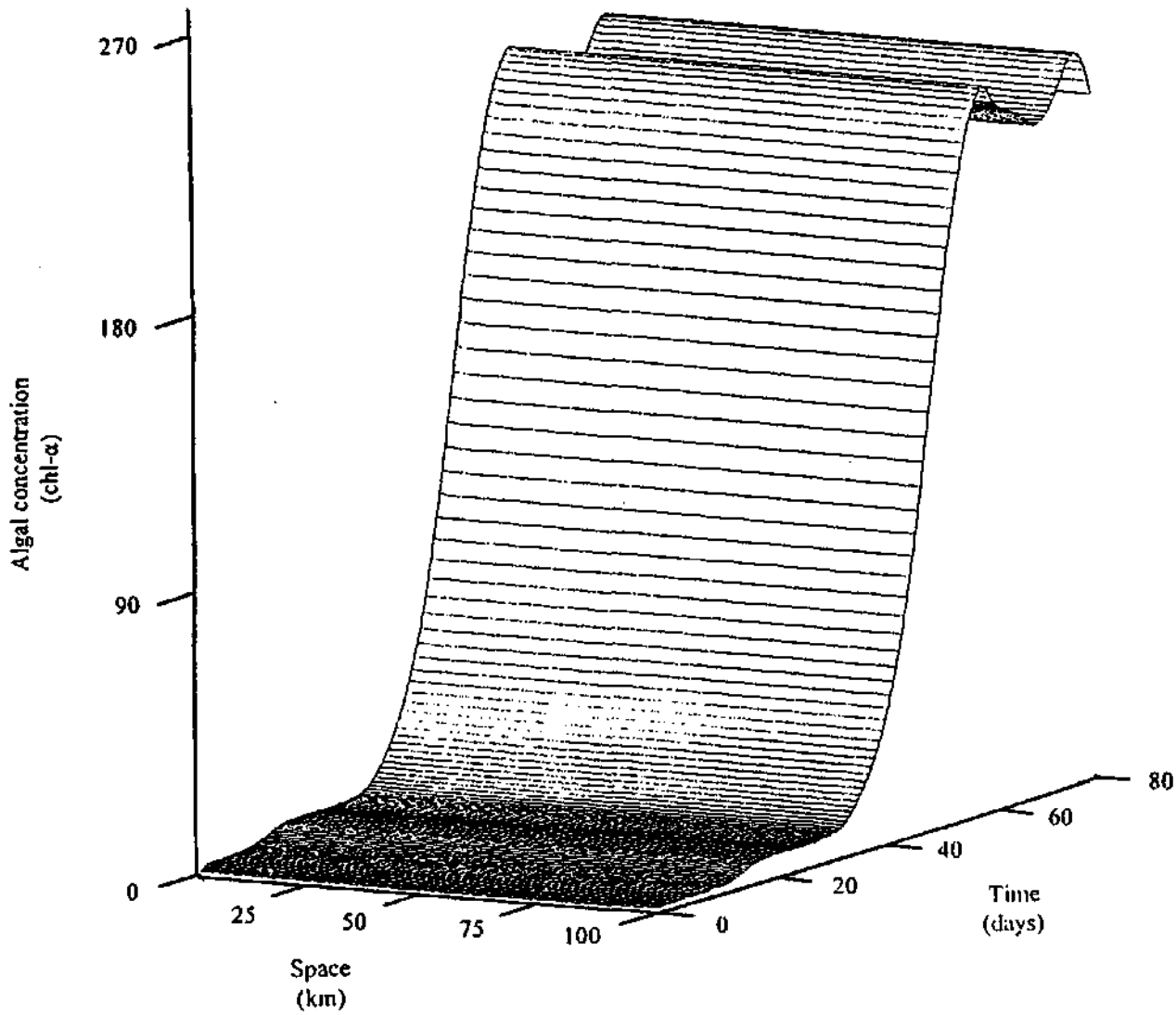


Figure 6.4: Algal growth profile under the influence of drastically varied river flow. All other parameters kept constant in space.

## 6.6 The effect of spatial temperature variations on algal growth.

We next discuss the effect of varying environmental parameters *together with* the flow. From a sensitivity analysis conducted with the stationary model (described in chapter 7), it is clear that temperature variations have the most pronounced effect on algal growth. For this reason, and to avoid an unnecessarily complicated exposition, we shall limit ourselves at this point only to temperature variations together with flow.

To illustrate the effect of temperature variation on algal growth, the temperature was varied linearly in space, with the temperature at the end of the reach being 1° Celsius higher than that at the beginning of the reach over the whole time period. For a reference simulation the flow was kept constant, so that only the effect of temperature could be seen. The resultant growth profile is shown in Figure 6.5. From this profile it is clear that even a 1° C change in temperature over a distance of 100 km would have a pronounced effect on the algal growth profile.

Since the temperature variation caused strong spatial variation in algal concentrations, it seemed logical to expect that the effect of flow would no longer be negligible, because the concentration of algae moving into a control volume, due to the flow, was no longer necessarily equal to the concentration of algae moving out of the volume.

Further simulations were therefore done with the same temperature variation as in the control simulation described above, but this time with various non constant flow profiles.

Figure 6.6 shows the results of a simulation in which the flow was allowed to oscillate smoothly between 20 $m^3s^{-1}$ and 60 $m^3s^{-1}$, as before. Clearly, no changes due to flow effects are visible. An explanation for this is that the variation in flow was not severe enough to visibly influence the algal growth profile.

In another simulation, flow was varied more severely, with the discharge kept constant at 40 $m^3s^{-1}$ for some time, and then sharply increased over a very short time to 200 $m^3s^{-1}$. The discharge was kept constant at 200 $m^3s^{-1}$ for the remainder of the time. This results are shown in Figure 6.7. To show clearly that this type of drastic flow variation does indeed have a visible effect on algal growth, parts of Figures 6.5 and 6.7 were magnified in Figure 6.8.

Even in such a simulation with severe flow variations, however, the effect of flow on the algal growth profile was minimal (the algal concentration never changed by more than approximately 1% due to the flow). This effect may seem small considering the large variation in discharge, but it should be kept in mind that it is not the discharge as such, but rather the *velocity* of the flow, that influences the algal growth profile. In the simulations discussed above, a channel width of 40 m was used. This meant that the cross sectional area, $A$, was large, and so the flow velocity, defined as the discharge divided by the cross sectional area ($U = Q/A$), showed a much smaller variation than the discharge itself.

As said before, the reason that a visible effect of the flow *was* visible in the last set of simulations, while no effect was seen in the constant temperature experiments, is that the algal concentrations were not constant in the spatial dimension. Therefore, when the discharge was increased, a spatial "shift" of the algal concentrations took place. The flow caused algae that grew well at a certain temperature to be transported to a region in space where the temperature was no longer ideal for their growth. At the same time algae that were present in a region where temperature conditions were not ideal for optimum growth were moved to a more optimal temperature region, and grew accordingly. Since the flow remained constant after the sharp rise, algal concentrations were soon adapted to their new levels, and further flow influences were negligible.

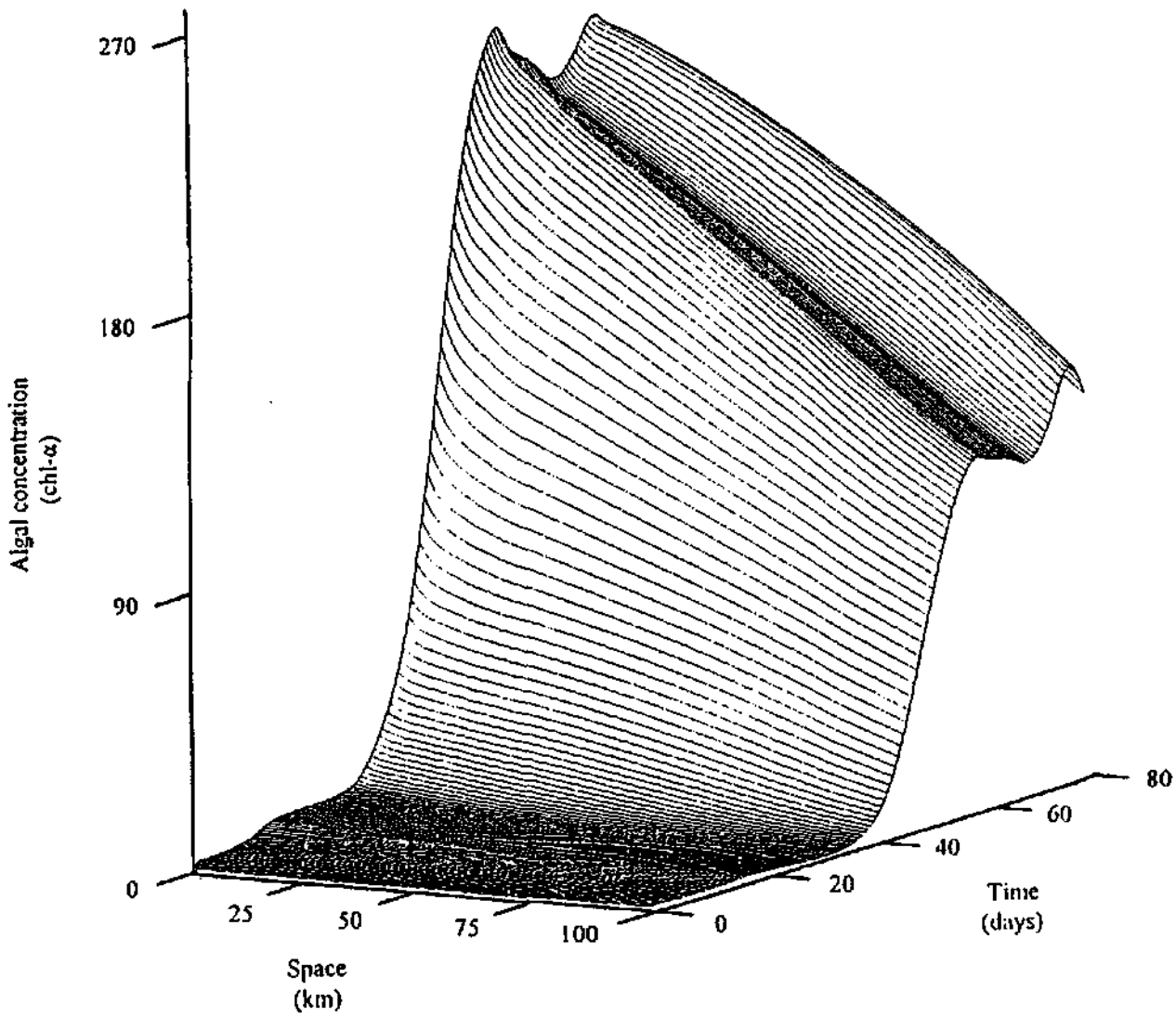


Figure 6.5: Reference algal growth profile. Temperature is linearly varied along the reach. River flow and all other environmental parameters are kept constant in space.

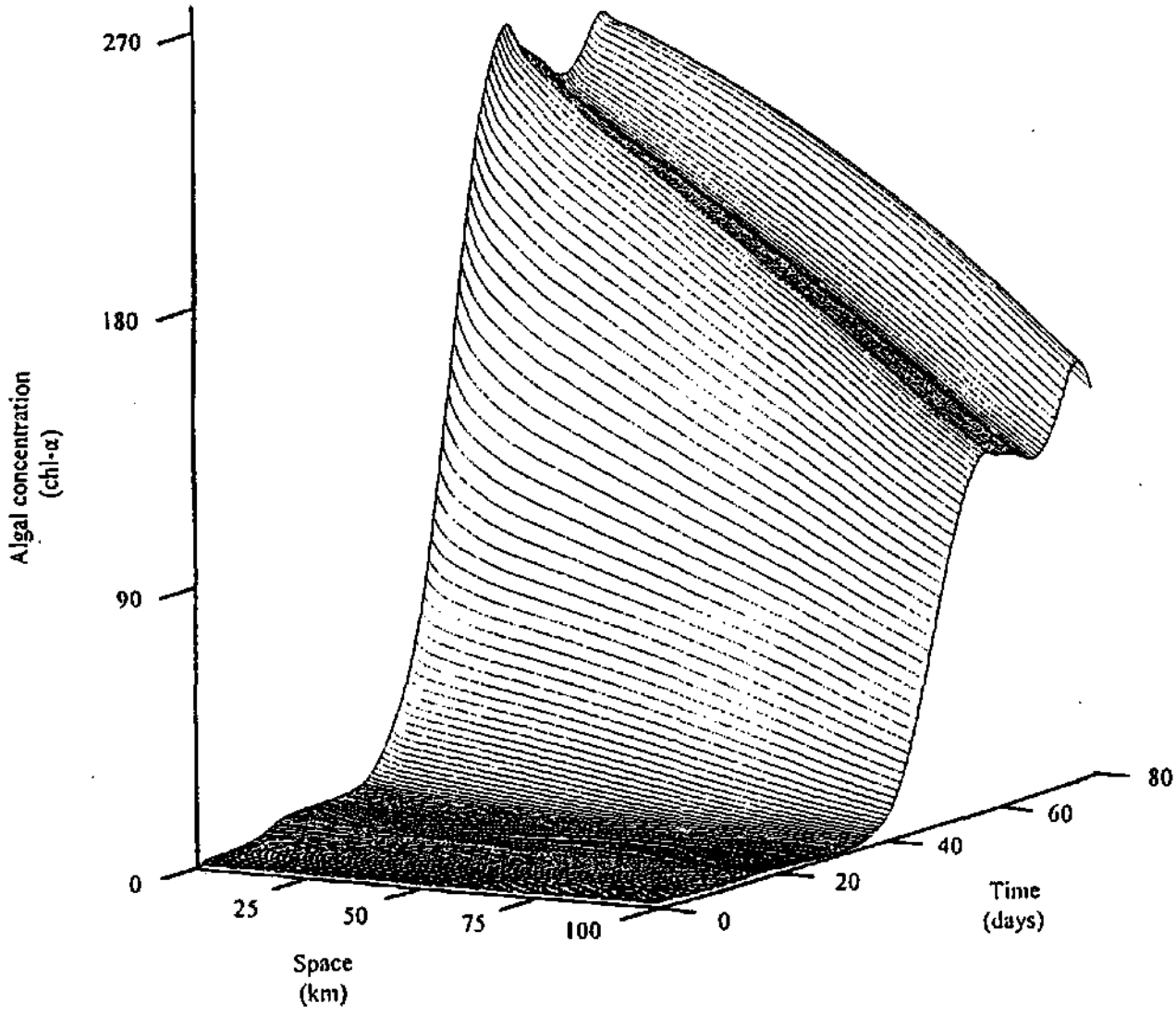


Figure 6.6: Algal growth profile affected by linearly varied temperature and gradual variations in river flow. All other parameters are constant in the space dimension.

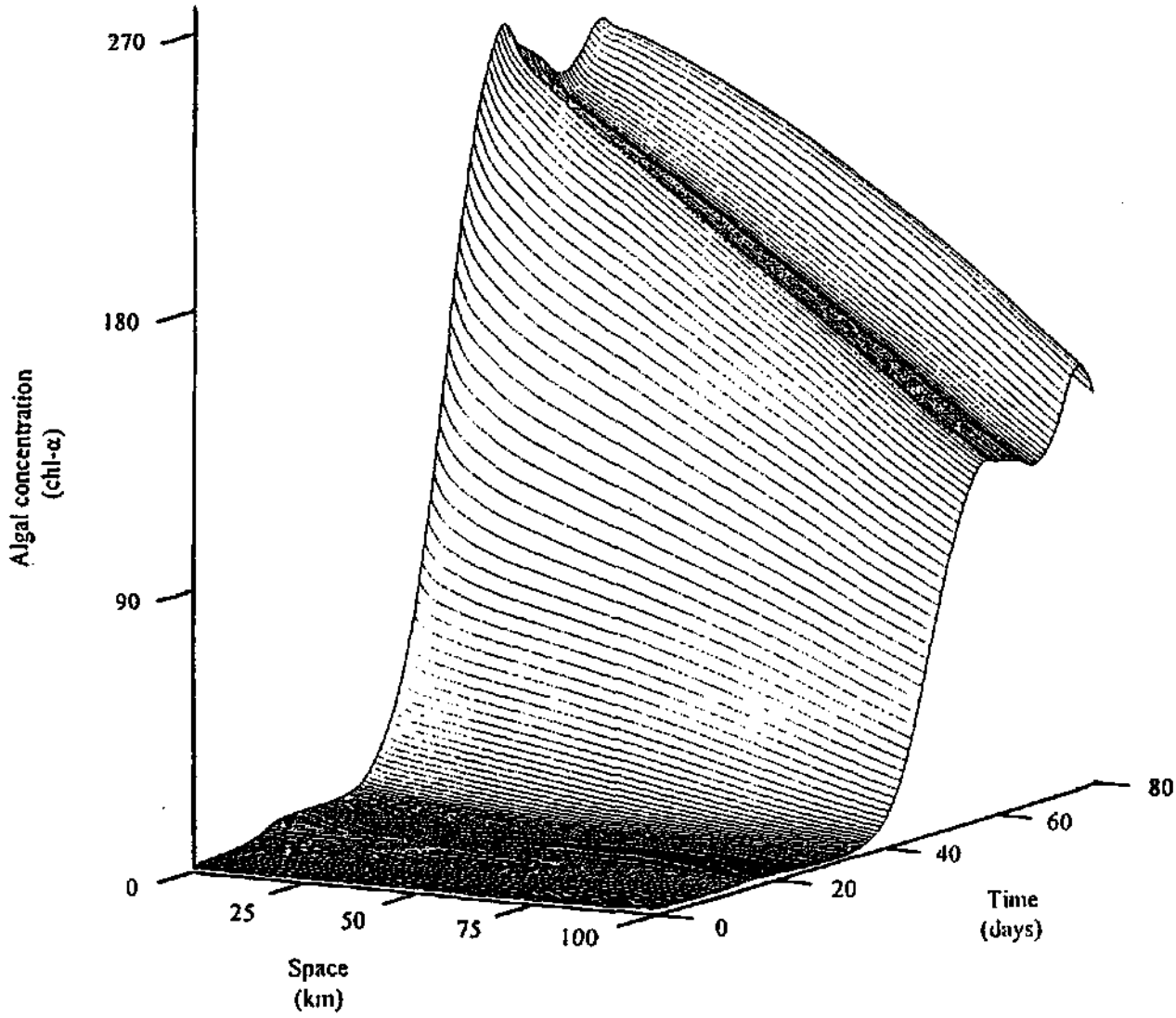


Figure 6.7: Algal growth profile affected by linearly varied temperature and drastic variations in river flow. All other parameters are constant in the space dimension.

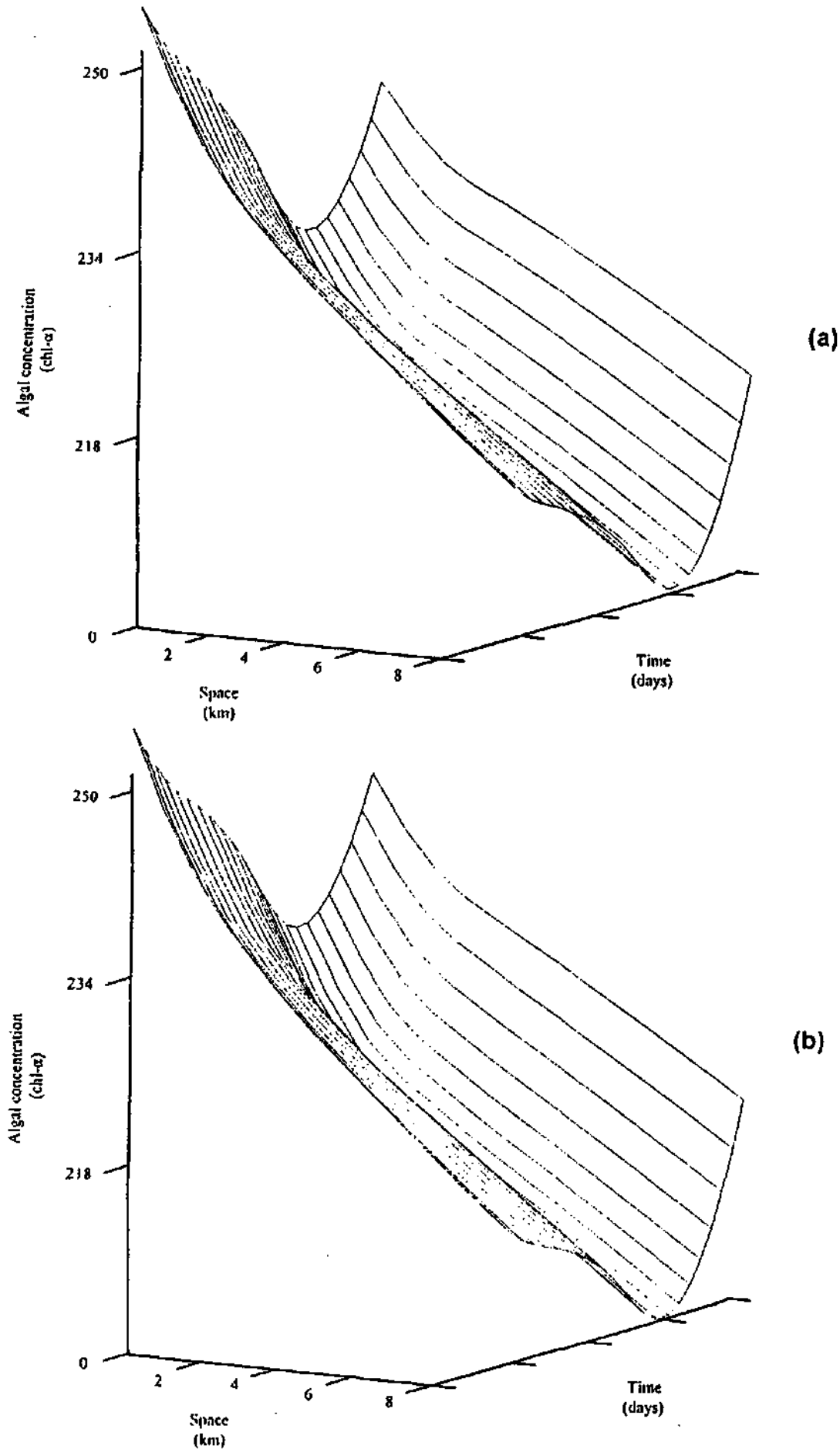


Figure 6.8: A magnified view of parts of the growth profiles in Figures 6.5 and 6.7, to accentuate changes due to flow variations.

# Chapter 7

# Sensitivity tests.

This chapter contains the results of various sensitivity tests of the model. These were typically performed by measuring variations in simulated chlorophyll-*a* concentration (i.e. model output) when varying input data by specified amounts.

All tests were carried out by using the simulated chlorophyll-*a* profile at Stilfontein during 1985 as a reference. (As shown earlier in this report, this particular profile corresponds very well with measured chlorophyll-*a* values.) Input parameters were then varied, one at a time, by a certain percentage, and simulated chlorophyll-*a* concentrations were recomputed and compared to the reference profile. There were typically three types of deviations from the reference profile:

1. Changes in the heights of the peaks (algal blooms) without affecting the overall shape of the profile too much.
2. Changes in the shapes of the peaks, without too much variation in their heights.
3. Shifts of the peaks along the time axis.

In an attempt to distinguish between these possibilities, two sensitivity coefficients $S_{val}$ and $S_{shape}$ were defined to describe amplitude and shape variations respectively:

$$S_{val} = \sqrt{\frac{\sum_t [\sum_{i=algae}(x_{i_1}(t) - \tilde{x}_{i_1}(t))]^2}{\sum_t [\sum_{i=algae} \tilde{x}_{i_1}(t)]^2}} \tag{7.1}$$

and

$$S_{shape} = \sqrt{\frac{\sum_t [\sum_{i=algae}(x'_{i_1}(t) - \tilde{x}'_{i_1}(t))]^2}{\sum_t [\sum_{i=algae} \tilde{x}_{i_1}(t)']^2}}, \tag{7.2}$$

where $x_{i_1}(t)$ represents the concentration of living algae of the i-th algal group at time $t$ and $x'_{i_1}(t)$ its time-derivative. Symbols with a " ˜ " on top refer to the reference data set.

The parameters considered were nitrogen concentration ($N$), phosphorus concentration ($P$), the $N/P$ ratio, light available for growth ($I$), turbidity $Tur$, and water temperature

$T$. In each test each of these parameters were varied quite independently, keeping all the others at the reference values. In the case of the three nutrient parameters these variations were of course quite artificial, since normally changes in $P$ and/or $N$ would also affect $N/P$, whereas, for the purpose of the sensitivity analysis, these parameters were treated as if they were completely independent of one another. When varying any of the parameters off the reference values, care was taken to ensure that its perturbed values remained realistic in the Vaal River context, in the sense that they were still well in the range of all available reported measurements.

Values of the sensitivity coefficients $S_{shape}$ and $S_{val}$ were calculated in the case of each of the parameters, for variations of between 50% below and 50% above the reference values. The results are displayed graphically in Figures 7.1 and 7.2. Note that the nearer each curve is to vertical, the more sensitive the model is for variations of the corresponding parameter.

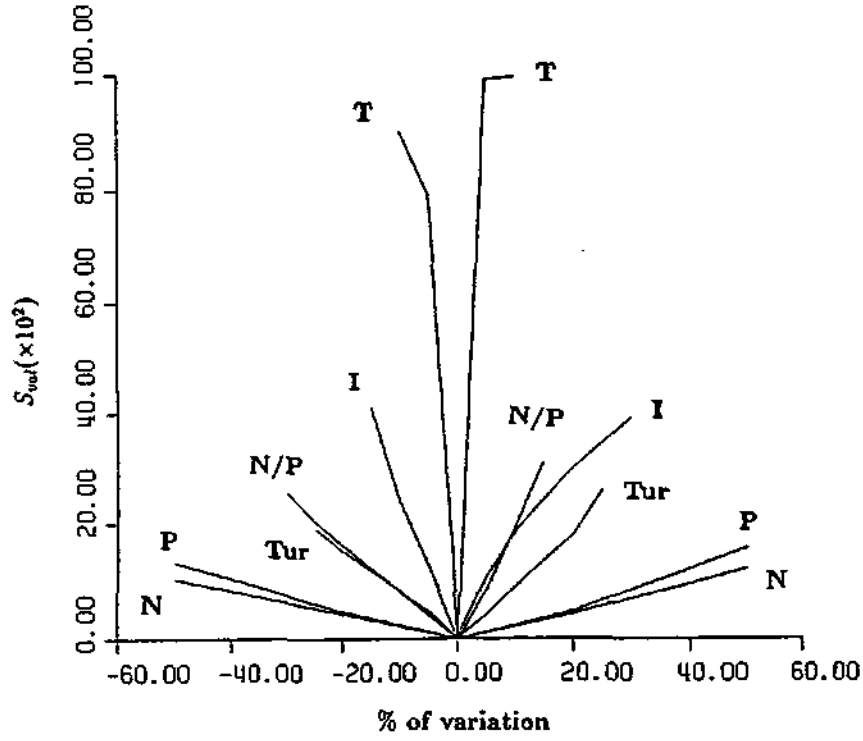


Figure 7.1: The sensitivity coefficient $S_{val}$ as a function of variations in $N$, $P$, $N/P$, $T$, $I$ and $Tur$. More vertical graphs correspond to parameters for which the model is more sensitive.

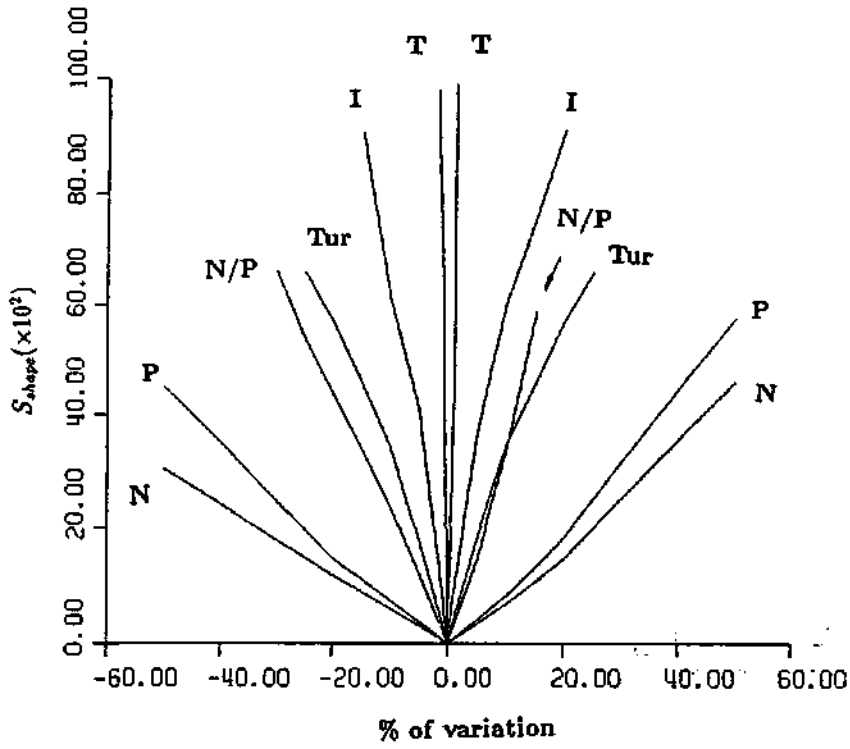


Figure 7.2: The sensitivity coefficient $S_{shape}$ as a function of variations in $N$, $P$, $N/P$, $T$, $I$ and $Tur$. More vertical graphs correspond to parameters for which the model is more sensitive.

These figures show clearly that the model is by far the most sensitive to temperature variations, followed by light, turbidity and $N/P$ ratio (more or less in that order, although the sensitivity coefficients for these last three are pretty much of the same order of magnitude). The model is least sensitive to dissolved nitrogen concentration, and only slightly less to dissolved phosphorus concentration.

Figures 7.3 through 7.8 also show deviations in chlorophyll-*a* profiles for certain variations of these parameters. As could be expected, the most dramatic effects are seen when the most sensitive parameter, temperature, is varied off the reference values (see Figure 7.8). In this case not only the heights (amplitudes) and shapes of the peaks in the profile are altered, but the entire profile is changed significantly.

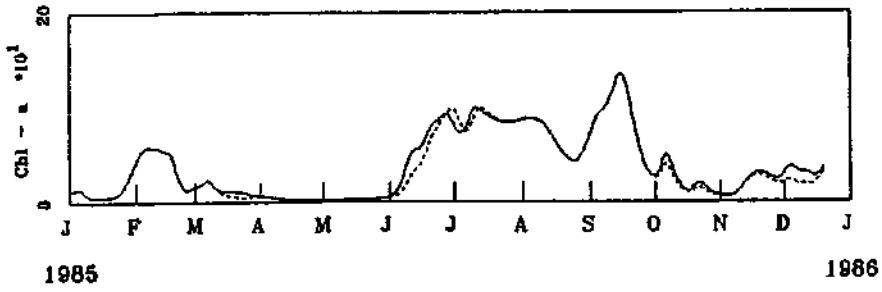


Figure 7.3: Computed Chl-*a* profile for a 50% *increase* in $N$ (smooth line). The reference computed profile is also given for comparison purposes (dashed line).

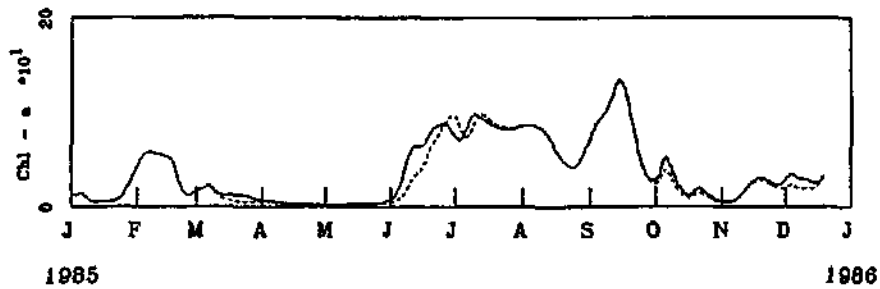


Figure 7.4: Computed Chl-*a* profile for a 50% *increase* in $P$ (smooth line). The reference computed profile is also given for comparison purposes (dashed line).

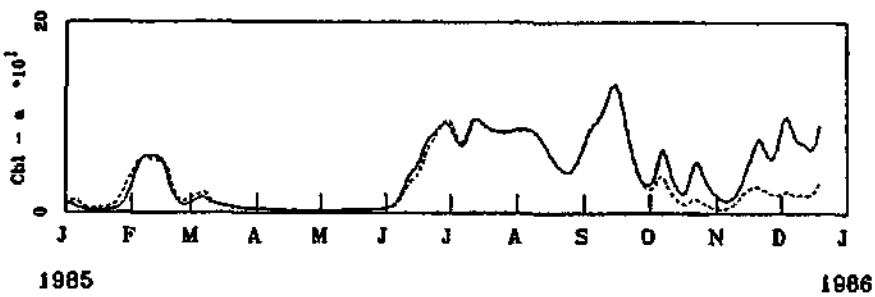


Figure 7.5: Computed Chl-*a* profile for a 15% *increase* in $N/P$ ratio (smooth line). The reference computed profile is also given for comparison purposes (dashed line).

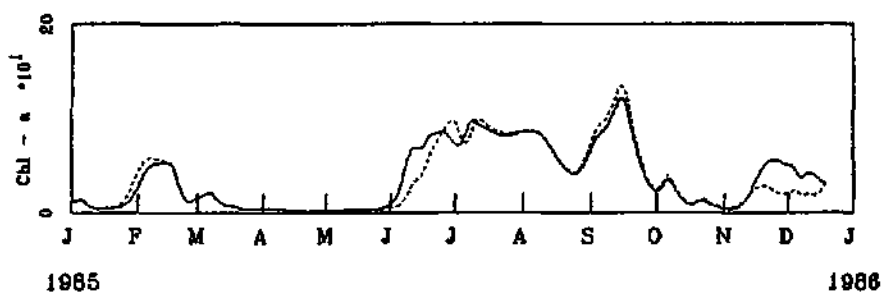


Figure 7.6: Computed Chl-*a* profile for a 25% *increase* in $Tur$ (smooth line).The reference computed profile is also given for comparison purposes (dashed line).

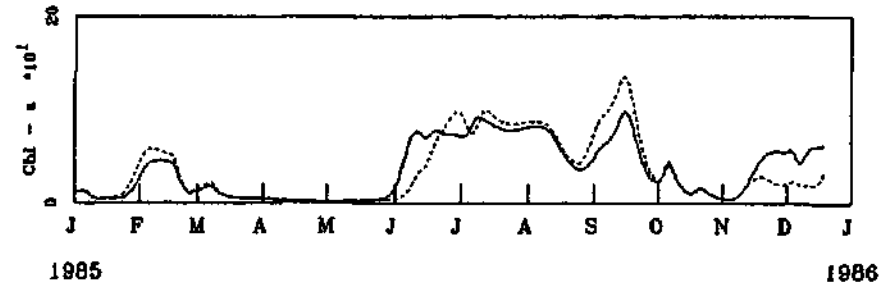


Figure 7.7: Computed Chl-*a* profile for a 15% *decrease* in $I$ (smooth line). The reference computed profile is also given for comparison purposes (dashed line).

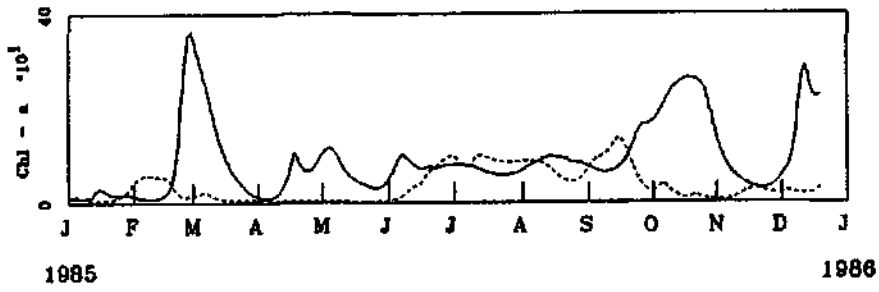


Figure 7.8: Computed Chl-*a* profile for a 20% *decrease* in $T$ (smooth line). The reference computed profile is also given for comparison purposes (dashed line).

The way changes in the various parameters affect the chlorophyll-*a* profile is summarised in Table 7.1 below.

| Parameter | Way profile is affected | | |
|---|---|---|---|
| | Amplitude | Shape | Entire profile |
| $T$ | × | × | × |
| $I$ | × | × | |
| $Tur$ | × | × | |
| $N/P$ | × | × | |
| $P$ | × | | |
| $N$ | × | | |

Table 7.1: Sensitivity properties of $N, P, N/P, Tur, I, T$. Parameters are listed in the order most sensitive to least sensitive.

# Chapter 8

# Verification of the mathematical model

In this chapter the predictive abilities of the static model (described in chapters 1 through 5) are demonstrated.

## 8.1 Verification after calibration with the Stilfontein-1985 data

In chapter 5 a calibration of the model was given, using six algal categories, which enabled a fairly good simulation of the 1985 chlorophyll-*a* profile at Stilfontein during 1985. To verify the model with this calibration, the input data set for the three year period 1985 up to 1987 (displayed in Figures 8.1 through 8.4 ) was used to carry out a simulation over this entire period. The simulated chlorophyll-*a* profile is shown in Figure 8.5. A careful study of this figure reveals that some of the algal blooms during 1986, and also to a less accurate extent some during 1987, are correctly predicted by the model. In Figures 8.6 and 8.7 the computed contribution of two of the individual algal groups are shown, and it would seem that some of the algal groups which bloomed during 1985, were also, at least partly, responsible for algal blooms in 1986 and 1987. It is also evident that, even though the model failed to predict some blooms, it certainly did not predict any spurious blooms (i.e. blooms which were not in fact observed).

It would therefore seem that the calibration up to this point (taking into account that only six algal groups were used) is fairly correct, and that the predictive abilities of the model could be extended by adding more algal groups.

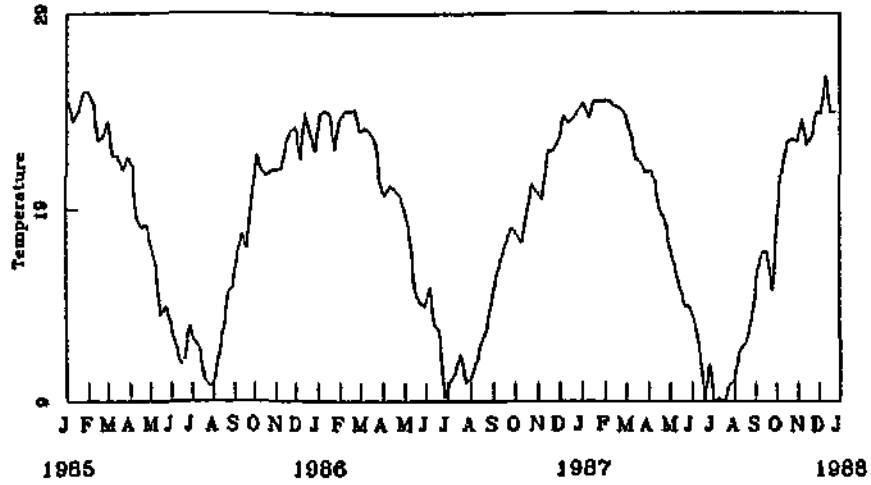


Figure 8.1: Measured temperatures at Stilfontein over the three year period 1985-1987.

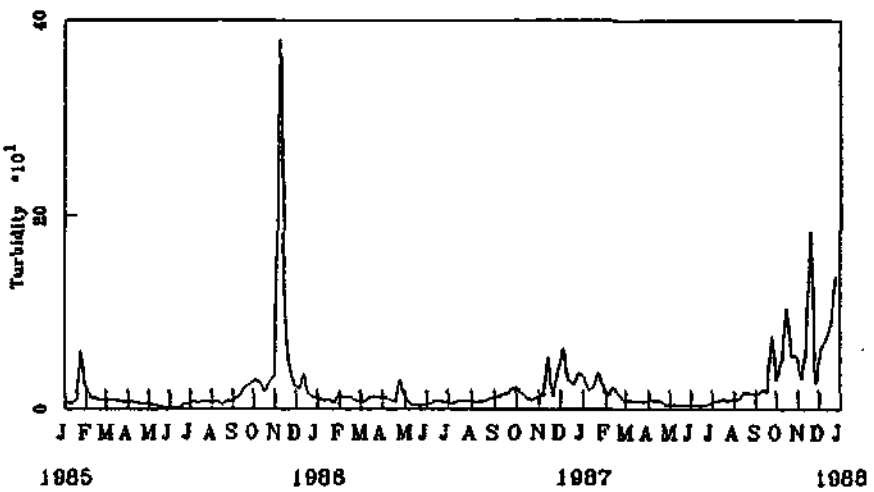


Figure 8.2: Measured turbidity at Stilfontein over the three year period 1985-1987.

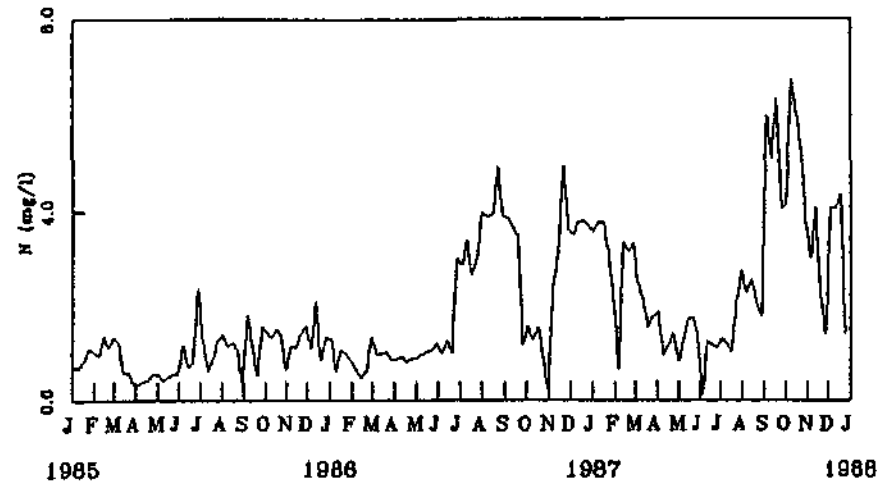


Figure 8.3: Measured dissolved nitrogen concentration at Stilfontein over the three year period 1985-1987.

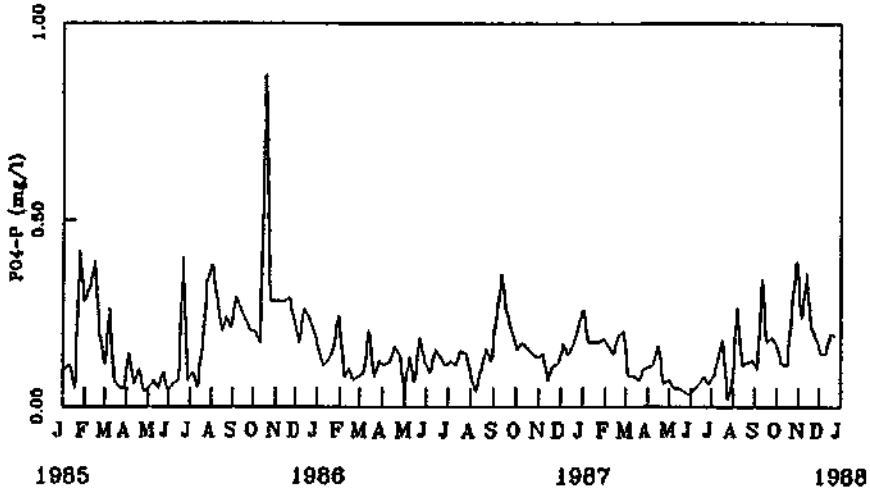


Figure 8.4: Measured dissolved phosphate concentration at Stilfontein over the three year period 1985-1987.

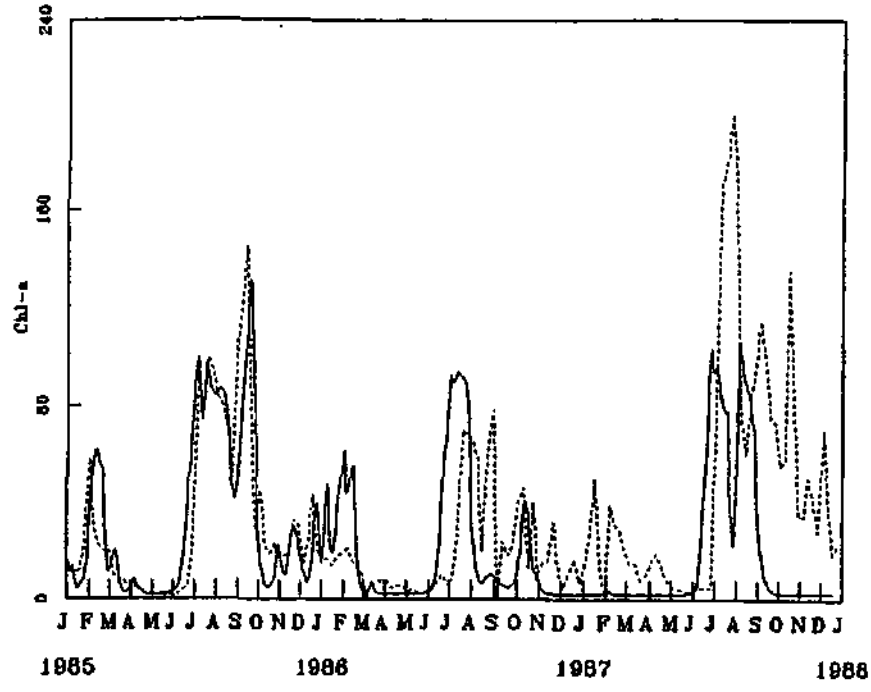


Figure 8.5: Computed total chlorophyll-*a* values over the three year period 1985-1987. Measured data are shown for comparison purposes (dashed line).

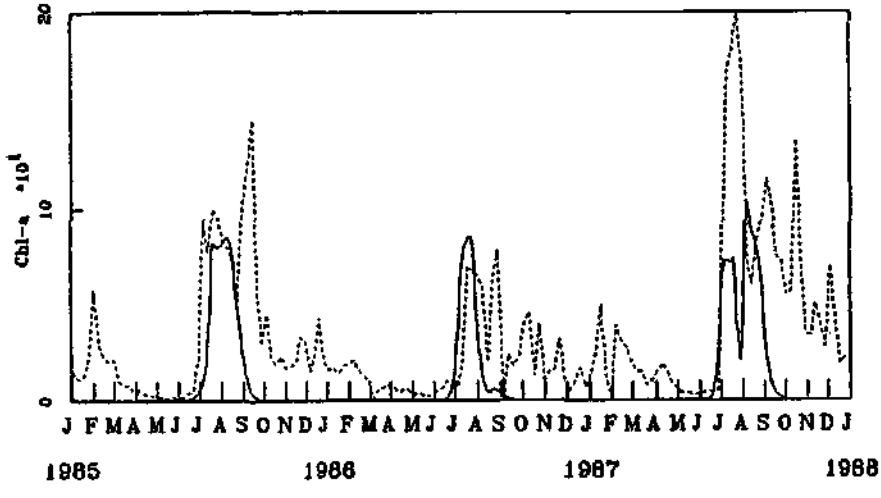


Figure 8.6: Computed contribution of alga 2 towards the total chlorophyll-*a* profile over the three year period 1985-1987. Measured data are shown for comparison purposes (dashed line).

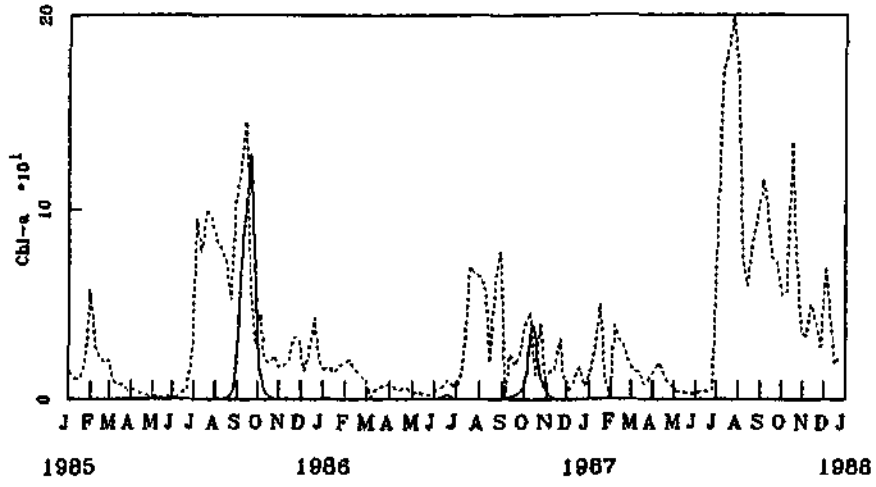


Figure 8.7: Computed contribution of alga 3 towards the total chlorophyll-*a* profile over the 3 year period 1985-1987. Measured data are shown for comparison purposes (dashed line).

## 8.2 Verification of the model calibrated with 14 algal groups

Since the six algal groups used in the calibration of the model using the 1985 data at Stilfontein proved to be insufficient to predict all major algal blooms after 1985, more algal groups had to be added. The parameter set of each of the six current algal groups were left unchanged (since they did not create inconsistencies, such as the simulation of algal blooms which were not observed), and eight more groups were added during a further calibration during which the model output was first fitted onto the 1986 chlorophyll-*a* profile observed at Stilfontein, and then also onto the 1987 observed chlorophyll-*a* profile. The parameter sets associated with the 14 algal groups are listed in Appendix C.

To test the consistency of the new calibration, another simulation over the entire period 1985 to 1987 was performed. The results are shown in Figures 8.8 through 8.10. Then the model, with the improved calibration, was verified by simulating the chlorophyll-*a* profile at Stilfontein during the years 1992 to 1994. The results of this simulation are shown in Figures 8.11 through 8.13. Figures 8.14 through 8.19 also show a comparison between computed and observed pH values during the years 1985 to 1987 and 1992 to 1994. In all cases there is a fair agreement (at least qualitatively) between predicted and observed algal blooms during the years 1992 to 1994. This is also true for the projected pH values.

During the years 1992 to 1994 the genera of dominant algae were recorded during some of the algal blooms. The genera observed are listed in Table 8.1, and Figures 8.20 and 8.21 indicate when each was observed. Figures 8.20 through 8.27 also show the contributions of some of the algal groups used in the model to parts of the 1992 to 1994 chlorophyll-*a*

profile. This breakdown was used to suggest associations between these algal groups and some of the observed genera. These suggestions can be seen in Table 8.2.

| Legend | Chlorophyta | Chrysophyta | Cyanobacteria |
|---|---|---|---|
| a | | Cyclotella | |
| b | | Melosira | |
| c | | Stephanodiscus | |
| d | Chlamydomonas | | |
| e | Trachelomonas | | |
| f | Euglena | | |
| g | | | Oscillatoria |

Table 8.1: Observed genera at Stilfontein during 1992-94. The legends a-g are used in Figures 8.20 to 8.27.

| Algal data bank | Genus |
|---|---|
| Alga 2 | Cyclotella |
| Alga 3 | Cyclotella |
| Alga 8 | Cyclotella |
| Alga 10 | Melosira |
| Alga 11 | Chlamydomonas |
| Alga 13 | Chlamydomonas |
| Alga 14 | Trachelomonas |

Table 8.2: Possible genera of algal groups in the model

The credibility of the calibrated parameter set (and of the model) is enhanced by the fact that this association of algal groups with observed genera did not lead to contradictions, in the sense that one algal group was seen to correspond with one particular genus in some blooms, and with another in other blooms.

On the other hand, although the diatom algal groups 2 and 3 are correctly matched with diatom genera, the nondiatom groups 8 and 10 are also matched with diatom genera! The fact that the model performed well nonetheless is probably due to the fact that these two groups were, both during calibration and verification, involved in fairly small algal blooms. Thus there was no strong depletion of dissolved silicon, so that this nutrient could not have a significant limiting effect on diatom growth.

Finally we wish to point out that the data bank consisting of calibrated parameters for 14 algal groups (of which some seem to correspond to known algal genera) can by no means be considered to be complete. It can, however, be used as a starting point for a further calibration process, in which more data is used to add more algal groups, when required. As the algal data bank is refined, the predictive abilities of the model should improve even further.

We should also warn that, since the present calibration and model verification were performed with data obtained from Stilfontein, the model might need some recalibration when used at other sites. The reason for this is mainly that environmental factors which were not explicitly taken into account, and which could differ from site to site, nevertheless could have had an effect on the values assigned to model parameters during calibration.

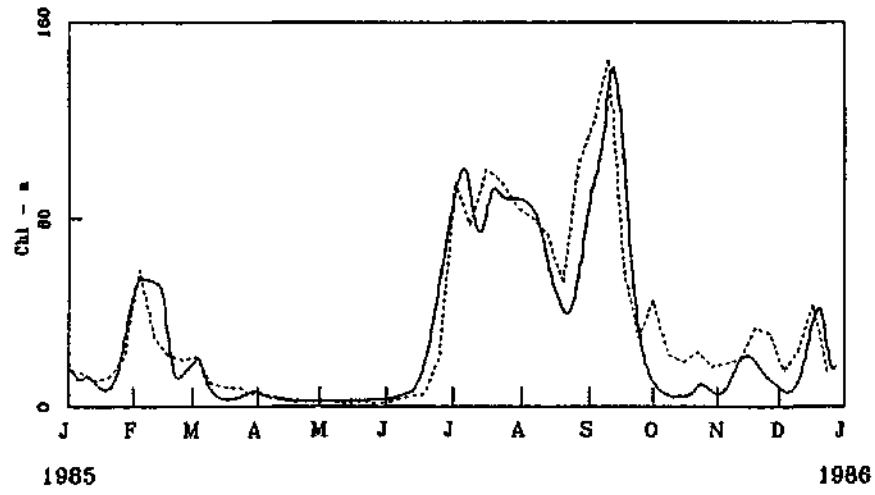


Figure 8.8: Total chlorophyll-*a* values computed by the model, calibrated with 14 algal groups, over the year 1985 at Stilfontein (smooth line). Measured data (dashed line) are provided for comparison purposes.

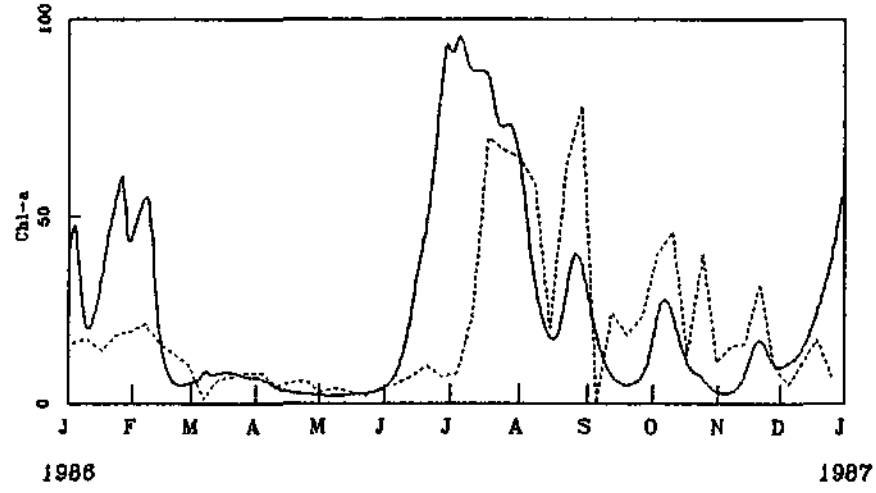


Figure 8.9: Total chlorophyll-*a* values computed by the model, calibrated with 14 algal groups, over the year 1986 at Stilfontein (smooth line). Measured data (dashed line) are provided for comparison purposes.

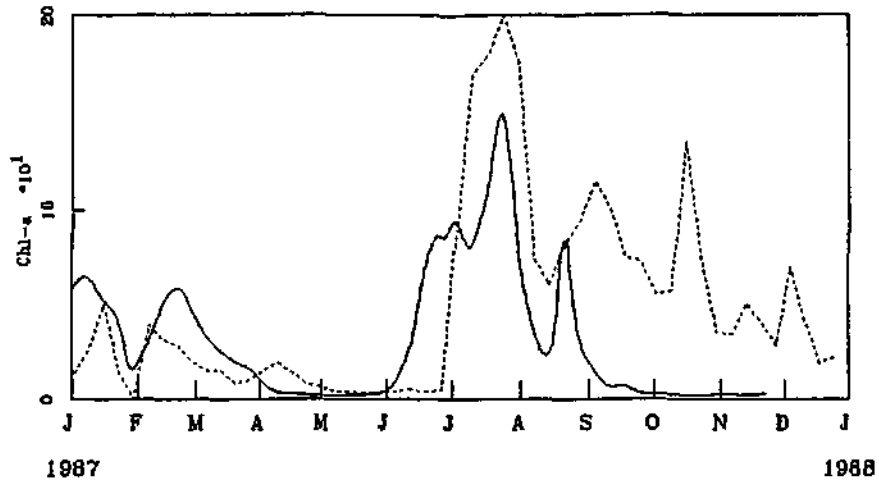


Figure 8.10: Total chlorophyll-*a* values computed by the model, calibrated with 14 algal groups, over the year 1987 at Stilfontein (smooth line). Measured data (dashed line) are provided for comparison purposes.

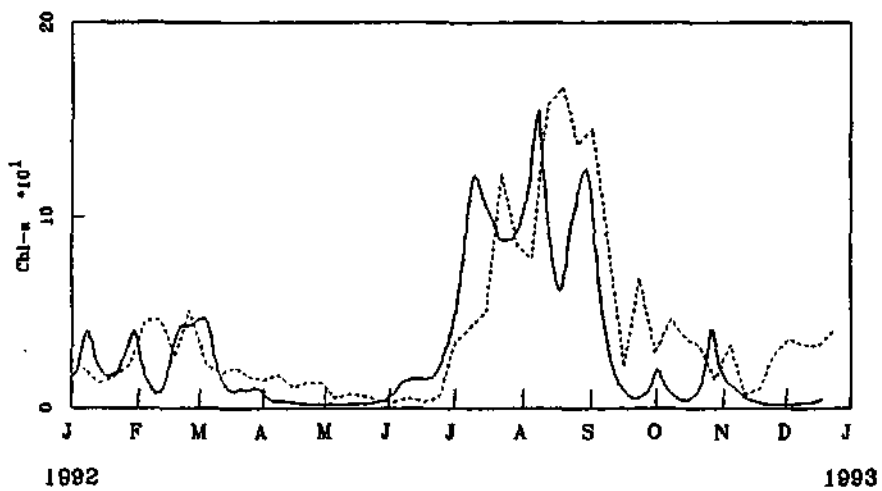


Figure 8.11: Total chlorophyll-*a* values computed by the model, calibrated with 14 algal groups, over the year 1992 at Stilfontein (smooth line). Measured data (dashed line) are provided for comparison purposes.

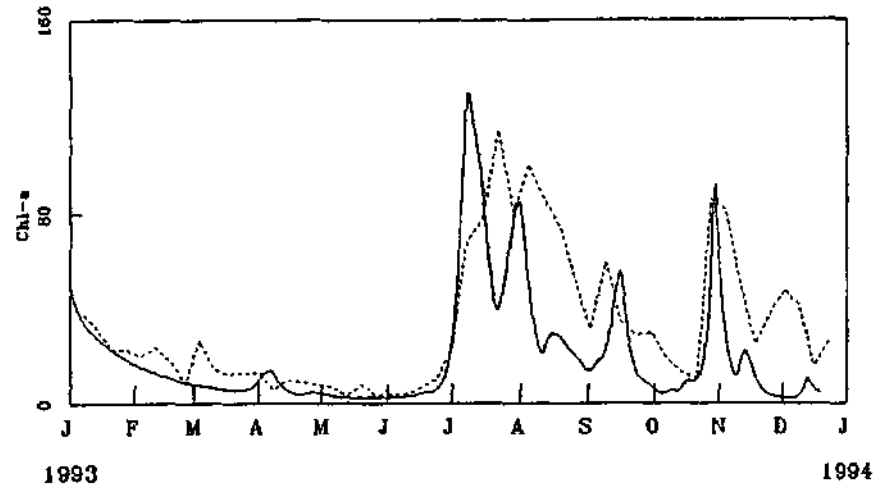


Figure 8.12: Total chlorophyll-*a* values computed by the model, calibrated with 14 algal groups, over the year 1993 at Stilfontein (smooth line). Measured data (dashed line) are provided for comparison purposes.

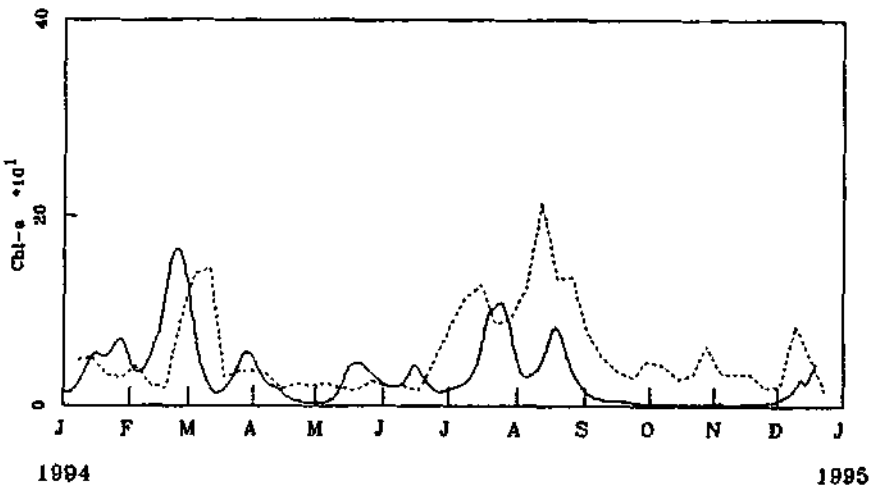


Figure 8.13: Total chlorophyll-*a* values computed by the model, calibrated with 14 algal groups, over the year 1994 at Stilfontein (smooth line). Measured data (dashed line) are provided for comparison purposes.

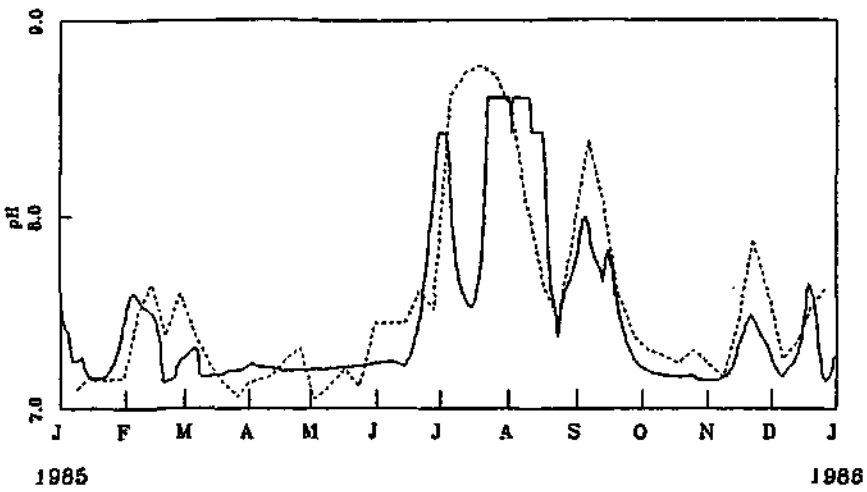


Figure 8.14: pH values computed by the model, calibrated with 14 algal groups, over the year 1985 at Stilfontein (smooth line). Measured data (dashed line) are provided for comparison purposes.

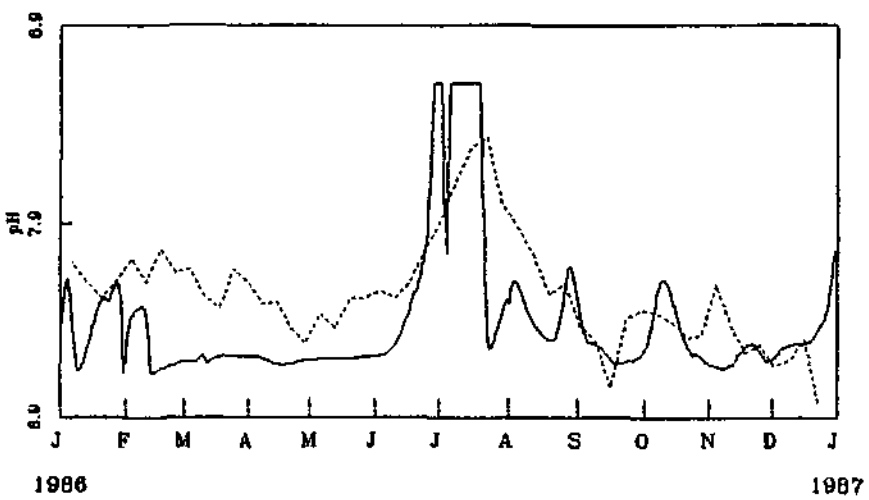


Figure 8.15: pH values computed by the model, calibrated with 14 algal groups, over the year 1986 at Stilfontein (smooth line). Measured data (dashed line) are provided for comparison purposes.

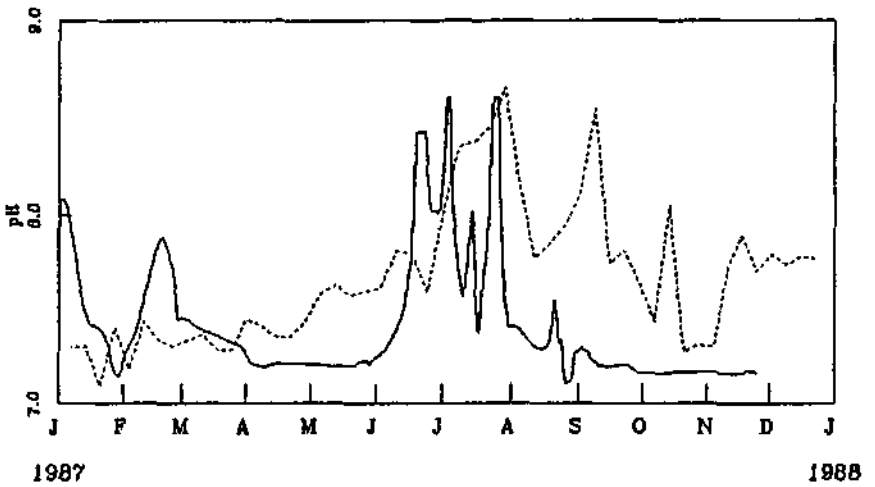


Figure 8.16: pH values computed by the model, calibrated with 14 algal groups, over the year 1987 at Stilfontein (smooth line). Measured data (dashed line) are provided for comparison purposes.

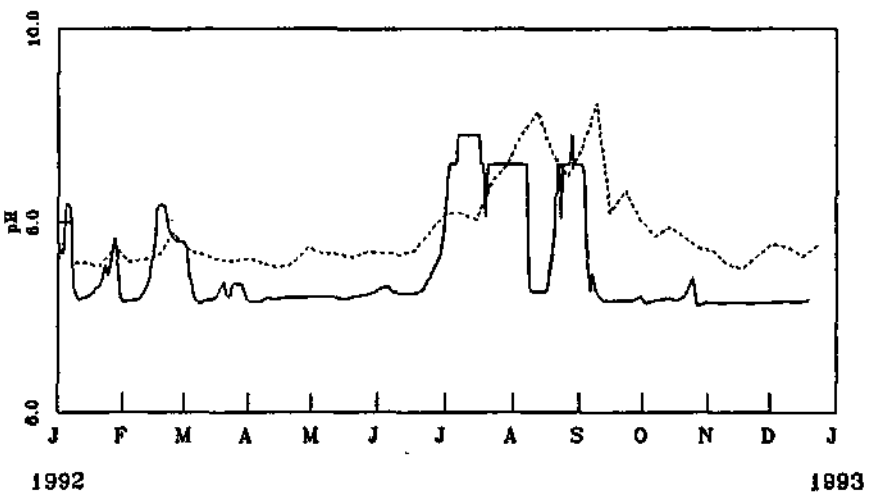


Figure 8.17: pH values computed by the model, calibrated with 14 algal groups, over the year 1992 at Stilfontein (smooth line). Measured data (dashed line) are provided for comparison purposes.

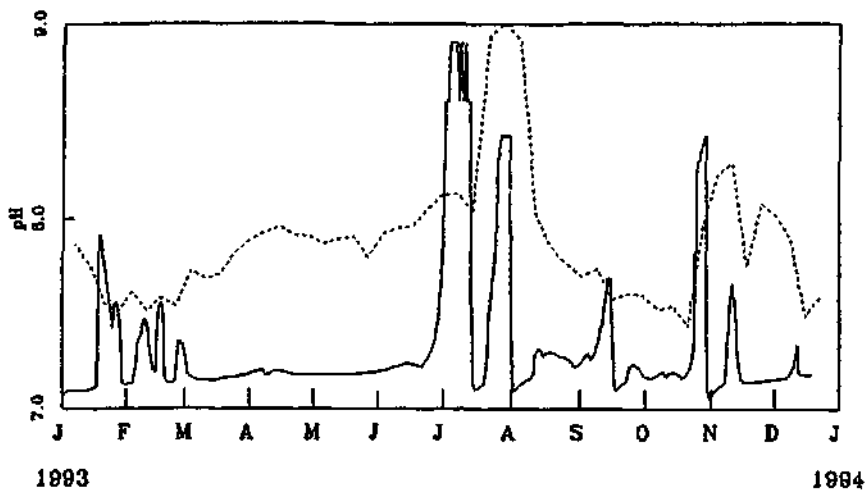


Figure 8.18: pH values computed by the model, calibrated with 14 algal groups, over the year 1993 at Stilfontein (smooth line). Measured data (dashed line) are provided for comparison purposes.

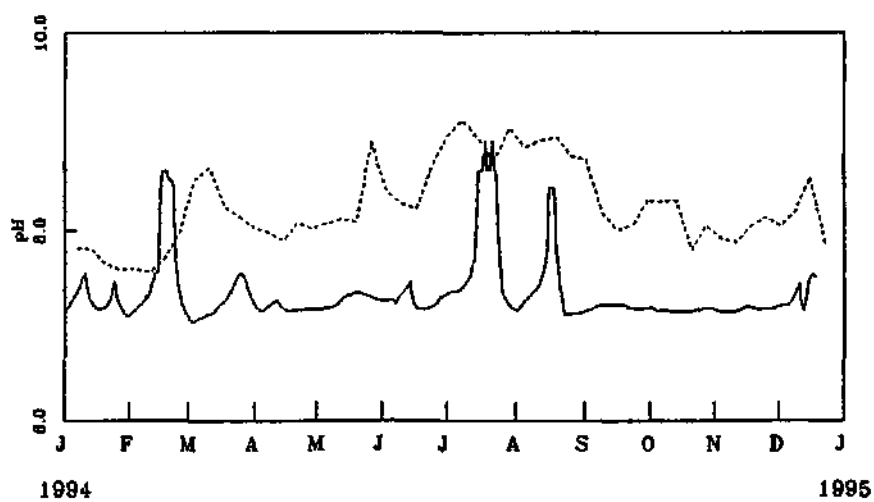


Figure 8.19: pH values computed by the model, calibrated with 14 algal groups, over the year 1994 at Stilfontein (smooth line). Measured data (dashed line) are provided for comparison purposes.

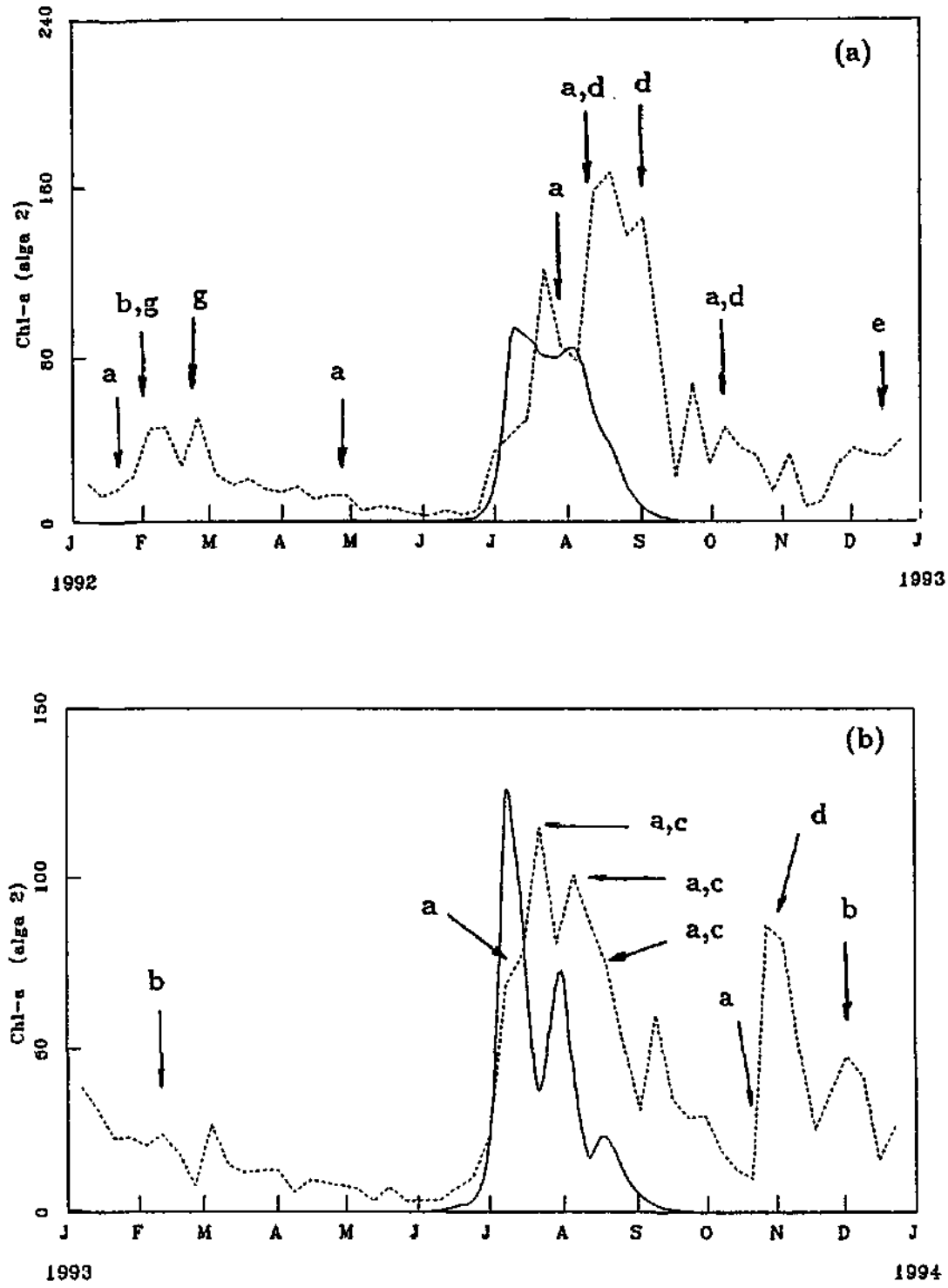


Figure 8.20: Computed contribution of alga 2 towards the chlorophyll-*a* profile at the Stilfontein site, using the 14 algal group calibration, over the year 1992 (a) and 1993 (b) (solid lines). Measured data are shown as dashed lines. The legends a-f denote the observed algal genera listed in Table 8.1.

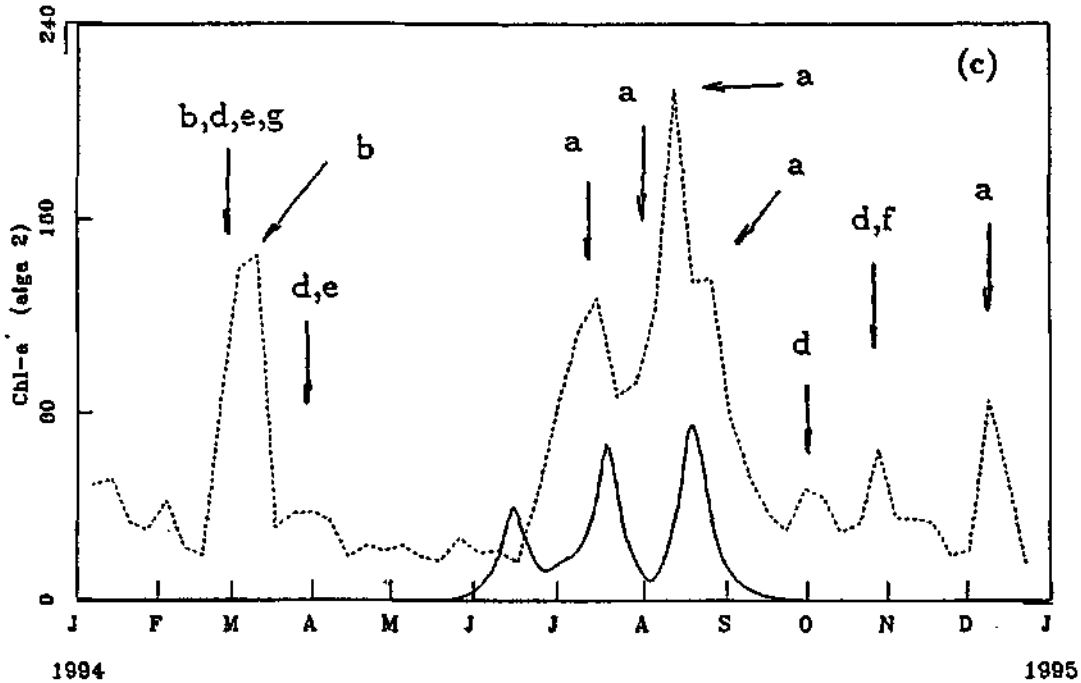


Figure 8.21: Computed contribution of alga 2 towards the chlorophyll-*a* profile at the Stilfontein site, using the 14 algal group calibration, over the year 1994 (solid line). Measured data are shown as a dashed line. The legends a-f denote the observed algal genera listed in Table 8.1.

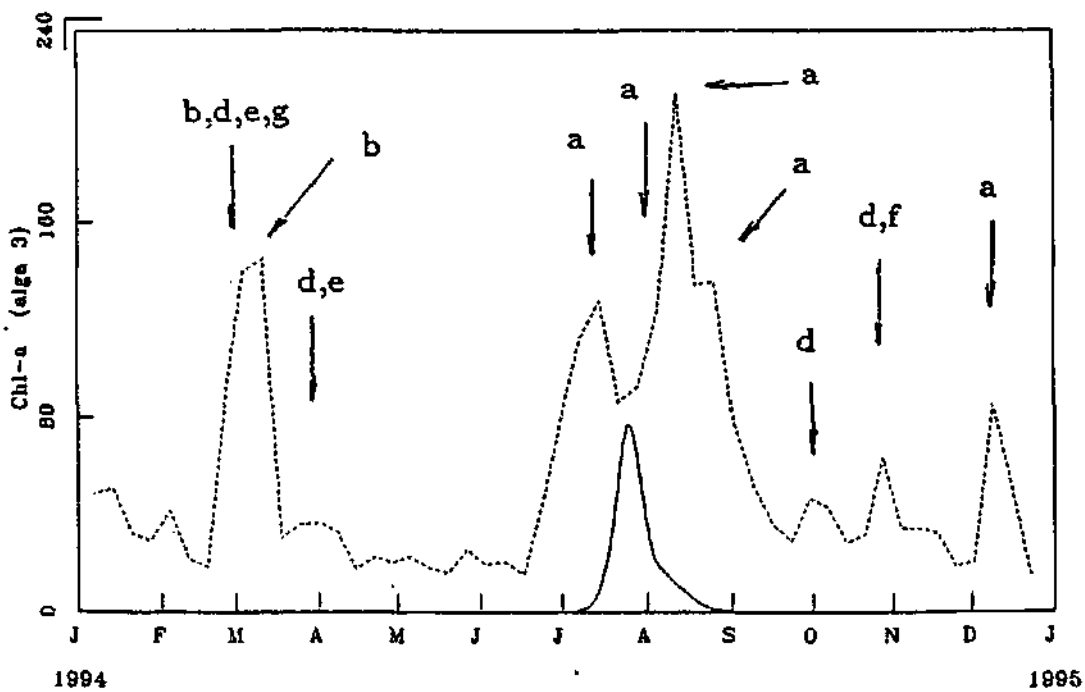


Figure 8.22: Computed contribution of alga 3 towards the chlorophyll-*a* profile at the Stilfontein site, using the 14 algal group calibration, over the year 1994 (solid line). Measured data are shown as a dashed line. The legends a-f denote the observed algal genera listed in Table 8.1.

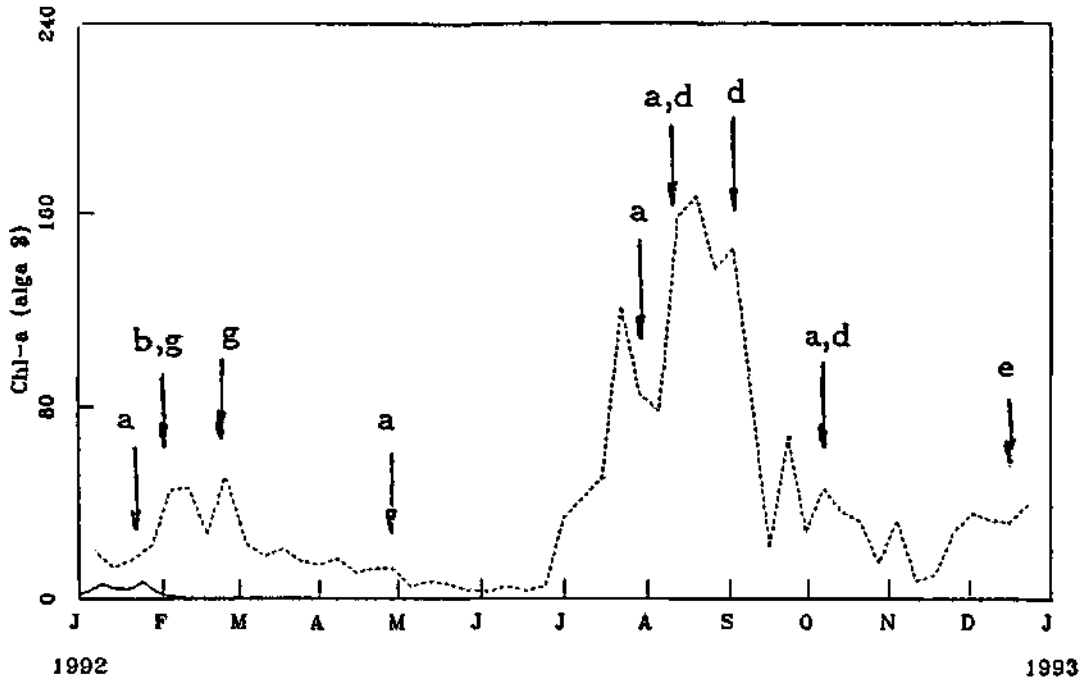


Figure 8.23: Computed contribution of alga 8 towards the chlorophyll-*a* profile at the Stilfontein site, using the 14 algal group calibration, over the year 1992 (solid line). Measured data are shown as a dashed line. The legends a-f denote the observed algal genera listed in Table 8.1.

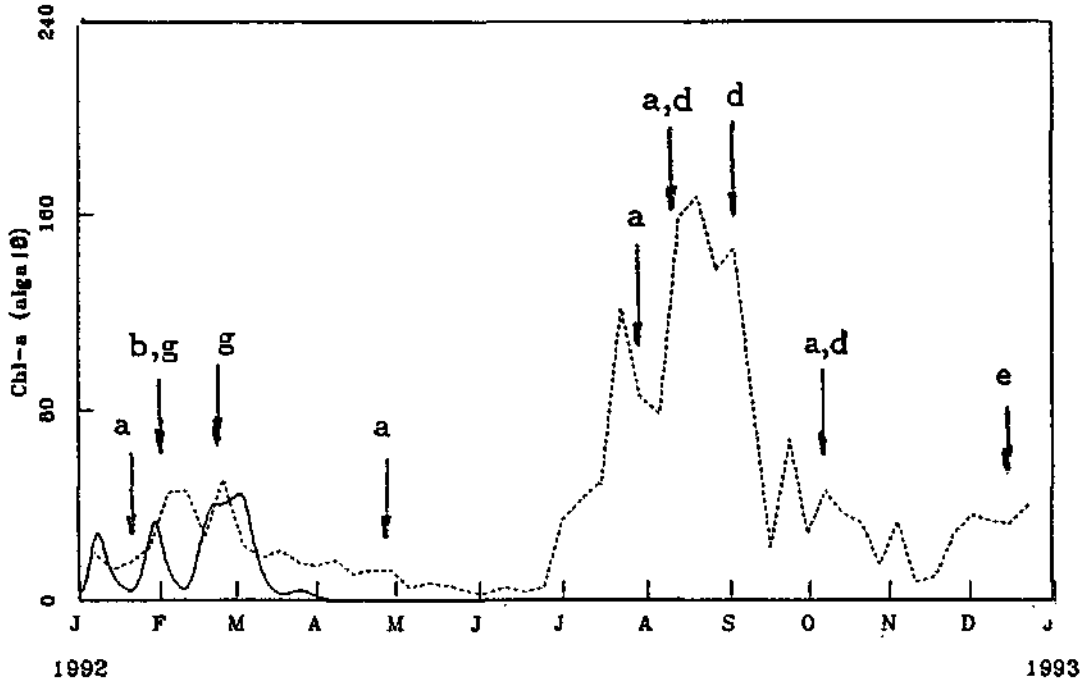


Figure 8.24: Computed contribution of alga 10 towards the chlorophyll-*a* profile at the Stilfontein site, using the 14 algal group calibration, over the year 1994 (solid line). Measured data are shown as a dashed line. The legends a-f denote the observed algal genera listed in Table 8.1.

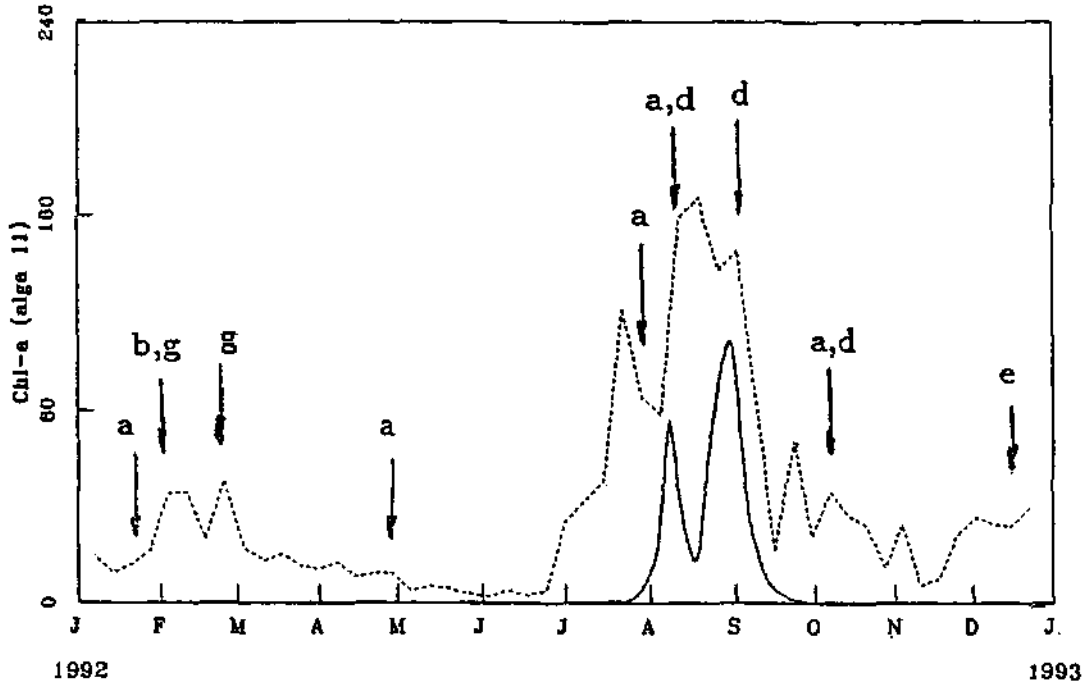


Figure 8.25: Same as Figure 8.24 but for alga 11.

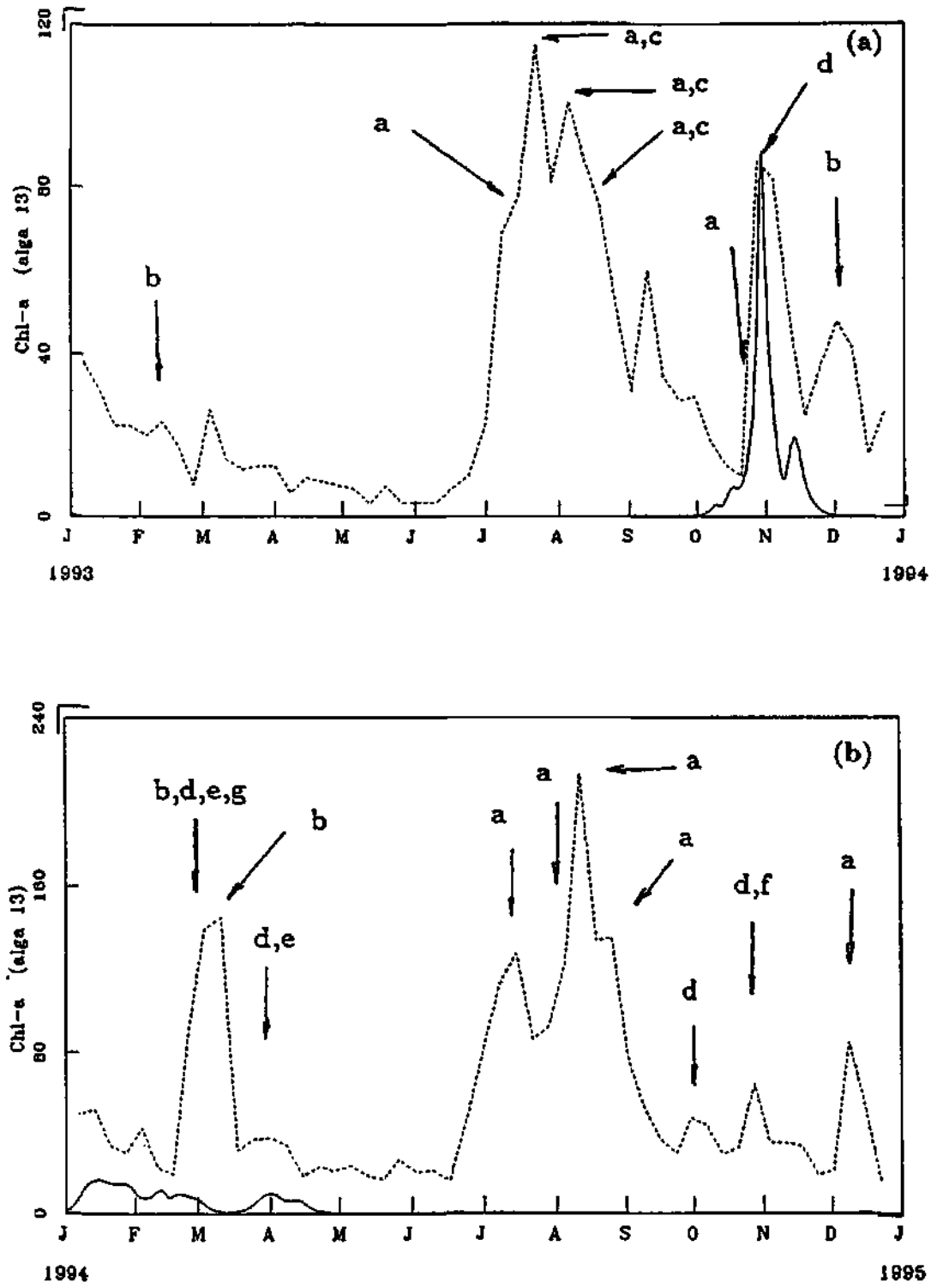


Figure 8.26: Computed contribution of alga 13 towards the chlorophyll-*a* profile at the Stilfontein site, using the 14 algal group calibration, over the year 1993 (a) and 1994 (b) (solid lines). Measured data are shown as a dashed line. The legends a-f denote the observed algal genera listed in Table 8.1.

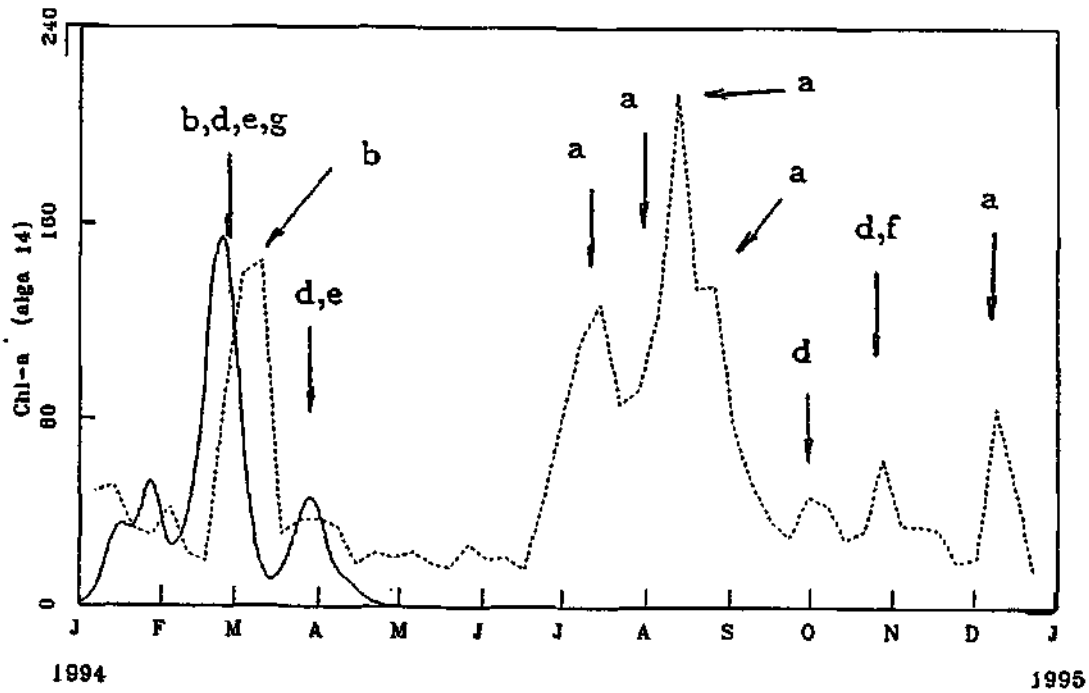


Figure 8.27: *Computed contribution of algae 14 towards the chlorophyll-a profile at the* Stilfontein site, using the 14 algal group calibration, over the year 1994 (solid line). Measured data are shown as a dashed line. The legends a-f denote the observed algal genera listed in Table 8.1.

# Chapter 9

# Concluding remarks

Although both a stationary and a flow dependent version of the model were developed, the incorporation of flow effects as described in chapter 6 were rather limited. Moreover, only the six major environmental parameters, i.e. temperature, light, turbidity, dissolved silicon, dissolved nitrogen and dissolved phosphorus were taken into account. Since the model was calibrated by fitting model output onto measured chlorophyll-*a* concentration, environmental factors which were not explicitly incorporated into the model, nevertheless had an effect on the values of parameters which were included.

Thus the model is effectively site dependent, in the sense that when used at a different site in the river, a recalibration might be necessary. (Even for the flow dependent version, this might be true.) The verifications in chapter 8 showed that the calibration with the Stilfontein data, at least, is fairly robust. Even though data of 1985 to 1987 was used for this calibration, good predictions of algal blooms could still be made for the much later three year period 1992 to 1994. It would seem, therefore, that at a particular site a recalibration would not be necessary too often, and that useful predictions could be made at that site.

A unique feature of the model is its ability to distinguish between different types of algae. Not only can this be used at a particular site to predict which algae are likely to cause an algal bloom under given conditions, but it could also facilitate an analysis of an observed bloom.

This model should be quite useful to water quality experts at the various water purification plants along the river. Due to its site dependence, however, it needs some modification before it can easily be used as a water quality management tool for the whole river system, or even significant river stretches. Such modifications should effectively remove the site dependence of the model by incorporating more of the significant environmental parameters, and by taking flow effects into account in a more comprehensive way than that described in chapter 6. In addition the model itself should be included as a sub model in a more comprehensive water quality model which involves all relevant hydraulical, chemical and biological aspects. This, however, is a major undertaking, and would justify a new project by itself.

This does not mean that it would be impossible to use the model, as it stands, for managing the river system. One possibility would be to feed the output of a classical water quality model into the algal growth model as input. Unfortunately this approach would make it impossible to take the effect of algal growth on water chemistry into account. The other possibility would be to calibrate the model at a restricted number of sites, and simulate algal growth only at these sites. This should give the managers of the river system a quick idea of the general effects of a planned action on the river.

Another extension to the work reported in this document would be to build a comprehensive data bank of algal groups. In this report a calibration involving 14 algal groups are described, with at least some of them associated with known algal genera. By continuing the calibration-verification process described in section 8, using more data sets, it would be possible to parameterise more algal groups, and eventually compile a library of parameter sets for algal genera which occur in the river.

# Appendix A

# The dynamical response of an uni-algal light dependent model

The light dependent model described in section 3.1 is the most fundamental building block of the model. Hence it is worthwhile to describe some basic analysis which investigates the response of this model to changes in the under water light climate. Only a single algal group will be considered, since the presence of more than one of these would add the phenomenon of competition between algal groups for available light, which would complicate the analysis too much at this stage. The interested reader is referred to Cloot and Schoombie (1994), where an analysis of this aspect is described extensively.

With a single algal group, the system (3.1) of $2N$ differential equations is reduced to two, namely

$$\dot{x} = [-k_D + k_{G_{opt}} g e^{1-g}]x \tag{A.1}$$

$$\dot{y} = k_D x - k_S y, \tag{A.2}$$

where $x$ and $y$ respectively denote the mass per unit volume of suspended living and dead algae in the water, as before, and where

$$\begin{aligned} g(x,y,t,D) &= \frac{\bar{I}(t)}{I_{opt}} \\ &= \frac{\mu(t) I_{max}(1 - R_\beta(t))}{z_0 I_{opt}[k_w + c_s S + k_x(x+y)]}. \end{aligned} \tag{A.3}$$

Because of the presence of the time dependent factors $\mu$ and $R_\beta$ in (A.3), an analysis of the system (A.1) and (A.2) is not trivial. These time dependent factors are periodic functions of time, however, since light intensity varies on both a 24 hour cycle and a 365 day one, the time dependence can be partly removed by taking averages over each 24 hour cycle. This leads to the following system:

$$\dot{X} = (-k_D + k_{G_{opt}} \bar{g} e^{1-\bar{g}})X \tag{A.4}$$

$$\dot{Y} = (k_D X - k_S Y), \tag{A.5}$$

where

$$\bar{g} = \frac{I_{max}\bar{F}}{z_0 I_{opt}(k_w + c_s S) + k_x(X+Y)}, \tag{A.6}$$

and where

$$\bar{F} = \overline{(1 - R_\beta)\mu} \tag{A.7}$$

is the average over a 24 hour period of the time dependent quantity $(1 - R_\beta(t))\mu(t)$. The quantity $\bar{F}$ will still vary from day to day, but this would be a relatively slow variation, and over a period of a few days it could be treated approximately as a constant. The systems (A.1), (A.2) and (A.4) and (A.5) are closely related in the sense that equilibria of (A.4), (A.5) correspond to solutions of (A.1), (A.2) which oscillate with small amplitude about these equilibria. A mathematical proof of this can be found in Cloot and Schoombie (1994), together with numerical calculations comparing solutions of (A.1), (A.2), sampled once a day, to equilibria of (A.4), (A.5) as they evolve with daily adjustments of $\bar{F}$.

It should also be noted that (A.4), (A.5) could serve as a model in its own right. In fact, the model proposed by Wofsy (1983) uses a time averaged light intensity.

It will be shown below that the stability of the equilibria , and in fact the qualitative behaviour of the solutions of (A.4), (A.5) are very much affected by the value of $\bar{F}$.

The system has three equilibrium points, namely $X = Y = 0$ and two others defined by

$$Y = (k_D/k_S)X \equiv MX \tag{A.8}$$

and the two roots of the equation

$$\bar{g}e^{1-\bar{g}} = (k_D/k_{G_{opt}}) \equiv K. \tag{A.9}$$

If we denote a equilibrium point of (A.4) and (A.5) as $(X, Y) = (a, b)$, then the three equilibria of the system are $(0, 0)$, $(a_1, b_1)$ and $(a_2, b_2)$, where for i=1,2

$$a_i = \frac{\epsilon\bar{F}/\Gamma_i - C}{k_x(1+M)} \tag{A.10}$$

$$b_i = Ma_i \tag{A.11}$$

and where $\Gamma_1$ and $\Gamma_2$ are the two roots of (A.9) such that

$$0 < \Gamma_1 < 1 < \Gamma_2 \tag{A.12}$$

(assuming that $K < 1$). For the equilibrium point $(0, 0)$, $\bar{g}$ assumes the value

$$\bar{g} = \frac{\epsilon\bar{F}}{C} \equiv \Gamma_3. \tag{A.13}$$

Note that $\Gamma_1$ and $\Gamma_2$ depend solely on the value of $K = k_D/k_{G_{opt}}$, whereas $\Gamma_3$ is directly proportional to the average irradiance $\bar{F}$.

The equilibrium point $(0, 0)$ of (A.4) , (A.5) corresponds to the the equilibrium point $(0, 0)$ of the system (A.1), (A.2), but the equilibria $(a_i, b_i)$ correspond to periodic orbits of (A.1),

(A.2), which deviate from $(a_i, b_i)$ by small quantities and being of the same stability types as these equilibria. (See the theorem quoted in Cloot and Schoombie (1994).)

We now consider the stability of the three equilibria. The Jacobian matrix of the system (A.4), (A.5) evaluated at $(X, Y) = (0, 0)$, is

$$J = \begin{pmatrix} -k_D + k_G\Gamma_3 e^{1-\Gamma_3} & 0 \\ k_D & -k_S \end{pmatrix} \tag{A.14}$$

with eigenvalues $-k_S$ and $-k_D + k_G\Gamma_3 e^{1-\Gamma_3}$. Since $k_S$ is a positive constant, both eigenvalues are negative and hence the equilibrium point $(0, 0)$ is a stable node (attractor) provided that

$$\Gamma_3 e^{1-\Gamma_3} < K, \tag{A.15}$$

i.e either $\Gamma_3 < \Gamma_1$, or $\Gamma_3 > \Gamma_2$. On the other hand, if $\Gamma_1 < \Gamma_3 < \Gamma_2$, this equilibrium point becomes a saddle, and is therefore unstable.

For the equilibria $(a_i, b_i)$, $i = 1, 2$, the Jacobian matrix is

$$J = \begin{pmatrix} -A_i & -A_i \\ k_D & -k_S \end{pmatrix} \tag{A.16}$$

where, making use of (A.9) and (A.3),

$$\begin{aligned} A_i &= k_G a_i \left[\frac{\partial}{\partial X}(\bar{g}e^{1-\bar{g}})\right]_{(X,Y)=(a_i,b_i)} = k_G a_i \left[\frac{\partial}{\partial Y}(\bar{g}e^{1-\bar{g}})\right]_{(X,Y)=(a_i,b_i)} \\ &= k_G a_i [1-\Gamma_i] e^{1-\Gamma_i} \left[\frac{\partial \bar{g}}{\partial X}\right]_{(X,Y)=(a_i,b_i)} \\ &= k_G a_i [1-\Gamma_i][-k_x/\epsilon\bar{F}]\Gamma_i^2 e^{1-\Gamma_i} \\ &= \frac{-k_D k_x \Gamma_i (1-\Gamma_i) a_i}{\epsilon \bar{F}}. \end{aligned} \tag{A.17}$$

An equilibrium point $(a_i, b_i)$ will now be hyperbolic and stable (i.e. an attractor) provided that the real parts of both eigenvalues are negative. Necessary and sufficient conditions for this are

$$\det J > 0, \quad \text{tr } J < 0, \tag{A.18}$$

or

$$A_i(k_S + k_D) > 0, \quad -(A_i + k_S) < 0. \tag{A.19}$$

Thus, if $A_i > 0$, the equilibrium point $(a_i, b_i)$ will be an attractor. It is also not difficult to see that when $A_i < 0$, this equilibrium point will be a saddle, i.e. unstable. Since $\epsilon$, $\bar{F}$, $\Gamma_i$, $k_D$ and $k_x$ are all positive quantities, we may conclude from (A.17) that the equilibrium point $(a_i, b_i)$ will be an attractor if

$$a_i(1-\Gamma_i) < 0, \tag{A.20}$$

and a saddle if this product is negative. Thus the equilibrium point $(a_1, b_1)$ is an attractor only if $a_1 > 0$ (since $\Gamma_1 < 1$), and the equilibrium point $(a_2, b_2)$ is an attractor only if $a_2 < 0$ (since $\Gamma_2 > 1$). From (A.10) and (A.13) we see that $a_i > 0$ if $\Gamma_i < \Gamma_3$, and $a_i < 0$ if $\Gamma_i > \Gamma_3$.

We can now identify three distinct possibilities, depending on the value of the parameter $\bar{F}$:

(I) $\Gamma_3 < \Gamma_1$, or $\bar{F} < \Gamma_1 C/\epsilon = z_0 I_{opt} \Gamma_1 (k_w + c_s S)/I_{max}$:

In this case the equilibrium point $(0,0)$ is a stable node. The values of $a_1$, $a_2$, $b_1$ and $b_2$ are all negative, with $a_1 > a_2$. The equilibrium point $(a_2, b_2)$ is therefore an attractor, while $(a_1, b_1)$, nearer to the origin in the $XY$ phase plane, is a saddle. Although both of these equilibria are in the third quadrant, their stability properties nevertheless have an influence on the orbits in the physically relevant first quadrant. Figure A.1 shows a typical phase diagram for this situation. All orbits in the first quadrant end at the origin, so that the water eventually becomes free from suspended algae. The biological interpretation is that the amount of suspended inorganic solids suspended in the water is just too much with respect to the available sunlight to cause the development of an algal bloom. This situation is most likely to occur in midwinter, when $\bar{F}$ is a minimum, or else after heavy rain, when $S$ is usually large.

(II) $\Gamma_1 < \Gamma_3 < \Gamma_2$, or $\Gamma_1 C/\epsilon < \bar{F} < \Gamma_2 C/\epsilon$:

In this case $(0,0)$ is a saddle, and $(a_1, b_1)$ is in the first quadrant, while $(a_2, b_2)$ is in the third quadrant of the phase plane. Moreover, both $(a_1, b_1)$ and $(a_2, b_2)$ are now attractors. A typical phase diagram of this type is shown in Figure A.2. All orbits in the first quadrant (except $X \equiv 0$) are attracted to the equilibrium point $(a_1, b_1)$. This represents a stable algal concentration in the water, and if the value of $a_1$ is sufficiently large, an algal bloom will develop. In this particular situation, the water can not be completely free from algae. Biologically this means that conditions are favourable for the development of an algal bloom, at least as far as the availability of photosynthetic light is concerned.

(III) $\Gamma_3 > \Gamma_2$, or $\bar{F} > \Gamma_2 C/\epsilon = z_0 I_{opt} \Gamma_2 (k_w + c_s S)/I_{max}$:

Once more $(0,0)$ is an attractor, and both $(a_1, b_1)$ and $(a_2, b_2)$ are in the first quadrant. $(a_2, b_2)$ is now a saddle, while $(a_1, b_1)$, which is further away from the origin, is an attractor. Figure A.3 shows a typical phase diagram. Orbits originating far enough from the origin will end up at $(a_1, b_1)$, while those starting nearer to $(0,0)$ will end up there. The first quadrant is thus divided into a relatively small basin of attraction for $(0,0)$, and a large one for $(a_1, b_1)$. The two orbits ending at the saddle $(a_2, b_2)$ are the separatrices between these two basins of attraction. The situation is therefore very much dependent on the initial condition.

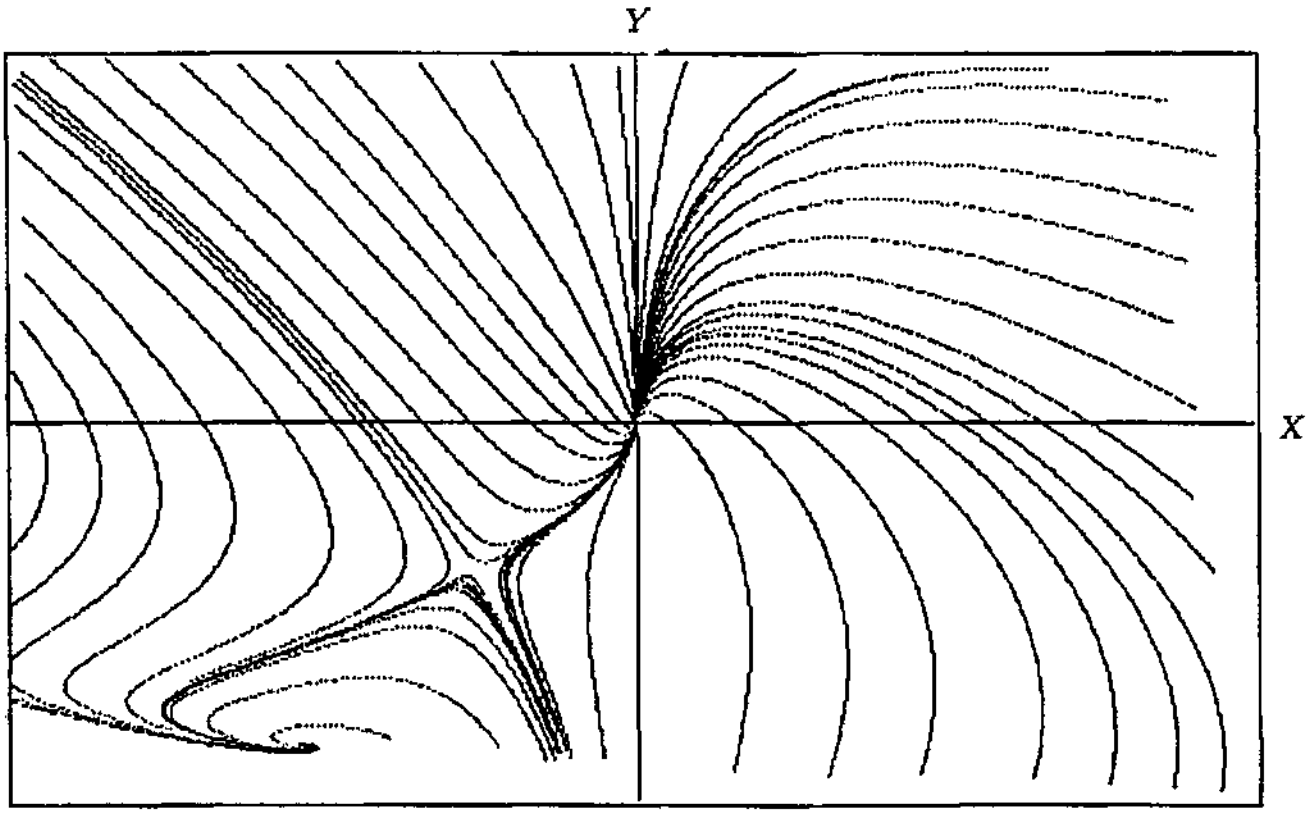


Figure A.1: Typical phase diagram for case (I), i.e. $g_3 < g_1$.

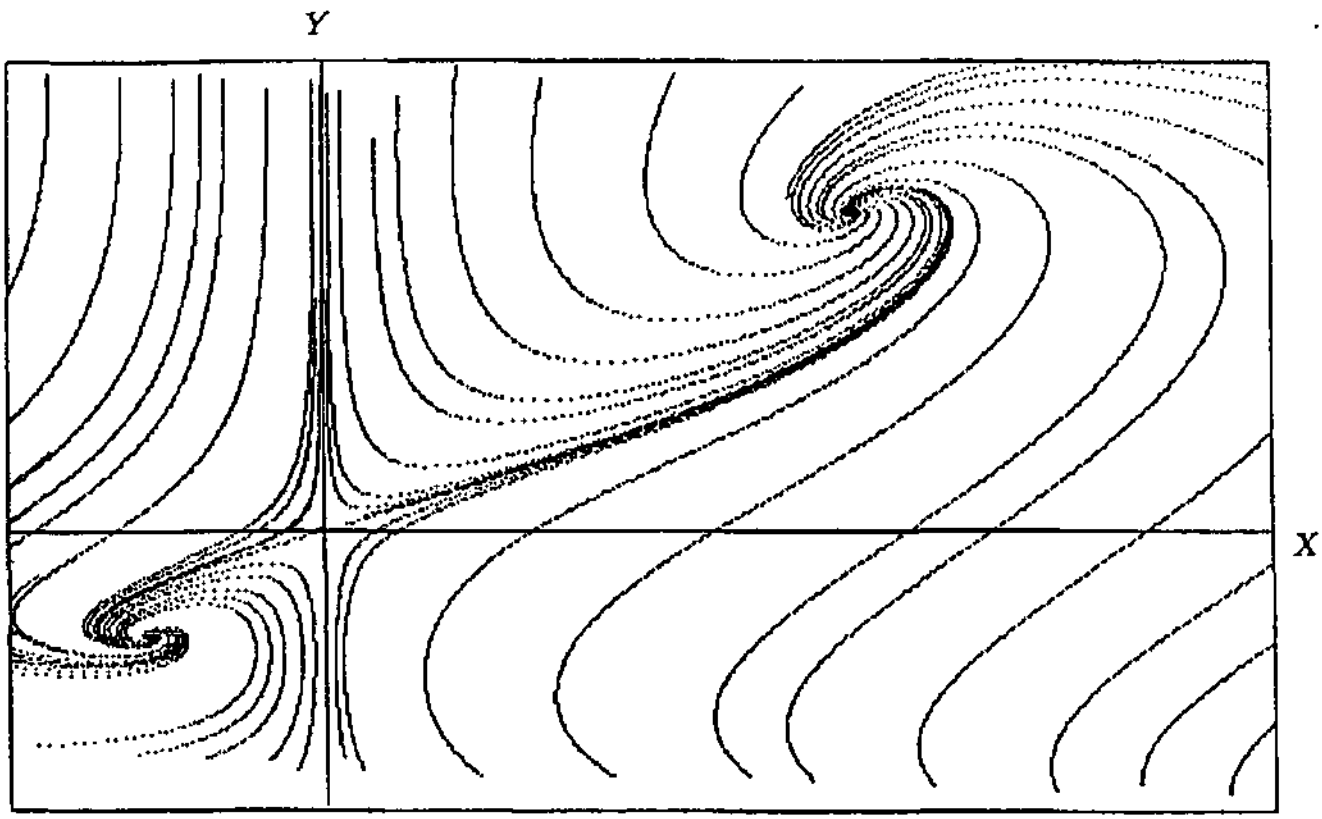


Figure A.2: Typical phase diagram for case (II), i.e. $g_1 < g_3 < g_2$.

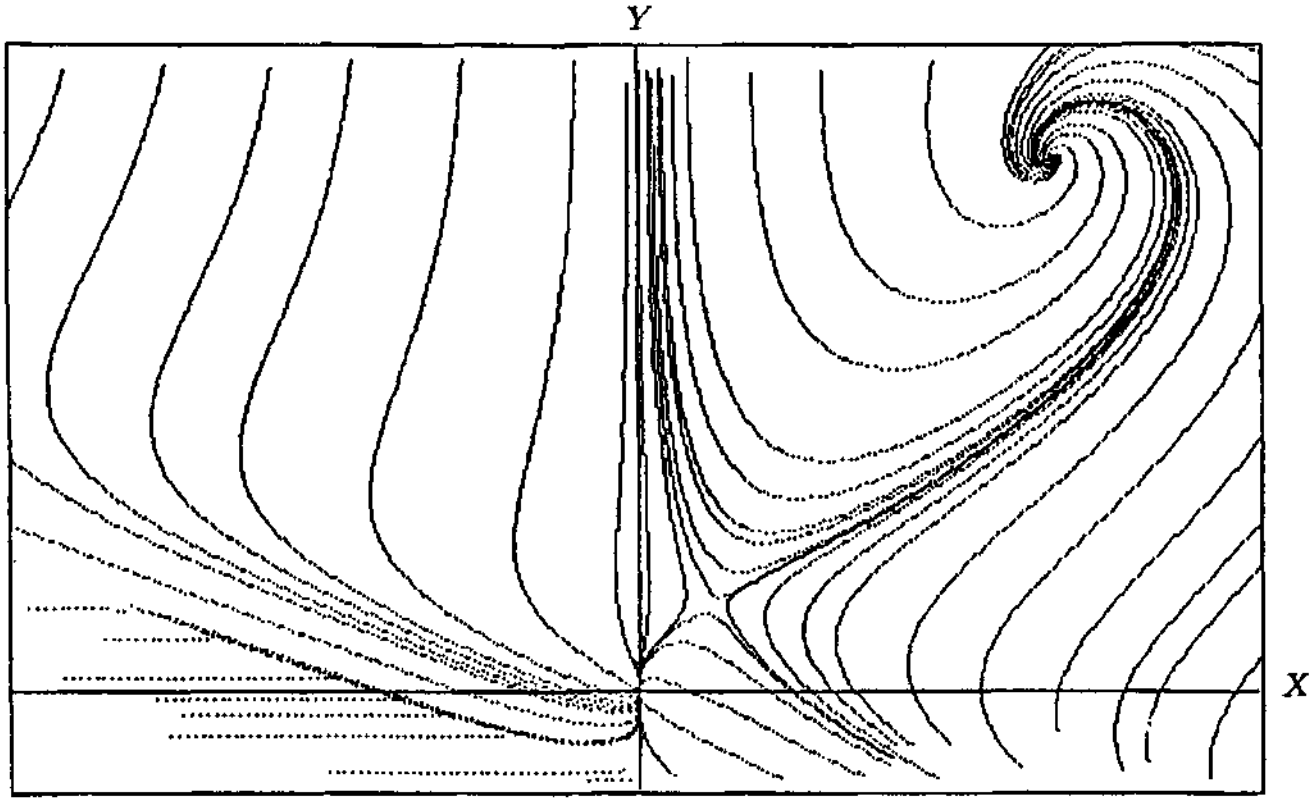


Figure A.3: Typical phase diagram for case (III), i.e. $g_3 > g_2$.

Biologically the interpretation is that the light available for photosynthesis is severely superoptimal, causing a decline in the algal concentration, unless there are initially sufficient living and dead algal cells suspended to provide enough self shading for the algal population to stabilize. Thus, with enough algae present initially, the development of an algal bloom will take place.

Water resources management would find a situation where the development of algal blooms are least likely to occur most favourable for e.g. the purification of water for drinking purposes. The condition for this, according to our analysis, would be

$$I_{max}\,\overline{\mu(1-R_\beta)} < z_0 I_{opt}\Gamma_1(k_w + c_s S). \tag{A.21}$$

Of course, the analysis performed in this appendix is an asymptotic analysis, and can only give an approximate description of the actual behaviour of the model (A.1), (A.2). However, it can be demonstrated, by means of actual calculations, that the results of our analysis correspond fairly well with the behaviour of the model itself, as far as the qualitative behaviour is concerned, and that it can also give at least a rough indication of the levels of algal concentration at a specific time under specific environmental conditions. This technical aspect of the problem together with an analysis of the dynamics of a more complex situation involving the competition between two different types of algae is extensively discussed in Cloot and Schoombie (1994), and will not be repeated here.

# Appendix B

# Software user guide

Two versions were developed of the mathematical model described in this report. Both were implemented as FORTRAN computer programs. The first one was called ALGSTMOD, and is a local model in the sense that it does not make explicit provision for flow effects, and simulates algal growth at one specific site in the river at a time. (A full description of this version is given in chapters 3 through 5, as well as chapters 7 and 8.) The other version was called ALGDYMOD, and this version does make explicit provision for the flow of the river, and can be used to simulate algal growth along stretches of the river. (A description of the flow effects incorporated into this version can be found in chapter 6 of the report.)

Both computer programs were written in FORTRAN 77. The source code of each program is distributed in the form of a single text file, namely ALGSTMOD.F and ALGDYMOD.F respectively. The user should use a suitable FORTRAN 77 compiler to compile this source code before using it. The reason why the source code is distributed rather than a compiled version, is to ensure maximum portability. However, should any user experience difficulties due to lack of a suitable compiler, he should feel free to contact the authors of this report at the address provided at the end of this user guide.

We will now provide instructions for the use of each of the two programs.

## B.1 Program ALGSTMOD

As explained above, the first step to get this program ready and running, is to compile the FORTRAN source file ALGSTMOD.F, using a FORTRAN 77 compiler suitable for the particular computer and operating system which the user wishes to use for the model. (The model runs quite well on a 486 or Pentium PC with at least 8 Mb of RAM memory.)

Along with ALGSTMOD.F and ALGDYMOD.F a short FORTRAN program called PREPRO.F is also distributed. This program should also be compiled, and should be run before running either ALGSTMOD or ALGDYMOD for the first time. PREPRO creates all the

output files used by both programs, and should be run once only. Care should be taken that PREPRO is saved and run in the same working directory as ALGSTMOD and/or ALGDYMOD.

The next step is to provide input data for ALGSTMOD, and, after running the program, to interpret the output. These will be explained in the next two subsections.

### B.1.1 Input data

Again for maximum portability, a very basic method was used to make the input data available to the program. All input data is entered into five text files. The master input data file contains environmental data and the algal data set, and should always be saved as DATA.DAT. The other four files contain respectively temperature data, turbidity data, nitrogen data and phosphorus data. The names of these files can be specified by the user, as long as these names are also included in the appropriate positions in the file DATA.DAT. Also note that some operating systems do not allow file names with more than eight characters (e.g. MS DOS, MS WINDOWS 3.x).

Each file has one, or at most two data entries per line. When there are two entries in a line, these should be separated by spaces. Any text editor or word processing software which have the capability to generate ASCI text files (e.g. the MS DOS editor, or MS WORD) can be used to enter data into these files. When using MS Word, enter the data, then use the "save as" option and choose the type "MS DOS text with line breaks".

We next describe the data which should be entered into the file DATA.DAT.

The first sixteen lines consists of some general and environmental data:

**Line 1:** Enter the latitude of the site (in degrees East). For instance, if the latitude is 33° E, enter 33.

**Line 2:** Enter the number of the day in the particular year at which the simulation should start, taking day zero as September 21. The table below can be used as a convenient guide to pick the correct day number. (Ignore February 29 in a leap year.)

**Line 3:** Enter the number of days during which the simulation should take place, i.e. if a two month simulation is required starting at June 1, enter 61.

**Line 4:** Enter the time step for the numerical solution of the differential equations as a fraction of an hour. We usually used five minute steps, which means an entry of 0.08333 on this line. A smaller time step would mean more accurate solutions of the equations, but more computer time, and a larger step would mean less accurate solutions and also less computer time used during the simulation.

**Line 5:** Enter the number of times you wish to have output during the simulation, i.e. if you wish to have weekly output during a two month simulation, enter 8.

| Date | Day number |
|---|---|
| January 1 | -263 |
| February 1 | -232 |
| March 1 | -204 |
| April 1 | -173 |
| May 1 | -143 |
| June 1 | -112 |
| July 1 | -82 |
| August 1 | -51 |
| September 1 | -20 |
| October 1 | 10 |
| November 1 | 41 |
| December 1 | 71 |

Table B.1: Day numbers for the file DATA.DAT

**Line 6:** Enter the name of the file in which the measured and/or expected water temperatures were saved. If this data was saved in a file FILTEMP, enter the character string FILTEMP on this line.

**Line 7:** Enter the name of the file in which the measured and/or expected water turbidity was saved, e.g. FILSED.

**Line 8:** Enter the name of the file in which the measured and/or expected dissolved nitrogen concentrations were saved, e.g. FILNO3.

**Line 9:** Enter the name of the file in which the measured and/or expected dissolved phosphate concentrations were saved, e.g. FILPO4.

**Line 10:** On this line, enter the depth of the mixed layer (in meters). (This corresponds to the variable $z_0$ in (3.6).)

The rest of the file DATA.DAT consists of values assigned to various parameters during model calibration. The user could use the values from line 11 to the end of the file DATA.DAT, distributed with the program, as a starting point. Once the model is calibrated, these values need not be changed until a recalibration of the model should become necessary. (See also section B.3.3 of this appendix.)

**Line 11:** Enter the value of the specific extinction coefficient $c_s$ for suspended inorganic solids, in $(\text{mg.m})^{-1}$. (See equation (3.6)).

**Line 12:** Enter the inverse of the characteristic time of restitution for dissolved silicon in the water, in $(\text{day})^{-1}$. (The variable $k_{\text{Si}}$ in (4.10).) This is about 0.14286 for the Vaal River.

**Line 13:** Enter the inverse of the characteristic time of restitution for dissolved oxygen in the water, in $(\text{day})^{-1}$. (The variable $K_{O_2}$ in (5.15).)

**Line 14:** Enter the inverse of the characteristic time of restitution for dissolved carbon dioxide in the water, in $(\text{day})^{-1}$. (The variable $K_{CO_2}$ in (5.13).)

**Line 15:** Enter the inverse of the characteristic time of restitution for dissolved phosphate in the water, in $(\text{day})^{-1}$. (The variable $K_{PO_4}$ in 5.36.)

**Line 16:** Enter the time period $\tau_D$ (in days) during which dead algae decompose.

The next set of data entered into DATA.DAT is the values of the calibrated algal parameters. They are preceded by the following two lines:

**Line 17:** The number of algal groups used. The maximum permitted by the program is 15. For the Stilfontein calibration this number is 14.

**Line 18:** The number of diatom algal groups used during the simulation.

For easy reference, the entries in the first 18 lines of DATA.DAT are also tabulated in Table B.2, together with the corresponding FORTRAN variables in the program and the appropriate units.

Next follows the sets of algal parameters, 18 for each algal group (25 for diatoms). Each set consists of 19 data lines for diatom algal groups, and 12 data lines for others. The data sets for diatom algal groups should be entered first, one after the other, and then those of the other algal groups. The data sets for the 14 algal group calibration at Stilfontein are tabulated in Appendix C, and can also be found in the file DATA.DAT distributed with the program.

For each algal group, the parameters are entered in the order as given in Table B.3. In this table the FORTRAN variables used in the program are also given.

| FORTRAN Parameter | unit | Description |
|---|---|---|
| DLAT | degrees | Latitude of the site |
| DAYI | day | Initial day from which simulation is started. Day 0 is September 21. |
| TDAY | day | Number of days of simulation. |
| TSTEP | h | Time step for integration in fraction of hours |
| KOUT | | Number of outputs required during the integration. |
| | | Name of the file containing water temperature data. |
| | | Name of the file containing water turbidity data. |
| | | Name of the file containing dissolved Nitrogen concentration data. |
| | | Name of the file containing dissolved Phosphate concentration data. |
| Z0 | m | Depth of the mixing layer |
| SIK | L/(mg.m) | specific extinction coefficient for silt |
| DKSIPR | $(day)^{-1}$ | Inverse of the characteristic restitution time for dissolved silicon in the water body |
| REARE | $(day)^{-1}$ | Inverse of the characteristic restitution time for dissolved oxygen in the water body |
| DIFCO2 | $(day)^{-1}$ | Inverse of the characteristic restitution time for dissolved carbon dioxide in the water body |
| DKPO4S | $(day)^{-1}$ | Inverse of the characteristic restitution time for dissolved phosphate in the water body |
| IDELAY | day | Time necessary for decomposition of dead algae |
| NALG | | Number of algal groups (Max =15) |
| NDIAT | | Number of diatom groups |

Table B.2: Environmental data in first 18 lines of DATA.DAT.

The final entries in the file DATA.DAT are the initial concentrations for the algal groups. The first value entered for the $i$-th algal group must be the initial concentration in living algae $x_{1_i}$ followed by the concentration of dead algae in suspension in the water $x_{2_i}$, i.e. the initial concentrations should be entered as follows for $N$ algal groups:

$$
\begin{array}{l}
Alga1 \left\{ \begin{array}{l} x_{1_1} \\ x_{2_1} \end{array} \right. \\
Alga2 \left\{ \begin{array}{l} x_{1_2} \\ x_{2_2} \end{array} \right. \\
Alga3 \left\{ \begin{array}{l} x_{1_3} \\ x_{2_3} \end{array} \right. \\
\vdots \\
AlgaN \left\{ \begin{array}{l} x_{1_N} \\ x_{2_N} \end{array} \right.
\end{array}
$$

In Section B.3 more will be said about suitable choices for these initial concentrations.

| Variable | unit | Description |
|---|---|---|
| GKM | $(\text{day})^{-1}$ | Maximum growth rate $k_{G_{opt}}$ |
| TI, TOP | $°C$, $°C$ | Minimum and Optimal temperatures $T_{min}$ and $T_{opt}$ for growth |
| DK | $(\text{day})^{-1}$ | Dying rate $k_D$ |
| OPLI | cal/(cm$^2$.min) | Optimal light intensity $I_{opt}$ for growth |
| SK | $(\text{day})^{-1}$ | Sedimentation rate $k_S$ |
| AK | l/($\mu$ g Chl-$a$.m) | Self-shading coefficient $k_x$ |
| PSMAX, TOPS | mg C/(mg Chl-$a$.h), $°C$ | Maximum photosynthetic rate $PS_{max}$ and optimal temp. $T_{PS}^{opt}$ for photosynthesis |
| DPSDI | cal/(cm$^2$.min) | Slope of photosynthetic rate vs light at the origin ($\chi_{PS}$) |
| DPSN, DPSP, RNPS | mg/L, mg/L, no unit | Saturation concentration for $N$, $P$ and optimal $N/P$ ratio ($N_{sat}$, $P_{sat}$, $(N/P)^{opt}$) |
| DISP, ENP | no unit, no unit | Dispersion factor $\chi_{(N/P)}$ and exponent $n$ in equations (5.5) and (5.6) |
| CORESP | no unit | Respiration rate as a % of the photosynthetic rate $PS_{max}$ |
| CO2SAT, XCO2 | mg $CO_2$, no unit | Saturation concentration and dispersion coefficient for $CO_2$ absorption ($CO_{2_s}$, $K_{CO_2}$) |
| *The following data are needed only for diatoms* | | |
| SISAT | mg Si/L | Saturation concentration $Si^{cr}$ of dissolved silicon for algal uptake |
| SIMIN | mg Si/L | Minimum concentration $Si^{min}$ of dissolved silicon for algal uptake |
| CHSI | no unit | Dispersion coefficient $\chi$ for Si transfer function for uptake |
| DKSIUP | $\mu$ Si/($\mu$ Chl-$a$. day) | Maximum rate $V_{max}$ of silicon absorption by algae |
| SISAG | mg Si/L | Saturation concentration $\tilde{Si}^{cr}$ of dissolved silicon for algal growth |
| SIMIG | mg Si/L | Minimum concentration $\tilde{Si}^{min}$ of dissolved silicon for algal growth |
| CHSIG | $\times$ | Dispersion coefficient $\tilde{\chi}$ for Si transfer function for growth |

Table B.3: Algal parameters in DATA.DAT

To summarise: A complete input file DATA.DAT for N algal categories, of which ND are diatoms, should have the following structure:

Environmental parameters

$\vdots$

Number of algal groups (i.e. N)
Number of diatom groups (i.e. ND)

$\vdots$

Algal parameters: Alga 1 (Diatoms)

$\vdots$

Algal parameters: Alga ND (Diatoms)
Algal parameters: Alga ND+1 (Non-diatoms)

$\vdots$

Algal parameters: Alga N (Non-diatoms)

$$\begin{array}{l} Alga1 \left\{ \begin{array}{l} x_{1_1} \\ x_{2_1} \end{array} \right. \\ Alga2 \left\{ \begin{array}{l} x_{1_2} \\ x_{2_2} \end{array} \right. \\ \vdots \\ AlgaN \left\{ \begin{array}{l} x_{1_N} \\ x_{2_N} \end{array} \right. \end{array}$$

The temperature, turbidity, nitrogen and phosphorus data files all have the same structure. Each of these files consists of a single column of numbers, representing weekly values of these factors. It is important that a value should be entered for *each* week from the first week of the year under consideration, up to at least a week after the last week in the simulation.

As an example, let us suppose we called the temperature data file FILTEMP, and that we wish to run a simulation from a day somewhere in the third week of a given year, up to a day somewhere in the fifth week of the same year. Then FILTEMP must contain at least the following entries:

$T_1$
$T_2$
$T_3$
$T_4$
$T_5$
$T_6$
$\vdots$

where $T_i$ is the average water temperature of the $i$-th week of that particular year. (Week 1 is the first week of the year starting on 1 January.) The other three data files should contain entries for the same weeks. The data should be in the following units:

temperature : $^{\circ}C$
turbidity : NTU
nitrogen : mgN/L
phosphorus : mgP/L

In Section B.3 more guidelines will be given about the preparation of these data sets.

### B.1.2 Output data

The program produces a number of output files. Each file consists of two columns of numbers. The first column consists of day numbers, and the second column of the values of some quantity computed for these days. These data can be imported into some graphics software package (e.g. Harvard Graphics) or a good spread sheet program with graphing capabilities (e.g. MS Excell), to produce graphs of the output.

The output file P10.DAT contains the simulated total chlorophyll-*a* concentrations on a daily basis. Next follows a sequence of files P11.DAT, P12.dat. P13.DAT, ... Each file P"10+i".DAT contains the computed chlorophyll-*a* concentrations of only the $i$-th algal group. (If there were 5 algal groups, their chlorophyll-*a* concentrations would be in the files P11.DAT, P12.DAT, P13.DAT, P14.DAT and P15.DAT.)

Finally there are nine output files, described in Table B.4, which contain computed data describing the effect of the algae on their environment.

Together with the program ALGSTMOD some input and output files are also distributed, in order to help the user to run the program correctly.

The input files were those used to compute the total chlorophyll-*a* profile for 1992 at Stilfontein, using the fourteen algal group calibration described in Chapter 8. Besides the file DATA.DAT, the four input files TEM92.DAT, TUR92.DAT, TNS92.DAT and PO492.DAT are provided, containing the temperature, turbidity, nitrogen and phosphate data respectively.

The output files P10.DAT, P12.DAT and PH.DAT are also provided, containing computed total chlorophyll-*a*, computed chlorophyll-*a* for the second algal group and computed pH values respectively. After running the program with the provided input files, the user can compare his own output with those in the provided output files.

| File | Description | unit |
|---|---|---|
| SI.DAT | Computed values of dissolved Si concentration in the water body | mg Si/L |
| O2.DAT | Computed values of dissolved $O_2$ concentration in the water body | mg $O_2$/L |
| CO2.DAT | Computed values of dissolved $CO_2$ concentration in the water body | mg $CO_2$/L |
| NH4-N.DAT | Computed values of dissolved $NH_4$ concentration in the water body | $\mu$ gN/L |
| NO3-N.DAT | Computed values of dissolved $NO_3$ concentration in the water body | mgN/L |
| PO4-P.DAT | Computed values of dissolved $PO_4$ concentration in the water body | mgP/L |
| TEMP-N.DAT | Computed rates of variation of dissolved nitrogen concentration, $dN/dt$, due to algal activity | $\mu$ gN/h |
| TEMP-P.DAT | Computed rates of variation of dissolved phosphate concentration, $dP/dt$, due to algal activity | $\mu$ gP/h |
| PH.DAT | Computed $pH$ values in the water body | |

Table B.4: Output files containing computed quantities describing the effect of algae on the environment

## B.2 Program ALGDYMOD

The FORTRAN source file which should be compiled with a FORTRAN 77 compiler, is ALGDYMOD.F. Since this program uses much more computer resources than ALGSTMOD, at least a PENTIUM personal computer is recommended for this program, with at least 16 Mb RAM memory.

Before running ALGDYMOD for the first time, make sure that PREPRO has been run to create all necessary output files. (If PREPRO has already been run to prepare files for ALGSTMOD, it should not be run again, unless a different directory (or folder) is used.)

After compiling, the user should provide input data to the program, and after running the program, he should also be able to interpret the output data. Instructions for these are given in the next two subsections.

### B.2.1 Input data

Input data is again entered into a master data file DYDATA.DAT, together with the four files containing the temperature, turbidity, nitrate and phosphate data as discussed in Section B.1.1, and an extra data file which describes the width of the flow channel at all points used during the simulation.

*The file DYDATA.DAT is similar to the file DATA.DAT used by ALGSTMOD, except* that it contains some channel flow data at the beginning. These consists of nine, ten or eleven lines of data, depending on the flow type considered.

Enter this data as follows:

**Line 1:** Enter the name of the file in which the width of the river is to be specified at various points, e.g. if this data is to be saved as FILRIVER, enter FILRIVER.

**Line 2:** Enter the length of the flow channel (i.e. the length of the river stretch) in kilometers.

**Line 3:** Enter the step length in space used for numerical integration of the partial differential equations as a distance in kilometers. This step length should always be the length of the flow channel (entered in Line 2) divided by some positive integer. For instance, if the length of the flow channel is 2 km, which is to be divided into 100 smaller stretches for the purposes of solving the equations numerically, enter 0.02. The smaller the number entered, the more accurately the equations will be solved, but the more computer resources will also be used.

**Line 4:** Enter an initial water depth in meters.

**Line 5:** Enter an initial flow discharge in cubic meters per second.

**Line 6:** Specify the flow type by entering either 1, 2 or 3. This allows a choice between constant flow (enter 1), smoothly oscillating flow as described in Chapter 6 (enter 2), or drastically varied flow as described in chapter 6 (enter 3). If 1 was entered here, lines 7 and 8 below are skipped.

**Line 7:** If 2 was entered on the previous line, enter the strength of the oscillation here as a percentage of the initial discharge, and skip line 8. If 3 was entered on the previous line, enter the size of the jump in the discharge rate here as a percentage of the initial discharge.

**Line 8:** If 3 was entered on Line 6, enter here the percentage of time spent at the initial discharge rate before jumping to the new discharge rate.

**Lines 9, 10 and 11:** On these lines should be entered the values of three coefficients C1, C2 and C3 respectively. These are the coefficients of a quadratic expression

$$Q = C1 \times A^2 + C2 \times A + C3$$

which is used as an extra downstream boundary condition to ensure more stability in the computation. C1, C2 and C3 depend on the initial water depth (Line 4) and initial flow discharge (Line 5), as well as the data in the file named on Line 1. A special FORTRAN program, GETPARAM.F, is distributed with ALGDYMOD to calculate these coefficients. The reason why this is done in a separate program, is to save computational time, since C1, C2 and C3 need not be recalculated unless the initial channel parameters and the river profile is changed. Instructions for the use of GETPARAM will be given in Section B.2.3.

The entries in the rest of the file DYDATA.DAT are exactly the same as the entries in DATA.DAT described in section B.1.1.

Table B.5 shows the flow data entries together with the corresponding FORTRAN variables in the program.

| Parameter | unit | Description |
|---|---|---|
| | | Name of the file containing the width of the flow channel at each of the spatial nodes |
| SPACE | km | The length of the flow channel |
| XSTEP | km | The size of the steps used in the spatial integration. The size of XSTEP must be such that the number of spatial nodes (=SPACE/XSTEP) is an integer value. |
| HINIT | m | The initial water depth |
| QINIT | m | The initial flow discharge |
| FLOWTYPE | | This variable allows a choice between 3 different flow types:<br>1 = constant flow<br>2 = smoothly oscillating flow<br>3 = drastically varied flow |
| *The following is entered only if FLOWTYPE=2* | | |
| PERCENT | % | A measure of the strength of the oscillation in the discharge (as a percentage of the initial discharge) |
| *The following is entered only if FLOWTYPE=3* | | |
| PERCENT1 | % | A measure of the size of the jump in the discharge rate (as a percentage of the initial discharge) |
| PERCENT2 | % | The percentage of time spent at the initial discharge rate, before the jump to the new discharge rate takes place |
| C1 | | Coefficient to be calculated by GETPARAM |
| C2 | | Coefficient to be calculated by GETPARAM |
| C3 | | Coefficient to be calculated by GETPARAM |

Table B.5: Channel flow data for ALGDYMOD

The temperature, turbidity, dissolved nitrogen and dissolved phosphorus data files are also prepared exactly as described in section B.1.1. The extra data file named on line 1 of the file DYDATA.DAT is described next.

To understand the nature of the data to be entered into this file, it should be understood that all calculations are done only at a fixed number of discrete points (also called nodes) along the flow channel, each a distance apart which was specified on line 3 of DYDATA.DAT. In this file, which might be called FILRIVER or some other convenient name, the top width and the bottom width of the river are both to be specified at each node, in the following format:

$$
\begin{array}{ll}
BW_1 & TW_1 \\
BW_2 & TW_2 \\
BW_3 & TW_3 \\
BW_4 & TW_4 \\
BW_5 & TW_5 \\
BW_6 & TW_6 \\
\vdots & \vdots
\end{array}
$$

where $BW_i$ is the bottom width and $TW_i$ the top width at the $i$-th node. These widths should be entered in meters.

### B.2.2 Output Data

ALGDYMOD produces much larger output files than ALGSTMOD, since all quantities are computed at all the nodes for every simulation day.

If there are $M$ nodes, and simulation is over $N$ days, and a computed quantity $X$ is in a particular output file, then this file will have the following format:

$$
\begin{array}{l}
M \quad N \\
X(0,0) \\
X(1,0) \\
\vdots \\
X(M-1,0) \\
\\
X(0,1) \\
X(1,1) \\
\vdots \\
X(M-1,1) \\
\\
\quad \vdots \\
\\
X(0,N-1) \\
X(1,N-1) \\
\vdots \\
X(M-1,N-1)
\end{array}
$$

In other words, on the first line of the file appears the numbers $M$ and $N$, followed by values of $X$ computed from day 0 to day $N-1$ at node 0, followed by the values of $X$ computed for all these days at node 1, etc.

This data could be imported into a spread sheet or graphics software for a two or three dimensional plot. Note that the actual node coordinates or dates are not included in these files—the user would have to specify these on the axes when plotting.

The output file P10.DAT contains total chlorophyll-*a* concentrations, while P11.DAT, P12.DAT, ... contains the chlorophyll-*a* concentrations due to algal group 1,2,... as in the case of ALGSTMOD.

As in the case of ALGSTMOD, a number of output files are also produced with data which show the simulated effect of algal activities on the environment. These files have the same names as in Table B.4, and contain simulated values of the quantities described in that table (except of course that the data is now in the two dimensional format described above).

The program also produces five output files containing flow related data. A description of the data in these files are given in Table B.6. This data is not in the format above, since it is essentially spatial.

| File | Description | unit |
|---|---|---|
| ADATA.DAT | The initial and final cross-sectional areas of the river at each of the spatial nodes | $m^2$ |
| UDATA.DAT | The initial and final flow velocities of the river at each of the spatial nodes | m/s |
| QDATA.DAT | The initial and final discharge rates of the river at each of the spatial nodes | $m^3/s$ |
| HDATA.DAT | The initial and final river depths of the river at each of the spatial nodes | m |

Table B.6: Flow related output files for ALGDYMOD

A sample file DYDATA.DAT is distributed with ALGDYMOD, together with a river data file RIVER.DAT, containing the widths of the flow channel at the spatial nodes. These were the data files used to perform the simulations reported in Chapter 6.

### B.2.3 The program GETPARAM

This program actually does a short flow computation, and thus needs some of the data in DYDATA.DAT. After compiling the source file, the program can be run straight away. The user will be prompted to enter certain information, after which the program will display some output on the screen, together with the computed values of the coefficients C1, C2 and C3 at the very end.

The information required is the following:

1. First the program will prompt the user to enter the name of the file containing

the river data. This should be the same filename entered on the first line of DYDATA.DAT.

2. Next the user will be asked to enter the total integration time in seconds. We recommend a time period of 5000 seconds.

3. Next the user is prompted to enter the length of the flow channel. This should be the same as the entry on the second line of DYDATA.DAT.

4. The next entry is the step length in space. This should be the number on the third line of DYDATA.DAT.

5. The next entry is the initial water depth, as on the fourth line of DYDATA.DAT.

6. Finally the user should enter the initial flow discharge, which should be the same as on the fifth line of DYDATA.DAT.

## B.3 Guidelines and tips

In this section a few guidelines are given for the preparation of input files. Some tricks which proved helpful to the developers of this model are also discussed,

### B.3.1 Initial concentrations of algal groups

In section B.1.1 it was stated that the last part of the file DATA.DAT should contain the initial concentrations of living algae ($x_{1_i}$) and dead algae ($x_{2_i}$) in suspension in the water. These concentrations should be specified for each algal group separately.

Usually the purpose of a simulation would be to make a prediction of future algal growth, but such a simulation would have to have some connection with current conditions, so that it should at least start at a time at which recorded data about algal concentrations and environmental conditions are available. Unfortunately only the *total* chlorophyll-*a* concentration is usually recorded, with at most some indication of the algae which were dominant at the time. This makes it difficult, if not impossible, to specify the initial concentrations for individual algal groups. Fortunately, however, precise initial conditions need not be necessary, as long as they are of the correct orders of magnitude. The dynamics of the model have a limited self-correcting mechanism, which would eventually pick up the correct algal concentration levels even if the initial values were not exactly correct.

The following guidelines and tricks could be helpful to the user when specifying these initial conditions:

- The total chlorophyll-*a* concentration as calculated by the model should be seen as the sum of the concentrations of living algae ($x_1$ variables) belonging to all the algal

groups. When specifying initial concentrations, the concentrations of dead algae ($x_2$ variables) must also be given. To do this, equation (A.8) in Appendix A can be used as a guideline, i.e. as a general rule of thumb, the initial $x_2$ concentrations can be specified by multiplying the assigned $x_1$ value by the ratio $k_D/k_S$ for that particular algal group. (This is the ratio of the FORTRAN variables DK to SK, with DK and SK specified in Appendix C.)

- To specify the $x_1$ variables, the user should first try to find an initial day for the simulation on which the total chlorophyll-*a* concentration was very low. Then arbitrary low initial values can be assigned to the $x_1$ variables of all algal groups.

- If it turns out to be impossible or undesirable to start at low algal concentrations, the user could start the simulation on a day with higher algal concentrations, provided that the sum of the assigned initial values for the $x_1$ variables is equal to the recorded total chlorophyll-*a* concentration for that day. If certain algal groups were known to be dominant on that day, this should also be reflected in the initial values assigned. It would also be advisable to include at least two weeks into the simulation for which recorded data is available, so that the simulated values for that time can be compared to recorded values, with adjustments to the initial algal concentrations if necessary.

- Another trick would be to use one "phantom" algal group, with a very low growth rate and a very high death rate. The assigned value for the initial $x_1$ variable of this group could be put equal to very nearly the total recorded chlorophyll-*a* concentration, with low chlorophyll-*a* concentrations assigned to the other algal groups. The effect of this would be that the "phantom" group would disappear very quickly and never reappear, while the other groups should grow to their correct values. Again this type of simulation should be verified by comparing to recorded values for the initial two or more weeks.

### B.3.2 Temperature, turbidity, nitrogen and phosphorus data

Before making a simulation of future algal growth, the user's estimates of future temperature, turbidity and dissolved nitrogen and phosphorus concentrations should be entered into the four input files described before. The user might want to test several scenarios in this way. However, it is always advisable for the first part of the simulation to cover a time period in the past, for which algal growth figures have been recorded. This would ensure that any transient spurious behaviour of the model due to inaccurate initial algal concentrations would have been dampened out before the actual time period of interest. Moreover, the data files have to start at the beginning of the year in which the simulation is to be done, which would usually also necessitate the inclusion of existing data.

Recorded data are not always available on a weekly basis, as required by the program. In cases where available data is available more infrequently, the user should make use of interpolation techniques to obtain weekly figures. In cases where data is available biweekly, linear interpolation would often be sufficient, but when the data base is more sparse, higher order interpolation such as quadratic or cubic should be considered. For

convenience, we give simple (though not the most efficient) formulae for linear, quadratic and cubic interpolation:

1. *Linear interpolation:* Let us suppose that temperatures (say) of $T_1$ and $T_2$ were measured at times $t_1$ and $t_2$ respectively. Then the temperature $T(t)$ at any time $t$ in between is estimated by means of linear interpolation as follows:

$$T(t) \approx T_1\left(\frac{(t-t_2)}{(t_1-t_2)}\right) + T_2\left(\frac{(t-t_1)}{(t_2-t_1)}\right).$$

2. *Quadratic interpolation:* If temperatures of $T_1$, $T_2$ and $T_3$ were measured at the times $t_1$, $t_2$ and $t_3$ respectively, then the temperature $T(t)$ at some time in between these three times would be estimated by means of quadratic interpolation as follows:

$$\begin{aligned} T(t) \approx\ & T_1\left(\frac{(t-t_2)(t-t_3)}{(t_1-t_2)(t_1-t_3)}\right) + T_2\left(\frac{(t-t_1)(t-t_3)}{(t_2-t_1)(t_2-t_3)}\right) \\ & + T_3\left(\frac{(t-t_1)(t-t_2)}{(t_3-t_1)(t_3-t_2)}\right). \end{aligned}$$

3. *Cubic interpolation:* If temperatures of $T_1$, $T_2$, $T_3$ and $T_4$ were measured at the times $t_1$, $t_2$, $t_3$ and $t_4$ respectively, then the temperature $T(t)$ at some time $t$ between two of these four times can be estimated by means of cubic interpolation as follows:

$$\begin{aligned} T(t) \approx\ & T_1\left(\frac{(t-t_2)(t-t_3)(t-t_4)}{(t_1-t_2)(t_1-t_3)(t_1-t_4)}\right) + T_2\left(\frac{(t-t_1)(t-t_3)(t-t_4)}{(t_2-t_1)(t_2-t_3)(t_2-t_4)}\right) \\ & + T_3\left(\frac{(t-t_1)(t-t_2)(t-t_4)}{(t_3-t_1)(t_3-t_2)(t_3-t_4)}\right) + T_4\left(\frac{(t-t_1)(t-t_2)(t-t_3)}{(t_4-t_1)(t_4-t_2)(t_4-t_3)}\right). \end{aligned}$$

More efficient interpolation algorithms can be found in any good book on numerical mathematics.

### B.3.3 Calibration

The program file DATA.DAT distributed with the program contains the calibrated algal parameters for the Stilfontein site, given in Appendix C. Any user who wish to use this model at any other site, could start with this calibration, and verify the model at the new site. However, he would probably find it necessary to recalibrate the model. The Stilfontein calibration should be a good starting point for such a recalibration.

Anyone with modelling experience should have little trouble to perform such a recalibration, which is done by fitting the output of the model on to actual field measurements.

A user who need help to calibrate the model for his site, should feel free to contact the developers of the model at the address given in the next section.

Even though the model might be correctly calibrated for a certain site, recalibrations might still be necessary from time to time. Users should frequently verify the model.

## B.4 Further information

Users who wish to obtain further information or assistance, should contact Prof. S.W. Schoombie at (051) 4012329 or prof. A. Cloot at (051) 4012190. They can also be reached at the following address:

Department of Mathematics and Applied Mathematics
University of the Free State
PO Box 339
Bloemfontein 9300

Fax: (051) 4477980
E-mail: schooms@wis.nw.uovs.ac.za

# Appendix C

# Algal parameters for the Stilfontein site

## C.1 Diatom algal groups.

| Parameter | Alga 1 | Alga 2 | Alga 3 |
|---|---|---|---|
| GKM | 1.3 | 1.4 | 1.8 |
| TI, TOP | 0, 11.54 | 0, 10.55 | 0, 8.5 |
| DK | 0.105 | 0.100 | 0.150 |
| OPLI | 0.185 | 0.075 | 0.065 |
| SK | 0.05 | 0.05 | 0.05 |
| AK | 0.03 | 0.03 | 0.03 |
| PSMAX, TOPS | 9, 21 | 15, 21 | 15, 21 |
| DPSDI | 3.25 | 3.5 | 3.5 |
| DPSN, DPSP, RNPS | 0.17, 0.026, 20 | 0.17, 0.026, 13 | 0.17, 0.026, 50 |
| DISP, ENP | 0.05, 2 | 0.05, 2 | 0.05 2 |
| CORESP | 3.0 | 3.0 | 3.0 |
| CO2SAT, XCO2 | 0.02, 9 | 0.017, 5 | 0.015 5 |
| SISAT | 2 | 2 | 2 |
| SIMIN | 1 | 0.5 | 0 |
| CHSI | 9 | 7 | 7 |
| DKSIUP | 0.0035 | 0.006 | 0.006 |
| SISAG | 2 | 1 | 0.06 |
| SIMIG | 1.2 | 0.5 | 0 |
| CHSIG | 9 | 4 | 25 |

Table C.1: Parameters for the diatom algal groups 1, 2 and 3 at Stilfontein.

## C.2 Algal groups which do not represent diatoms

| Parameter | Alga 4 | Alga 5 | Alga 6 |
|---|---|---|---|
| GKM | 1.6 | 1.8 | 1.5 |
| TI, TOP | 5, 15 | 10, 25 | 10, 19.6 |
| DK | 0.14 | 0.15 | 0.15 |
| OPLI | 0.075 | 0.22 | 0.11 |
| SK | 0.05 | 0.1 | 0.06 |
| AK | 0.03 | 0.065 | 0.03 |
| PSMAX, TOPS | 4.75, 25 | 6, 35 | 8, 25 |
| DPSDI | 6 | 3.5 | 1.5 |
| DPSN, DPSP, RNPS | 0.17, 0.026, 5.65 | 0.17, 0.026, 5 | 0.17, 0.026, 3 |
| DISP, ENP | 0.1, 2 | 0.1, 4 | 0.1 4 |
| CORESP | 3.0 | 3.0 | 3.0 |
| CO2SAT, XCO2 | 0.015, 9 | 0.02, 5 | 0.01, 9 |

Table C.2: Parameters for algal groups 4, 5 and 6 at Stilfontein

| Parameter | Alga 7 | Alga 8 | Alga 9 |
|---|---|---|---|
| GKM | 1.3 | 1. | 1.6 |
| TI, TOP | 10, 20.5 | 10, 23.5 | 5, 13 |
| DK | 0.15 | 0.15 | 0.15 |
| OPLI | 0.1 | 0.05 | 0.04 |
| SK | 0.075 | 0.05 | 0.05 |
| AK | 0.03 | 0.03 | 0.03 |
| PSMAX, TOPS | 10, 35 | 5, 30 | 12, 20 |
| DPSDI | 3.1 | 3.1 | 3.5 |
| DPSN, DPSP, RNPS | 0.17, 0.026, 50 | 0.17, 0.026, 15 | 0.17, 0.026, 25 |
| DISP, ENP | 0.1, 4 | 0.1, 4 | 0.1 4 |
| CORESP | 3.0 | 3.0 | 3.0 |
| CO2SAT, XCO2 | 0.01, 5 | 0.03, 5 | 0.05, 10 |

Table C.3: Parameters for algal groups 7, 8 and 9 at Stilfontein

| Parameter | Alga 10 | Alga 11 | Alga 12 |
|---|---|---|---|
| GKM | 1.8 | 1.85 | 1.72 |
| TI, TOP | 10, 25 | 5, 13.5 | 5, 15.4 |
| DK | 0.15 | 0.15 | 0.15 |
| OPLI | 0.22 | 0.03 | 0.035 |
| SK | 0.1 | 0.05 | 0.1 |
| AK | 0.065 | 0.03 | 0.065 |
| PSMAX, TOPS | 9, 35 | 15, 23.5 | 15, 25.4 |
| DPSDI | 3 | 4 | 4.5 |
| DPSN, DPSP, RNPS | 0.17, 0.026, 22 | 0.17, 0.026, 13 | 0.17, 0.026, 21 |
| DISP, ENP | 0.1, 4 | 0.1, 4 | 0.1 4 |
| CORESP | 3.0 | 3.0 | 3.0 |
| CO2SAT, XCO2 | 0.05, 10 | 0.01, 7 | 0.02, 5 |

Table C.4: Parameters for algal groups 10, 11 and 12 at Stilfontein

| Parameter | Alga 13 | Alga 14 |
|---|---|---|
| GKM | 1.5 | 1.1 |
| TI, TOP | 10, 22 | 10, 23.5 |
| DK | 0.15 | 0.15 |
| OPLI | 0.038 | 0.03 |
| SK | 0.1 | 0.05 |
| AK | 0.065 | 0.065 |
| PSMAX, TOPS | 14, 32 | 15, 33.5 |
| DPSDI | 4 | 5 |
| DPSN, DPSP, RNPS | 0.17, 0.026, 10 | 0.17, 0.026, 12 |
| DISP, ENP | 0.1, 4 | 0.1, 4 |
| CORESP | 3.0 | 3.0 |
| CO2SAT, XCO2 | 0.02, 5 | 0.012, 5 |

Table C.5: Parameters for algal groups 13 and 14 at Stilfontein

# Bibliography


ABBOTT MB and BASCO DR (1989) Computational Fluid Dynamics. An Introduction for Engineers. Longman Scientific & Technical. New York.

CANALE RP and VOGEL AH (1974) Effects of temperature on phytoplankton growth. J. Envir. Engng. Div. Am. Soc. civ. Engrs. **100** 231-241.

CLOOT A and SCHOOMBIE SW (1994) Some aspects of the dynamics of a light-dependent bi-algal growth model, Quaest. Math. **17** (1) 95-136.

COLE GA (1975) Textbook on limnology. The C.V. Mosby company, St. Louis, 275pp.

EPPLEY RW (1977) The growth and culture of diatoms. In Werner D (ed.) *The biology of diatoms*. Blackwell Scientific Publ., Oxford **103** 24-64.

GARCIA-NAVARRO P and SAVIRON JM (1992) McCormack's Method for the Numerical Simulation of one-dimensional discontinuous unsteady open channel flow. *Journal of Hydraulic Research*. **30** (1), 95-105.

GARRELS RM and CHRIST CL (1965) Solutions, minerals and equilibria. Harper & Row, New-York, 435pp.

GOLTERMAN HL (1975) Physiological limnology: an approach to the physiology of lake ecosystems, Elsevier Scientific Publishing Co., Amsterdam.

GUCKENHEIMER PH and HOLMES P (1986) Nonlinear oscillations, dynamical systems and bifurcations of vector fields. Springer-Verlag, New-York, Berlin, Heidelberg and Tokyo.

HALE JK (1969) Ordinary differential equations. Wiley, NewYork.

JORGENSEN SE (1979) Handbook of enviromental data and ecological parameters. International Society for Ecological Modeling.

LAX P and WENDROFF B (1960) Systems of Conservation Laws. *Communications on Pure and Applied Mathematics*. **XIII** 217-237.

MAHMOOD K and YEVJEVICH V (eds.) (1975) Unsteady Flow In Open Channels. Water Resource Publications. Fort Collins.

PIETERSE AJH (1992) Private communication.

PIETERSE AJH and Toerien DF (1978) The phosphrus-chlorophyll relationship in Roodeplaat dam. Water SA 4 105-112.

ROACHE PJ (1977) Computational Fluid Dynamics. Hermosa. Albuquerque.

ROOS JC (1992) Primary productivity of the Vaal River phytoplankton. Ph. D. thesis, Dept. of Botany and Genetics, University of the Orange Free State, Bloemfontein, Republic of South Africa, 265 pp.

ROOS JC (1993) Private communication.

SHEN HW (1979) Modeling of Rivers. John Wiley & Sons. New York.

STEEMAN NIELSEN E (1975) Marine photosynthesis - with special emphasis on the ecological aspects. Elsevier Oceanography series **13** 141pp.

STUMM W and MORGAN JJ (1970) Aquatic chemistry - An introduction emphasizing equilibria in natural waters. Wiley-interscience, New-York, USA, 571 pp.

USEPA Report (1985) Rates, contants, and kinetics formulations in water quality modeling. US Environmental Protection Agency, EPA/600/3-85/040 455pp.

WALMSLEY RD and BUTTY M (1980) Guidelines for the control of eutrofication in South Africa. Water Research Commission and National Institute for Water Research, report ISBN 0 7988 1735 6.

WERNER D (1977) Silicate metabolism. In: Werner D. (ed) *The biology of diatoms.* Blackwell Scientific Publ., Oxford **103** 110-149.

WETZEL RG (1983) *Limnology.* Saunders College Pub., New-York, USA, 765 pp.

WHITEHEAD PG and HORNBERGER GM (1984) Modeling algal behaviour in the river Thames, *Water Res.* **18**, 945-953.

WOFSY SC (1983) A simple model to predict extinction coefficients and phytoplankton biomass in eutrophic waters, *Limnol. and Oceanogr.* **28**(6), 1144-1155.